Evaluation of LTPP Climatic Data for Use in Mechanistic-Empirical Pavement Design Guide Calibration and Other Pavement Analysis

PUBLICATION NO. FHWA-HRT-15-019

MAY 2015

U.S. Department of Transportation
Federal Highway Administration

Research, Development, and Technology
Turner-Fairbank Highway Research Center
6300 Georgetown Pike
McLean, VA 22101-2296

LTPP™

FOREWORD

This document presents the results of an evaluation of climate data from Modern-Era Retrospective Analysis for Research and Applications (MERRA) for use in the Long Term Pavement Performance (LTPP) Program and for other infrastructure applications. MERRA data were compared against the best available ground-based observations both statistically and in terms of effects on pavement performance as predicted using the Mechanistic-Empirical Pavement Design Guide (MEPDG). These analyses included a systematic quantitative evaluation of the sensitivity of MEPDG performance predictions to variations in fundamental climate parameters.

A more extensive analysis of MERRA data included additional statistical analysis comparing operating weather station (OWS) and MERRA data, evaluation of the correctness of MEPDG surface shortwave radiation (SSR) calculations and comparison of MEPDG pavement performance predictions using OWS and MERRA climate data for more sections. The principal conclusion from these evaluations was that the MERRA climate data were as good as and in many cases substantially better than equivalent ground-based OWSs. MERRA is strongly recommended as the new future source for climate data in LTPP. Recommendations are provided for incorporating hourly MERRA data into the LTPP database.

The LTPP program is an ongoing and active program. To obtain current information and access to other technical references, LTPP data users should visit the LTPP Web site at http://www.tfhrc.gov/pavement/ltpp/ltpp.htm. LTPP data requests, technical questions, and data user feedback can be submitted to LTPP customer service via e-mail at ltppinfo@fhwa.dot.gov.

Jorge E. Pagán-Ortiz
Director, Office of Infrastructure
Research and Development

TECHNICAL DOCUMENTATION PAGE

1. Report No. FHWA-HRT-15-019	2. Government Accession No.	3. Recipient's Catalog No.
4. Title and Subtitle Evaluation of Long-Term Pavement Performance (LTTP) Climatic Data for Use in Mechanistic-Empirical Pavement Design Guide(MEPDG) Calibration and Other Pavement Analysis		5. Report Date May 2015 6. Performing Organization Code
7. Author(s) Charles W. Schwartz, Gary E. Elkins, Rui Li, Beth A. Visintine, Barton Forman, Gonzalo R. Rada, Jonathan L. Groeger		8. Performing Organization Report No.
9. Performing Organization Name and Address AMEC Environment and Infrastructure, Inc. 12000 Indian Creek Court, Suite F Beltsville, MD 20705-1242 University of Maryland—College Park Department of Civil and Environmental Engineering 1173 Glenn L. Martin Hall College Park, MD 20742		10. Work Unit No. (TRAIS) 11. Contract or Grant No. DTFH61-11-C-00030
12. Sponsoring Agency Name and Address Office of Infrastructure Research and Development Federal Highway Administration 6300 Georgetown Pike McLean, VA 22101-2296		13. Type of Report and Period Covered Final Report, May 2011–October 2014 14. Sponsoring Agency Code
15. Supplementary Notes The Contracting Officer's Representative (COR) was Larry Wiser.		

16. Abstract

Improvements in the Long-Term Pavement Performance (LTPP) Program's climate data are needed to support current and future research into climate effects on pavement materials, design, and performance. The calibration and enhancement of the *Mechanistic-Empirical Pavement Design Guide* (MEPDG) is just one example of these emerging needs. A newly emerging climate data source, the Modern-Era Retrospective Analysis for Research and Applications (MERRA), developed by the National Aeronautics and Space Administration (NASA) for its own in-house modeling needs, provides continuous hourly weather data starting in 1979 on a relatively fine-grained uniform grid. MERRA is based on a reanalysis model that combines computed model fields (e.g., atmospheric temperatures) with ground-, ocean-, atmospheric-, and satellite-based observations that are distributed irregularly in space and time. MERRA data are available at an hourly temporal resolution and 0.5 degrees latitude by 0.67 degrees longitude (approximately 31.1 by 37.30 mi at mid-latitudes) spatial resolution over the entire globe. MERRA data were compared against the best available ground-based observations both statistically and in terms of effects on pavement performance as predicted using the MEPDG. These analyses included a systematic quantitative evaluation of the sensitivity of MEPDG performance predictions to variations in fundamental climate parameters. More extensive analysis of MERRA data included additional statistical analysis comparing operating weather station (OWS) and MERRA data, evaluation of the correctness of MEPDG surface shortwave radiation (SSR) calculations and comparison of MEPDG pavement performance predictions using OWS and MERRA climate data for more sections. The principal conclusion from these evaluations was that the MERRA climate data were as good and in many cases substantially better than equivalent ground-based OWS data. Given these many benefits and very few if any significant limitations, MERRA is strongly recommended as the new future source for climate data in LTPP. Recommendations are provided for incorporating hourly MERRA data into the LTPP database.

17. Key Words Long-Term Pavement Performance, LTPP, climate data, pavement design, pavement performance, solar radiation, virtual weather stations, Modern-Era Retrospective Analysis for Research and Applications, MERRA, Mechanistic Empirical Pavement Design Guide, MEPDG, hourly weather data	18. Distribution Statement No restrictions. This document is available to the public through the National Technical Information Service, Springfield, VA 22161. http://www.ntis.gov

19. Security Classif. (of this report) Unclassified	20. Security Classif. (of this page) Unclassified	21. No. of Pages 138	22. Price

Form DOT F 1700.7 (8-72) Reproduction of completed page authorized

SI* (MODERN METRIC) CONVERSION FACTORS

APPROXIMATE CONVERSIONS TO SI UNITS

Symbol	When You Know	Multiply By	To Find	Symbol
		LENGTH		
in	inches	25.4	millimeters	mm
ft	feet	0.305	meters	m
yd	yards	0.914	meters	m
mi	miles	1.61	kilometers	km
		AREA		
in^2	square inches	645.2	square millimeters	mm^2
ft^2	square feet	0.093	square meters	m^2
yd^2	square yard	0.836	square meters	m^2
ac	acres	0.405	hectares	ha
mi^2	square miles	2.59	square kilometers	km^2
		VOLUME		
fl oz	fluid ounces	29.57	milliliters	mL
gal	gallons	3.785	liters	L
ft^3	cubic feet	0.028	cubic meters	m^3
yd^3	cubic yards	0.765	cubic meters	m^3
	NOTE: volumes greater than 1000 L shall be shown in m^3			
		MASS		
oz	ounces	28.35	grams	g
lb	pounds	0.454	kilograms	kg
T	short tons (2000 lb)	0.907	megagrams (or "metric ton")	Mg (or "t")
		TEMPERATURE (exact degrees)		
°F	Fahrenheit	5 (F-32)/9 or (F-32)/1.8	Celsius	°C
		ILLUMINATION		
fc	foot-candles	10.76	lux	lx
fl	foot-Lamberts	3.426	$candela/m^2$	cd/m^2
		FORCE and PRESSURE or STRESS		
lbf	poundforce	4.45	newtons	N
lbf/in^2	poundforce per square inch	6.89	kilopascals	kPa

APPROXIMATE CONVERSIONS FROM SI UNITS

Symbol	When You Know	Multiply By	To Find	Symbol
		LENGTH		
mm	millimeters	0.039	inches	in
m	meters	3.28	feet	ft
m	meters	1.09	yards	yd
km	kilometers	0.621	miles	mi
		AREA		
mm^2	square millimeters	0.0016	square inches	in^2
m^2	square meters	10.764	square feet	ft^2
m^2	square meters	1.195	square yards	yd^2
ha	hectares	2.47	acres	ac
km^2	square kilometers	0.386	square miles	mi^2
		VOLUME		
mL	milliliters	0.034	fluid ounces	fl oz
L	liters	0.264	gallons	gal
m^3	cubic meters	35.314	cubic feet	ft^3
m^3	cubic meters	1.307	cubic yards	yd^3
		MASS		
g	grams	0.035	ounces	oz
kg	kilograms	2.202	pounds	lb
Mg (or "t")	megagrams (or "metric ton")	1.103	short tons (2000 lb)	T
		TEMPERATURE (exact degrees)		
°C	Celsius	1.8C+32	Fahrenheit	°F
		ILLUMINATION		
lx	lux	0.0929	foot-candles	fc
cd/m^2	$candela/m^2$	0.2919	foot-Lamberts	fl
		FORCE and PRESSURE or STRESS		
N	newtons	0.225	poundforce	lbf
kPa	kilopascals	0.145	poundforce per square inch	lbf/in^2

*SI is the symbol for the International System of Units. Appropriate rounding should be made to comply with Section 4 of ASTM E380.
(Revised March 2003)

TABLE OF CONTENTS

LIST OF FIGURES

LIST OF TABLES

LIST OF ACRONYMS AND SYMBOLS

AADTT	Average Annual Daily Truck Traffic
AASHTO	American Association of State Highway and Transportation Officials
AC	Asphalt Concrete
AR	Asphalt Concrete Rutting
ASOS	Automated Surface Observing System
AWS	Automated Weather Station
CCC	Canadian Centre for Climate
CLM	Climate module (LTPP environment/climate data module)
CNCDIA	Canadian National Climate Data and Information Archive
COOP	Cooperative Observer Program
CRCP	Continuously Reinforced Concrete Pavement
DLND	Design Limit Normalized Difference
DST	Daylight Savings Time
EICM	Enhanced Integrated Climate Model
ESS	Environmental Sensor Station
ETG	Expert Task Group
F	Faulting
FAA	Federal Aviation Administration
FHWA	Federal Highway Administration
GEOS-5	Goddard Earth Observation System Version 5
GOES	Geostationary Operational Environmental Satellites
GPS	General Pavement Studies
GPSR	Global Position Satellite Receiver
GSI	Grid-Point Statistical Interpolation
HDF	Hierarchical Data Format
IAU	Incremental Analysis Update
IRI	International Roughness Index
JPCP	Jointed Plain Concrete Pavement
LC	Longitudinal Cracking
LTBP	Long-Term Bridge Performance
LTPP	Long-Term Pavement Performance
MDISC	Modeling and Assimilation Data and Information Services Center
MEPDG	Mechanistic-Empirical Pavement Design Guide
MERRA	Modern-Era Retrospective Analysis for Research and Application
METAR	Météorologique Aviation Régulière
NASA	National Aeronautics and Space Administration
NCDC	National Climate Data Center
NCHRP	National Cooperative Highway Research Program
NetCDF	Network Common Data Format
NOAA	National Oceanic and Atmospheric Administration
NSI	Normalized Sensitivity Index
NSRDB	National Solar Radiation Data Base
NWS	National Weather Service
OAT	One at a Time
OWS	Operating Weather Station

PCC	Portland Cement Concrete
PG	Performance Grade
PPDB	Pavement Performance Database
QA	Quality Assurance
QC	Quality Control
QCLCD	Quality Controlled Local Climatological Data
RCC	Regional Climatic Center
RMSE	Root Mean Squared Error
RWIS	Road Weather Information System
SC	Slab Cracking
SDR	Standard Data Release
SIRS	Solar Infrared Radiation System
SMP	Seasonal Monitoring Program
SPS	Specific Pavement Studies
SSR	Surface Shortwave Radiation
TMI	Thornthwaite Moisture Index
TR	Total Rutting
ULCD	Unedited Local Climatological Data
UMD	University of Maryland
USCRN	U.S. Climate Research Network
VWS	Virtual Weather Station

EXECUTIVE SUMMARY

The Long-Term Pavement Performance (LTPP) Program has performed pioneering work to characterize and summarize site-specific climatic data for use in evaluating the performance of its General Pavement Studies (GPS) and Specific Pavement Studies (SPS) test sections. Improvements in these data are needed to support current and future research into climate effects on pavement materials, design, and performance. The calibration and enhancement of the Mechanistic-Empirical Pavement Design Guide (MEPDG) is just one example of these emerging needs.

The original objectives of this study were the following: (1) examine current and emerging needs in climate data collection for transportation infrastructure applications such as the MEPDG, Superpave binder specification, and bridge and other types of asset management models; (2) develop a methodology for incorporating temporal changes in position and measurement characteristics of operating weather stations (OWS) into the computation of climate indices; (3) apply this new methodology to update the climate statistics in the LTPP database; (4) examine the need for additional climate-soils parameters, such as the Thornthwaite Moisture Index (TMI) to the LTPP database; and (5) examine the need for continued location-specific solar radiation measurements to capture the effects of climate change on pavement and other infrastructure performance. However, during the project, the study team discovered a newly emerging source of weather data that resulted in a change of direction. This data source, the Modern-Era Retrospective Analysis for Research and Applications (MERRA), developed by the National Aeronautics and Space Administration (NASA) for its own in-house modeling needs, provides continuous hourly weather data starting in 1979 on a relatively fine-grained uniform grid. MERRA is based on a reanalysis model that combines computed model fields (e.g., atmospheric temperatures) with ground-, ocean-, atmospheric-, and satellite-based observations that are distributed irregularly in space and time. The result is a uniformly gridded dataset of meteorological data derived from a consistent modeling and analysis system over the entire data history. MERRA data are provided at an hourly temporal resolution and a 0.5 degrees latitude by 0.67 degrees longitude (approximately 31.1 mi by 37.3 mi at mid-latitudes) spatial resolution over the entire globe.

The direction of the project was therefore shifted to evaluating whether MERRA is a viable alternative to conventional ground-based climate data sources and whether it satisfied (or made moot) all of the original project objectives. MERRA data were compared against the best available ground-based observations both statistically and in terms of effects on pavement performance as predicted using the MEPDG. These analyses included a systematic quantitative evaluation of the sensitivity of MEPDG performance predictions to variations in fundamental climate parameters. Key conclusions from these investigations are summarized as follows:

Sensitivity of MEPDG performance predictions to fundamental climate parameters

- Average annual temperature and average annual temperature range were the most sensitive climate characteristics for both flexible and rigid pavements. Average daily temperature range also had a very significant influence on jointed plain concrete pavement (JPCP) slab cracking but almost no effect on flexible pavement performance. The sensitivity of JPCP slab cracking to percent sunshine was also very high.

- Percent sunshine and wind speed were moderately important climate characteristics for both flexible and rigid pavements.

- Precipitation had negligible influence on either flexible or rigid pavement performance. This was sensible given that the current version of the MEPDG does not include the effects of surface infiltration in its modeling of temperature and moisture within the pavement.

- Asphalt rutting, total rutting, and longitudinal cracking were the flexible pavement distresses that were most sensitive to climate characteristics.

- Slab cracking was the rigid pavement distress most sensitive to climate characteristics.

Comparisons of MERRA versus Automated Weather Station (AWS) and OWS weather data statistics

- There was generally good agreement in air temperature, precipitation, and relative humidity frequency distributions and statistics from all data sources.

- There was generally poorer agreement in percent sunshine and wind speed frequency distributions and statistics from the various data sources. These discrepancies may be the result of the methods used to infer some data elements (percent sunshine for AWS), unexplained anomalies in the recorded data (wind speed for OWS), discrete versus continuous recording of data (wind speed), and potentially inaccurate quantification of cloud cover conditions (wind speed for OWS).

Comparison of MEPDG distress predictions using MERRA versus AWS/OWS weather data

- About a third of the 12 sites analyzed exhibited generally good agreement between the MERRA- and AWS/OWS-based distress predictions.

- There were no systematic patterns in the discrepancies of MEPDG predicted distresses using AWS versus MERRA versus virtual weather station (VWS) versus OWS weather data sources. The results suggest that the match between MERRA and AWS data in overall terms is at least as good as the agreement between VWS/OWS and AWS data.

- Weak trends were observed between differences in MEPDG distress predictions using MERRA versus OWS weather inputs and site terrain and latitude. Good agreement of MEPDG distress predictions was more likely for flat terrain and northern sites while poorer agreement was more likely for varying/mountainous terrain and southern sites.

- Total incoming shortwave radiation, a key driver for pavement temperatures, must be determined indirectly from the OWS data using estimates of top-of-atmosphere incoming solar radiation, measured percent sunshine/cloud cover, and an empirical relation for atmospheric diffuse scattering and absorption. Total incoming shortwave

radiation is provided explicitly in the MERRA data, but it cannot be used directly as an input in the current version of the MEPDG.

- Examination of the underlying formulation of the Enhanced Integrated Climate Model (EICM) in the MEPDG in the context of MERRA versus OWS weather inputs suggests that discrepancies in MEPDG predictions using the two data sources are related to differences in absorbed energy at the surface of the pavement, and more specifically, to differences in incoming shortwave solar radiation at the pavement surface from the two data sources.

These conclusions strongly support recommendation of MERRA as a source of climate data for LTPP and for weather inputs for the MEPDG and other infrastructure applications. MERRA data satisfy all of the major study objectives. They meet the climate data needs for current infrastructure applications such as the MEPDG, LTPPBind, HIPERPAV®, and bridge management. The broad range of MERRA data means that they will likely meet the climate data needs for future applications as well. The attention to quality and continuity in the MERRA data eliminates the need to deal with temporal changes in position and/or measurement details of OWS histories. The close and uniform spacing of MERRA grid points also eliminate the need for improved weather data interpolation and VWS. Lastly, MERRA makes moot the issue of continued location-specific solar radiation measurement, because MERRA provides this information directly at every grid point.

Initial evaluations of the MERRA data suggested that it is as good as, and in many ways superior to, weather data time series from conventional surface-based OWSs. The recommendations from these initial evaluations were that LTPP adopt MERRA as the data source for its next update to the climate data module and develop a tool to extract and use this data for engineering applications.

After review of the initial evaluations by the Transportation Research Board's Expert Task Group (ETG) on LTPP Special Activities, Federal Highway Administration (FHWA) experts, and LTPP staff, two primary comments necessitate additional analysis with the following primary objectives:

1. More extensive analysis of MERRA data.

2. Development of a tool to disseminate MERRA data.

The more extensive analysis of MERRA included the following specific study activities:

- If possible, establish an appropriate ground truth for climate data.

- Perform statistical comparisons of ground truth, OWS, and MERRA.

- Evaluate the correctness of MEPDG surface shortwave radiation (SSR) calculations.

- Compare MEPDG pavement performance predictions using ground truth, OWS, and MERRA climate data.

A variety of data sources were examined in this phase of the study. Ground-based climate data provided as part of the MEPDG served as the standard input for flexible and rigid pavement simulations using the Pavement ME Design® software. Additional data sources employed for comparisons with the MEPDG climate files include the U.S. Climate Research Network (USCRN), the National Weather Service (NWS) Cooperative Observer Program (COOP), the Department of Energy Solar Infrared Radiation System (SIRS) stations, and NASA's MERRA.

Statistical analyses were conducted comparing the different data sources relative to USCRN (i.e., USCRN treated as the reference measurement) for the approximately 17-year period of July 1, 1996, through September 1, 2013. This time period corresponds to the approximate temporal overlap of all of the available data sources used in this study. The emphasis of the statistical evaluation was on temperatures because prior studies had shown that pavement performance was most sensitive to these climate.[1,2] Wind speed and cloud cover are the next most sensitive climate inputs; however, the USCRN data do not contain these data elements and consequently they could not be evaluated. Although the MEPDG in its current form assumes no infiltration of surface water into the pavement layers, precipitation data from various climate data products were nevertheless compared. Cloud cover, wind speed, and humidity were also compared to a lesser extent. Cloud cover is important primarily because of its impact on incoming SSR at the ground surface. Although SSR is not a direct input in the MEPDG, it is the principal driver for pavement heating and cooling. To evaluate the SSR issue, SIRS observations were used to supplement the USCRN SSR observations. Hence, the following meteorological analyses were conducted in-depth: (1) near-surface air temperatures, (2) precipitation at the ground surface, and (3) shortwave radiation at the ground surface.

The overall conclusions from the statistical comparisons of the various climate data sources can be summarized as follows:

- Although in concept the USCRN data are the closest thing to ground truth, it is the opinion of the project team that the concept of ground truth does not truly exist for climate data. Given the inevitable measurement errors and the spatial variability of weather data over even short distances, even two ground truth stations separated by only a few hundred meters will inevitably give slightly different climate data time series.

- The statistical comparisons of hourly data found that the Quality Controlled Local Climatological Data (QCLCD) and MERRA data have small and roughly comparable differences from the USCRN values. The MERRA data are slightly warmer on average than the QCLCD values, but only by less than 2 °F.

- The statistical comparisons of daily temperature data found that the COOP and MERRA data have small but roughly comparable differences from the USCRN values. The MERRA data are slightly warmer than the COOP values, but in most cases by less than 1° F.

- The comparisons for MEPDG surface shortwave calculations against predicted MERRA and measured SIRS values found that the bias was generally small in comparison to peak solar radiation values. However, the MEPDG values had higher

positive bias and variability than MERRA during critical low-percent cloud cover conditions and hot summer months and lower positive bias during the less important late winter months. The project team recommends that the Pavement ME Design® Task Force explore the option of using SSR as a direct input rather than percent cloud cover.

Pavement performance as predicted by the MEDPG models incorporated in the Pavement ME Design® software was evaluated using the MEPDG weather data files provided with the software (derived from the QCLCD and Unedited Local Climatological Data products from the National Climate Data Center (NCDC)) and the MERRA climate data for collocated sites and congruent time series. A total of 20 sites were analyzed.

Both new flexible pavements and new JPCP were analyzed. The pavement structures, traffic loads, material properties, and other inputs for the analysis correspond to the medium traffic cases for the sensitivity analyses described in.[(1)] All analyses were performed using Version 2.0 of the Pavement ME Design® software.

Overall, the comparisons in MEPDG predicted performance for both flexible and rigid pavements using MERRA versus MEPDG weather data are close and acceptable for engineering design. Based on the earlier statistical comparisons among the various climate data sources, the agreement in predicted performance using MERRA versus USCRN ground truth and/or MEPDG versus USCRN would likely show similar agreement. However, it is impossible to demonstrate this agreement because the USCRN data lack the wind speed and cloud cover inputs required by the MEPDG software.

The results of the more extensive statistical and pavement performance comparisons reported here support the original recommendation that LTPP should adopt MERRA as a primary data source for its next update to the climate data module and develop a tool to extract and use this data for engineering applications.

MERRA offers the following benefits compared with conventional ground-based OWS data:

- **Denser, more uniform, and broader spatial coverage**. The network of first-order ground-based OWS provides data at approximately 1,000 locations in the contiguous United States. These locations are not distributed uniformly, and vast areas of the country have sparse or no coverage. MERRA data, by contrast, are currently available at more than 3,000 grid points in the contiguous United States. MERRA grid points are uniformly distributed at a horizontal spacing of approximately 31.1 by 37.3 mi; no point on the globe is more than 24.9 mi from the nearest MERRA grid point. This distance will become dramatically smaller when an enhanced MERRA having approximately 0.62 by 0.62 mi horizontal grid spacing is made available to the public within the next few years.

- **Better temporal frequency and continuity**. MERRA provides weather data at hourly time intervals as required by current state-of-the-art infrastructure modeling applications. Daily, monthly, and/or annual statistics are also available directly from MERRA or can be aggregated from the hourly data. There are no gaps in the MERRA

histories as often appear in the AWS data. All MERRA data are consistently referenced to Greenwich Mean Time.

- **Excellent data consistency and quality**. To meet its in-house needs for modeling and satellite retrieval algorithms, NASA performs rigorous and sophisticated quality control (QC) checks to ensure that all MERRA data are consistent and correct, even as the mix of satellites and other sources of measurement data inevitably change across time and location.

- **Focus on fundamental physical quantities.** MERRA data include data elements that are much more relevant to the fundamental inputs required by thermodynamics-based infrastructure modeling than are available from the OWS data. For example, MERRA directly provides the shortwave radiation fluxes at the top of atmosphere and at the ground surface. In the MEPDG, these quantities are estimated using empirical and semi-empirical relationships that are functions of location, time, and percent sunshine category. Given that net shortwave radiation flux at the surface is the primary driver for pavement temperature distributions, the MERRA data are much more suitable. The ready availability of MERRA data will likely foster improvements to current infrastructure modeling applications such as the MEPDG.

- **Richer and more versatile datasets.** To meet NASA's diverse modeling requirements, MERRA reports hundreds of data elements, although not all of these data elements are at the highest temporal and spatial resolutions. Many of these data elements may be useful to future infrastructure and other modeling applications.

- **Potential for automated updates to LTPP database**. The process of requesting MERRA data, downloading it from the server, extracting and processing the data elements relevant to LTPP needs, and importing these data into the LTPP database has the potential to be highly automated. This could enable more frequent updates to the climate (CLM) module at significantly less cost.

- **Improvement over time**. NASA is currently enhancing MERRA to an approximately 1 km spatial resolution. This means that no location will be more than 2,297 ft from the nearest MERRA grid point. Significant improvement in conventional ground-based OWS coverage is very unlikely.

- **Reliability analysis capabilities**. MERRA is only, albeit the most comprehensive, retrospective reanalysis system available. Others have been developed in Europe, Japan, and elsewhere. These various modeling applications could be applied simultaneously to develop ensembles of weather histories that can be characterized statistically for rationally quantifying the uncertainty of predicted infrastructure performance caused by the weather inputs.

MERRA offers many benefits and very few if any significant limitations for use as the source of climate data for transportation infrastructure modeling applications. Therefore, it is recommended that MERRA be the future source of climate data in LTPP. Guidelines are provided for incorporating hourly MERRA data into the LTPP database. Topics addressed

include unit conversions, elimination of VWS, new data elements, new table designs, nomenclature, data storage, and data release policies. Recommendations are also made for archiving of data in the current LTPP CLM module.

Data used in this effort were acquired as part of the activities of NASA's Science Mission Directorate and are archived and distributed by the Goddard Earth Sciences Data and Information Services Center.

CHAPTER 1. INTRODUCTION

STUDY BACKGROUND AND OBJECTIVES

The importance of climate to the performance of pavements and many other transportation infrastructure assets is beyond debate. The Long-Term Pavement Performance (LTPP) Program has performed pioneering work to characterize and summarize site-specific climatic data for its General Pavement Studies (GPS) and Specific Pavement Studies (SPS) test sections. However, improvements in climatic data collection are needed to support current and future research on climate effects pertaining to pavement materials, design, and performance. The calibration and enhancement of the *Mechanistic-Empirical Pavement Design Guide* (MEPDG) is just one example of these emerging needs.[(3)]

To address these needs, the study had the following original objectives:

- Examine current and emerging needs in climate data collection and engineering indices for use in MEPDG calibration, changes in Superpave binder performance grading, and development of future mechanistic-based infrastructure management applications, including pavement, bridge, and other types of asset management models.

- Develop a methodology for characterizing location-specific historical climate indices that includes temporal changes in the position and measurement characteristics of the operating weather stations (OWS) used for the computation. This new methodology will include an estimate of the variability or uncertainty caused by the spatial averaging process used to develop the baseline indices.

- Provide recommendations to update the climate statistics in the LTPP database.

- Examine the need to add a climate-soils parameter such as the Thornthwaite Moisture Index (TMI) to the LTPP database. Examine the applicability of TMI to other transportation infrastructure applications.

- Examine the need for continued location-specific solar radiation measurements to capture the effect of climate change on pavement and other infrastructure performance. Determine whether existing data sources can be used to fulfill this need.

TERMINOLOGY

Some clarification of terminology is appropriate here. The National Oceanic and Atmospheric Administration (NOAA) provides the following definitions:

"**Weather** refers to [atmospheric] conditions at a given point in time (e.g., today's high temperature), whereas **Climate** refers to the "average" weather conditions for an area over a long period of time (e.g., the average high temperature for today's date)."[(4)]

The Intergovernmental Panel on Climate Change provides the following even more specific definition:

"Climate in a narrow sense is usually defined as the "average weather," or more rigorously, as the statistical description in terms of the mean and variability of relevant quantities over a period ranging from months to thousands or millions of years. The classical period is 30 years, as defined by the World Meteorological Organization (WMO). These quantities are most often surface variables such as temperature, precipitation, and wind. Climate in a wider sense is the state, including a statistical description, of the climate system."[5]

The atmospheric data stored in the LTPP database are a combination of "weather," which is currently the daily extremes, and "climate" statistics summarized at the monthly and annual level. To minimize potential confusion, this report uses the general term "climate" to represent the larger subject area, but may also use weather data to describe specific short-term observations or measurements.

CHANGE IN PROJECT WORK PLAN

During the execution of Phase 2 of the project, the study team discovered a newly emerging source of weather data that resulted in a change of direction in the project work plan. This discovery is credited to the University of Maryland (UMD) members of the research project team. A UMD Civil Engineering faculty member advised the study team of the existence of a new source of weather and climate data based on his recent work at the Goddard Space Flight Center in Greenbelt, MD. The name of the data source is Modern-Era Retrospective Analysis for Research and Applications (MERRA). The primary attribute of this data source that motivated the project direction change is the availability of continuous hourly weather data starting in 1979 on a relatively fine-grained uniform grid. MERRA also contains more fundamental scientific data elements than are available from any of the other data sources identified in phase 1 of this project. If MERRA data proved to be a viable alternative, then all of the project objectives could be satisfied. Chapter 4 of this report provides more details and information on MERRA data.

The significant change in the phase 2 work plan was to evaluate MERRA data against available ground-based observations, both in statistical terms and using the MEPDG. The MEPDG, developed under National Cooperative Highway Research Program (NCHRP) Project 1-37A and recently officially adopted by the American Association of State Highway and Transportation Officials (AASHTO), was selected because it contains the most advanced models on pavement-climate interaction that have ever been officially adopted by AASHTO.[6,3] The MEPDG is also a major focus of the objectives of the present study. Chapter 5 documents the findings of the comparisons between MERRA and best available ground-based weather data sources with significant time coverage.

MORE EXTENSIVE ANALYSIS OF MERRA DATA

Initial evaluations of the MERRA data suggested that it is as good as, and in many ways superior to, weather data time series from conventional surface-based OWSs. The recommendations from these initial evaluations were that LTPP adopt MERRA as the data source for its next update to

the Climate (CLM) module and develop a tool to extract and use this data for engineering applications.

After review of the initial evaluations by the Transportation Research Board's Expert Task Group (ETG) on LTPP Special Activities, Federal Highway Administration (FHWA) experts, and LTPP staff, two primary comments necessitate additional analysis with the following primary objectives:

1. More extensive analysis of MERRA data.
2. Development of a tool to disseminate MERRA data.

The more extensive analysis of MERRA included the following specific study activities:

- If possible, establish an appropriate ground truth for climate data.
- Perform statistical comparisons of ground truth, OWS, and MERRA.
- Evaluate the correctness of MEPDG surface shortwave radiation (SSR) calculations.
- Compare MEPDG pavement performance predictions using ground truth, OWS, and MERRA climate data.

REPORT ORGANIZATION

To provide a complete overview of the status of climate data in the LTPP program, chapter 2 contains a summary of the legacy LTPP approach to climate data in current use. While some of this information is available in other LTPP documents, some new information is presented here that provides a context to evaluate MERRA data against the legacy approach, not only as used by LTPP, but also for other infrastructure applications.

Chapter 3 provides a summary of infrastructure climate data needs and candidate data sources reviewed by the study team. While most of this information was contained in the phase 1 report, it is being repeated in this document for reviewer convenience.

Chapter 4 contains a description of the MERRA product. This includes a conceptual description of the modeling approach, the data used and produced by MERRA, and comments on quality control (QC) procedures.

Chapter 5 presents the findings of the evaluation of MERRA data against existing ground-based observations both statistically and using the MEPDG models. The analyses include a systematic quantitative evaluation of the sensitivity of MEPDG predicted pavement distresses to climate inputs, a statistical comparison of MERRA versus ground-based weather history inputs, and a critical comparison of MEPDG predicted pavement distresses using MERRA versus ground-based weather history data.

Chapter 6 presents the findings of the more extensive analysis of MERRA data, including additional statistical analysis comparing OWS and MERRA data, evaluation of the correctness of

MEPDG SSR calculations, and comparison of MEPDG pavement performance predictions using OWS and MERRA climate data for more sections.

Chapter 7 presents the recommendations and findings of this research effort. These include the benefits of MERRA data, recommendations on inclusion of legacy climate indices, and initial concepts for implementation of MERRA data into the LTPP database.

CHAPTER 2. LEGACY LTPP APPROACH TO CLIMATE DATA

A brief overview of the current approach for collection, processing, and storage of data to represent climate conditions at each test site is presented in this chapter. This discussion is limited to the methodology to include continuous long-term data stored in the climate module for all test sections because this was the objective of this portion of the study.

VIRTUAL WEATHER STATION CONCEPT

To develop climate statistics to represent site conditions at each test site, LTPP developed the "virtual" weather station (VWS) concept. Because LTPP test sections are rarely located near an OWS, a method was needed to interpolate data from nearby sites over the required duration of the test section life. The methodology LTPP selected was to call the statistical climate data interpolated from nearby OWS a VWS.

The selection of the OWS to form the statistical basis for a VWS is a critical consideration. The objective of the OWS selection process was to identify weather measurement locations that are expected to be representative of conditions at the VWS site and that satisfy the data needs of the intended application. Some of the factors taken into consideration in the LTPP OWS selection process included the following:

- Distance between the OWS and VWS location.
- Elevation difference between the OWS and VWS location.
- Terrain features between OWS and VWS locations. Mountains and large bodies of water can influence temperature, precipitation, humidity, and wind patterns.
- Types of data available from OWS because weather stations vary in recorded data.
- OWS data reporting frequency. Some weather data measurement sources only include daily extremes while others contain hourly or more frequent data.
- Temporal coverage of data from the selected OWS.
- Data QC measures applied to OWS instrumentation.

The OWS selection method used by the LTPP program developed over time. It began with definition of a perfect weather station to describe the climate at LTPP test sections. The "perfect" weather station had to be within 5 mi and include data equivalent to a first order weather station.[7] In theory, only one perfect weather station is needed to describe the weather events occurring at a pavement test section location that can account for events affecting the performance of the test pavement structure. When it became apparent that no perfect weather stations existed for the LTPP test sections at the start of the program, the following OWS selection process was used based on first-order and cooperative weather stations in the United States. First-order weather stations are those maintained by the National Weather Service (NWS) that operate 24 hours a day with frequent data collection intervals collecting variables such as temperature, precipitation, surface pressure, humidity, wind speed and direction, cloud cover,

snow depth, visibility, and solar radiation; cooperative weather stations generally collect only temperature and/or precipitation at less frequent intervals, and collection is performed by volunteers. Equivalent categories of weather stations were also applied to available data from Canada. The following OWS selection process used by the LTPP program emerged over time:

A. Using automated methods, develop a list of candidate OWSs based on the following rules:

    1. Identify at least one active first-order weather station with at least 50-percent coverage of the desired time length.

    2. Identify the closest active cooperative weather stations satisfying the following criteria:

        i. Has at least 50-percent temporal coverage over the desired coverage period.

        ii. Has temporal coverage greater than or equal to pavement age or 5 years.

        iii. Contains the following mandatory data elements: minimum and maximum daily air temperature, daily precipitation, and daily snowfall (where applicable).

    3. Identify at least three other nearest active or inactive weather stations that provide data over the coverage time period.

B. Submit the list of candidate OWSs to LTPP regional contractors for further evaluation and development of recommendations on final selection of up to five weather stations. The following factors were taken into account by LTPP regional contractors in developing recommendations on the selected OWS:

    1. Correction of test section location coordinates when necessary. When LTPP started, the use of Global Position Satellite Receiver (GPSR) technology was limited, and many of the initial pavement test section coordinates were not correct. A manual plotting of test section coordinates on a suitable paper map and comparison to other information on the known location of a test section was the best available method to confirm test section location coordinates.

    2. Representativeness of the selected active first-order weather stations based on distance from the test section relative to elevation differences, mountains, large lakes, and other terrain features. The regional contractors were encouraged to contact State climatologists to obtain input on known micro-climate effects and other known OWS anomalies in the area. In some cases, it was not possible to associate a first-order weather station with a LTPP test section site.

    3. Representativeness of the selected active cooperative weather stations meeting the criteria listed under A.2 above, using the same criteria mentioned above for first-order weather stations.

    4. Representativeness of the other candidate OWSs.

C. Conduct a centralized evaluation of the recommended OWS list. Initial evaluation was based on reasonableness considerations on the basis for the recommended OWS, and secondarily on results of analysis of data obtained from the final list of selected OWS sites.

D. Repeat the OWS selection process over time as new test sections and test sites are added. In most instances, because new test sections in the SPS were added at existing LTPP test section sites, the same OWS previously selected could be used to generate the VWS statistics for the location. For the new pavement construction SPS experiments, i.e., SPS-1, SPS-2, and SPS-8, using the original concept of perfect weather stations, automated weather stations (AWS) were installed and operated by the LTPP program at or near the SPS projects.

As it turns out, based on LTPP experience, there is no such thing as a perfect weather station. As is subsequently explained, all weather measurement instrumentation requires continual monitoring, evaluation, and maintenance to provide reasonable data. This is compounded by secondary issues related to time conventions, equipment calibrations, and changes in measurement equipment over time.

Using the selected representative OWSs, LTPP used a VWS interpolation methodology based on a $1/R^2$ "gravity" model for combining data from up to five nearby weather stations. As illustrated conceptually in figure 1, the interpolated value for data element *V* for day *m* at the VWS location is determined from the data elements V_{mi} recorded at each of the *k* OWSs on day *m* as seen in figure 2 in which R_i is the distance of weather station *i* from the VWS location at the project site. In figure 1, OWS_3 is highlighted to represent the closest first-order weather station. As subsequently explained, 95 percent of the daily VWS weather statistics for wind and humidity are based on only one OWS, which is typically a first-order weather station.

The LTPP VWS interpolation methodology does not directly account for elevation differences between the measurement locations and project site. This is the reason that the selection criteria for the OWSs included a limit to the difference in elevation to the VWS site. (Note: The VWS algorithm in the MEPDG is very similar to that used by LTPP except that it does include an elevation correction using the temperature lapse rate.)

DATA PROCESSING AND STORAGE

The LTPP climate data obtained from external sources are stored in the CLM module in the pavement performance database (PPDB). A two-tiered data storage structure is used. The first tier contains raw and processed data from OWSs selected for use in computing the second tier VWS statistics.

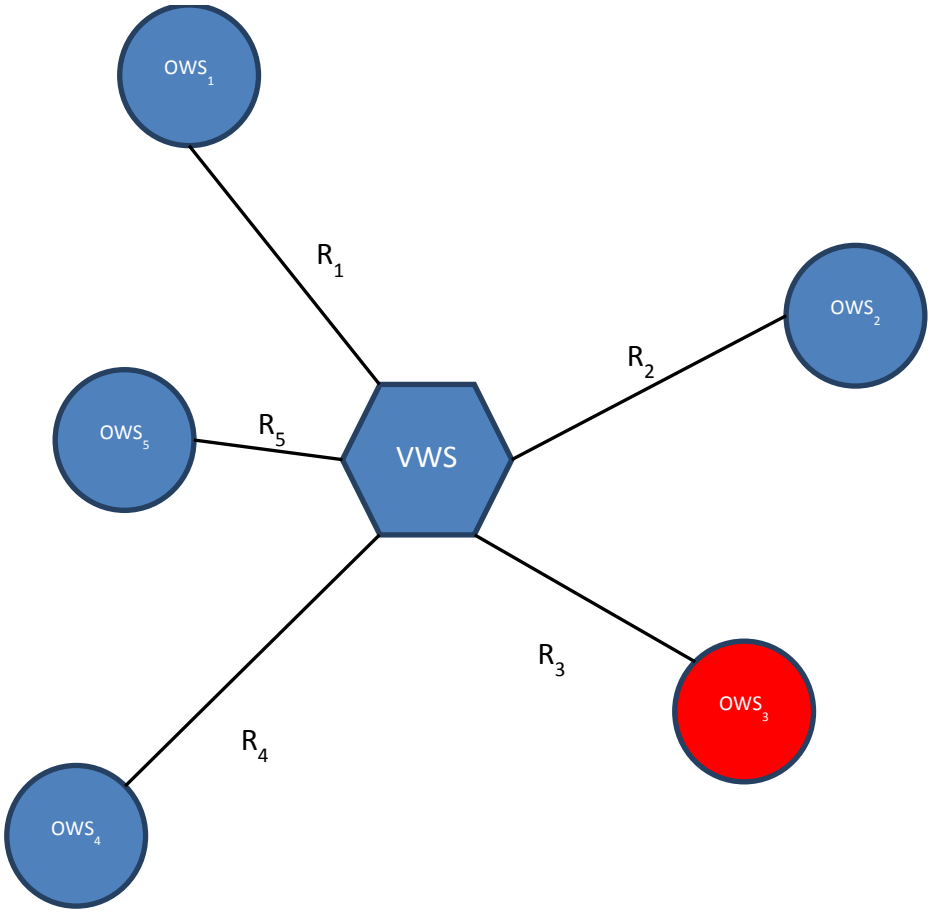

Figure 1. Illustration. Illustration of VWS concept.

$$V_m = \frac{\sum_{i=1}^{k} \frac{V_{mi}}{R_i^2}}{\sum_{i=1}^{k} \frac{1}{R_i^2}}$$

Figure 2. Equation. Gravity model equation.

All of the table names in the CLM module start with CLM as the first three-letter prefix. In the table relationship figures in this part of the report, the CLM prefix has been omitted for presentation convenience.

Figure 3 illustrates the organization of the CLM_OWS tables contained in the PPDB. Only the CLM_OWS_LOCATION table is distributed as a part of the LTPP Standard Data Release (SDR). All of the other CLM_OWS_* tables shown in this figure are stored centrally on the LTPP PPDB database server and are disseminated by request only. The data obtained from the United States and Canadian climate data sources, National Climate Data Center (NCDC) and Canadian Centre for Climate (CCC), respectively, are split into four data types and stored by time period, i.e., daily, monthly, and annual. This format was implemented in 2004 as part of the 2005 data release to address data discrepancies found in the raw data from NCDC.

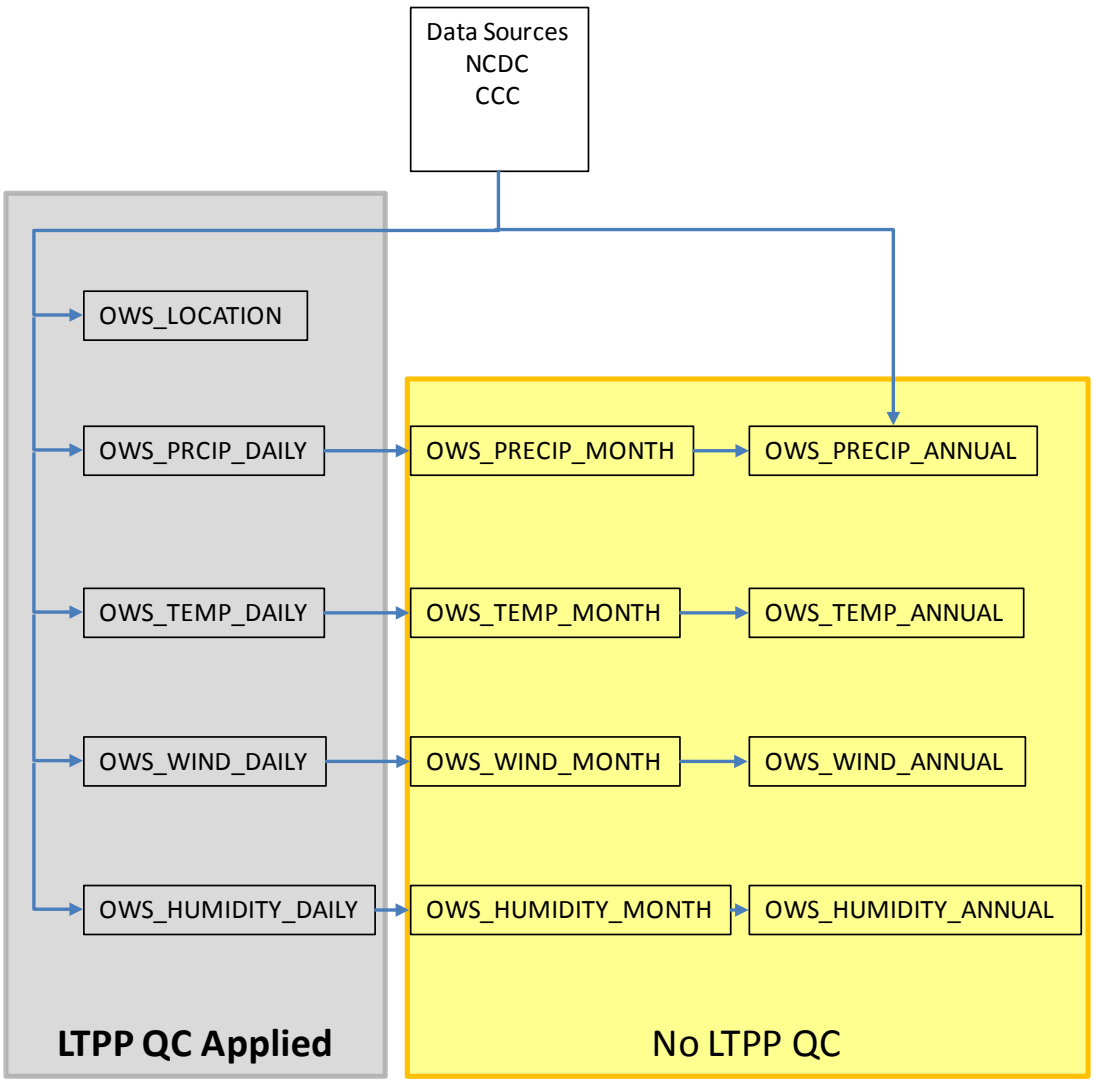

Figure 3. Illustration. LTPP parsing, QC checks, and data flow relationships among the CLM_OWS* tables obtained from external data sources.

Only the OWS_LOCATION and OWS_*data-type*_DAILY tables are subjected to automated LTPP QC checks because they are used in the computation process for the CLM_VWS tables contained in the SDR. The four data types include precipitation, temperature, wind, and humidity. The OWS monthly and annual tables are not subject to LTPP QC checks. These tables have been used in the past by the LTPP engineering staff to perform reasonableness checks on the results of the VWS monthly and annual tables. In essence, the monthly computations from the OWS sources are compared with those computed from the VWS daily data when a new data upload is performed.

Figure 4 illustrates the CLM VWS computational structure relationships. OWSs are linked to pavement test sections through a process that considers their locations relative to the test section locations. The results of this selection process are contained in the VWS_OWS_LINK table, which controls which OWS data are included in each VWS statistic. The SPS_GPS_LINK and SITE_VWS_LINK tables are used to associate CLM_VWS statistics with collocated test

sections at project sites with more than one test section. The dashed arrows in figure 4 show the hierarchical statistical summaries based on level E data from the underlying temporal statistics. Level E means that the data have passed all of the automated LTPP QC checks.

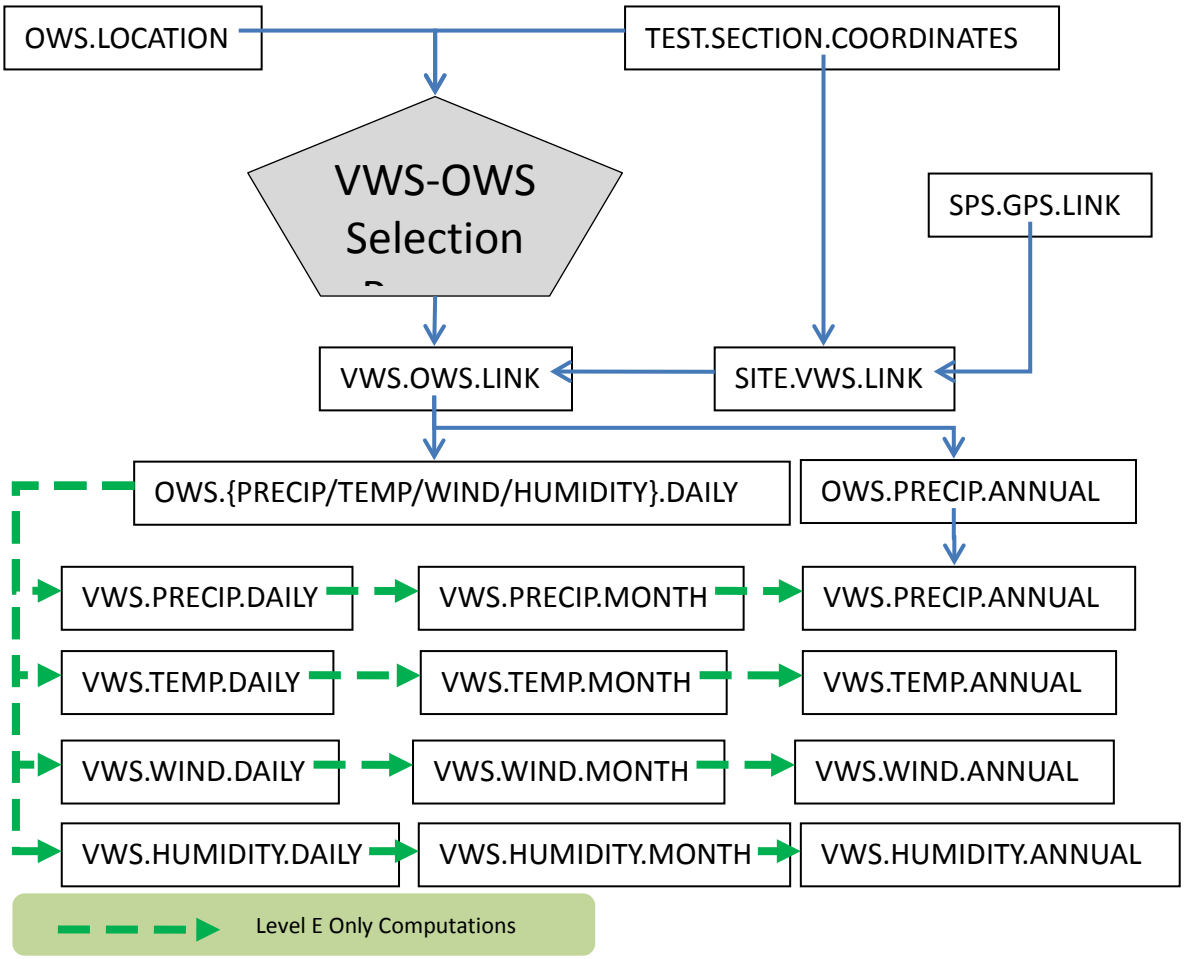

Figure 4. Illustration. LTPP CLM VWS computational relationship structure.

After the VWS daily tables are created, the VWS monthly tables are computed. The monthly tables are computed using daily data that have passed all of the daily data QC checks. In addition to the checks on the daily tables, the monthly data table calculations are subjected to QC checks on the number of valid days in each month's daily data. Likewise, annual statistics are based on the monthly statistics and subjected to QC checks related to the number of valid days in the year for which data for each data type is available.

The data in CLM_VWS_* tables contained in the SDR includes all data at all levels of RECORD_STATUS. While only level E data are used to compute the higher-level temporal aggregation statistics, data failing the QC checks were retained for research purposes.

The derived monthly and annual climate statistics and indices computed from the daily data are shown in table 1. In addition to common statistical descriptive measures, the LTPP CLM module includes the following climate indices:

- Freeze index.
- Freeze–thaw cycles
- Intense precipitation days.
- Number of wet days.
- Number of days above freezing.
- Number of days below freezing.

Table 1. Derived climatic data statistics and computed indices stored in the LTPP database.

	Monthly				Annual			
Data Element	**Average**	**Std. Dev.**	**No. of Days**	**Value**	**Average**	**Std. Dev.**	**No. of Days**	**Value**
Mean temperature	X	X	X		X		X	
Maximum temperature	X	X	X		X		X	
Minimum temperature	X	X	X		X		X	
Absolute maximum temperature				X				X
Absolute minimum temperature				X				X
Number of days above 90 °F			X				X	
Number of days below 32 °F			X				X	
Freeze index			X	X			X	X
Freeze–thaw cycles			X	X			X	X
Maximum humidity	X	X	X		X		X	
Minimum humidity	X	X	X		X		X	
Total precipitation			X	X			X	X
Number of intense precipitation days (daily precipitation > 0.5 inches)			X				X	
Number of wet days (daily precipitation > 0.01 inches)			X				X	
Total snowfall				X			X	X
Number of snow covered days							X	
Mean wind speed	X		X		X		X	
Maximum wind speed	X		X		X		X	

Std. Dev. = Standard Deviation

ISSUES WITH LEGACY LTPP CLIMATE DATA APPROACH

The legacy LTPP program approach to general climate statistics for test sections dates back to technology available in 1991. Over time, LTPP has pursued an active and informed approach to provision of climate data statistics that has altered and adapted to changing technology. The following are some difficulties, limitations, and issues with this approach that the program has attempted to deal with over the last 20 years and that represent future challenges to its legacy approach:

- Limited spatial and temporal coverage of ground-based OWSs, close enough to test sections to be used as part of the VWS computation process, result in an uneven number of OWSs by data type. Figure 5 shows the number of OWS that provide data for a LTPP VWS by data type. The vertical scale is percentage of total daily OWS observations in each VWS climate data category. The horizontal scale is the number of OWSs used in each daily VWS statistic. When wind and humidity data are available, 95 percent of the VWS daily data come from only one OWS, whereas less than 10 percent of the VWS daily data for temperature and precipitation come from one OWS. At the other extreme, almost 50 percent of the VWS statistics for temperature and precipitation are based on the maximum of five OWSs. This situation creates an uneven balance in the basis of the VWS computed parameters for each study site.

- Selected OWSs contain data gaps or do not provide temporal coverage over the desired timeframe.

- Existing OWSs change location over time while keeping the same name. This requires changes to the current LTPP CLM data storage and computational structures to accommodate.

- If all of the selected OWSs do not contain a desired data element, the resulting VWS climate data statistic is left null or a record is not included in the LTPP database.

- New OWSs are introduced over time. To proceed with the legacy LTPP climate approach requires a new OWS selection process. While technological advances have been made to make this process more streamlined than in the past, the OWS selection process requires expenditures of significant program resources.

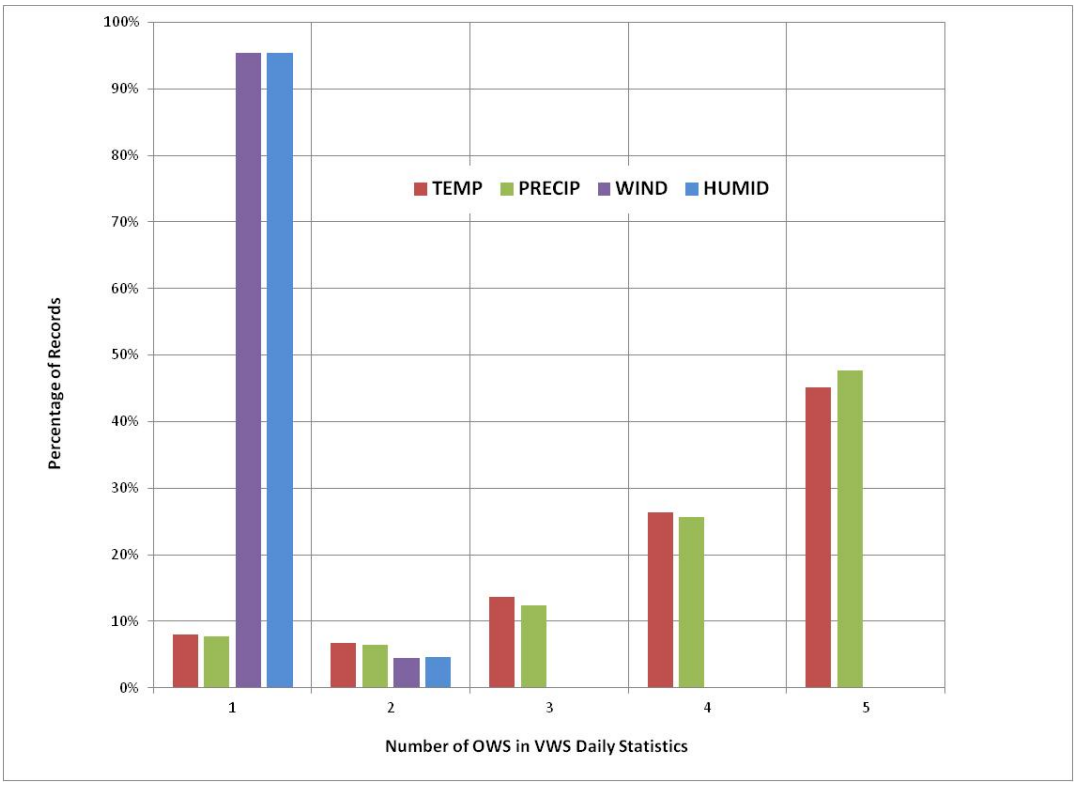

Figure 5. Graph. Percentage of OWSs represented in each daily VWS statistic by number of OWSs.

- The MEPDG software requires hourly climate inputs. The LTPP climate database contains only daily climate extremes.

- The existing onsite hourly weather measurements collected by LTPP as part of the AWS effort contain significant data gaps due to equipment failure and thus do not provide continuous coverage over the operational time period. This issue is the reason that the U.S. Climate Reference Network (USCRN) includes redundant measurement instrumentation at each site.

- No adjustments are made in the interpolation process to account for elevation differences between the OWS and VWS.

These issues are not criticisms of the LTPP program; they merely reflect the issues and challenges that all infrastructure research projects requiring sit- specific climate data have faced over the last 20 years. Even today, using ground-based weather data observations has some of these same issues.

The next chapter of this report contains a summary of climate data sources that are available to meet emerging needs of the modern generation of infrastructure design and performance prediction engineering models.

CHAPTER 3. CLIMATE DATA APPLICATIONS AND SOURCE CANDIDATES

INFRASTRUCTURE APPLICATIONS

Effective identification of potential climate data sources requires knowledge of the types of applications in which these data will be used. The following subsections describe current pavement and other infrastructure applications that require climate data as part of their inputs.

Empirical Pavement Design

Until very recently, most major pavements in the United States have been designed using the empirical AASHTO method.[8] This method includes climate influences and climate data inputs, but only in very indirect ways. For example, the design subgrade resilient modulus for both flexible and rigid pavement designs is specified as a seasonally averaged value reflecting the variations in foundation stiffness during the year, particularly in northern climates subjected to freeze–thaw cycles. However, climate data per se are not explicit inputs into the seasonal adjustment calculations. Both the flexible and rigid design procedures include drainage coefficients to account for the speed with which climate-related water infiltration is removed from the pavement structure. However, the climate data input for determining the drainage coefficients is nebulously defined in terms of the percentage of the year that the pavement layers will be at saturation levels near 100 percent. The only explicit climate input in the 1993 AASHTO method is the depth of frost penetration, which is used for computing serviceability loss due to frost heave; however, very few States use this part of the AASHTO design method. Explicit climate inputs in the 1998 AASHTO supplement for rigid pavements are the mean annual wind speed, temperature, and precipitation used for estimating the effective positive temperature differential through the concrete slab; however, relatively few States use the 1998 AASHTO supplement.

Mechanistic-Empirical Pavement Design

The lack of explicit treatment of climate influences in the most widely used empirical AASHTO design methods was one of the motivations for the development of mechanistic-empirical pavement design procedures. These procedures couple mechanistic calculation of pavement primary responses—e.g., stresses and strains at critical locations—resulting from traffic loads and climate influences with empirical predictions of pavement structural distresses—e.g., rutting and cracking in flexible pavements, joint faulting and slab cracking in rigid pavements, and reflection cracking in rehabilitation overlays. Mechanistic-empirical pavement design methods have been developed in the past by several State highway agencies (e.g., Illinois, Kentucky, and Washington) and by industry groups (e.g., Shell Oil, The Asphalt Institute, and the Portland Cement Association). The most recent and comprehensive of these procedures is the MEPDG developed under NCHRP Project 1-37A and recently officially adopted by AASHTO.[6.3] The MEPDG procedures are implemented in the AASHTOWare Pavement ME Design® software released by AASHTO in April 2011.

The temperature and moisture analyses performed by the MEPDG's Enhanced Integrated Climate Model (EICM) require five weather-related parameters on an hourly basis over the entire design life of the project: air temperature, wind speed, percent sunshine, relative humidity,

and precipitation. Details on how these weather history inputs are used in the EICM are presented later in chapter 5.

Weather history information is obtained from weather stations located near the project site. The MEPDG software includes a database of approximately 800 weather stations throughout the United States. If needed, interpolation of climatic data from multiple nearby stations can be stored as a VWS.

Although no formal, documented QC checks have been performed on the climatic data distributed with the current version of the MEPDG software, there is general consensus and concern that the information for some of the weather stations may be flawed. Studies by Zaghloul et al. and Johanneck and Khazanovich well-illustrate some of the reasons for these concerns.[9,10]

A major difficulty in evaluating the consequences of MEPDG weather data quality is that the sensitivity of the pavement performance predictions from the MEPDG to climatic inputs is largely unknown. Numerous studies have evaluated the sensitivity of MEPDG performance predictions to traffic, geometric, and material design input parameters, but no comprehensive sensitivity study of the effects of climate on performance predictions has been performed. Nearly all "sensitivity analyses" of MEPDG performance predictions to climatic inputs to date have simply compared results using one weather station to another, usually from a distinctly different climatic zone. (See references 11 through 26, 9, 27, and 28.) This type of anecdotal approach cannot provide any organized comprehensive insights. A recent study by Li et al. examined in a quantitative but very limited way the sensitivity MEPDG predicted performance to changes in average temperature and precipitation.[29] Some of the findings were unsurprising, e.g., asphalt rutting increases with increasing average temperature. However, other findings were more perplexing, e.g., alligator cracking decreased with decreasing average precipitation; although this might be intuitively expected, it is surprising to find this in the MEPDG predictions because, as described later in chapter 5, the current version of the MEDPG ignores any infiltration of precipitation into the pavement structure. Some insights into the influence of individual weather components on pavement performance can also be gleaned from the effective temperature relations for rutting and fatigue developed by El-Basyouny and Jeong, which are functions of annual average temperature, the variability of the maximum annual temperature, wind speed, percent sunshine, and precipitation as well as loading frequency and, for rutting, depth within the pavement.[30]

There have been many attempts to compare predictions of pavement temperature histories against measured values for the LTPP Seasonal Monitoring Program (SMP) using finite difference- or finite element-based transient heat balance simulation models (e.g., Hermansson, Zubair et al., and Ho and Romero). (See references 31 through 35.) These comparisons have been quite close in most studies. However, the predictions exhibited low sensitivity to some climate inputs and high sensitivity to other climate-related inputs that are not even measured (e.g., atmospheric down-welling longwave radiation and surface albedo, the inverse of surface shortwave absorptivity). Zuo et al. demonstrated that pavement critical responses (e.g., maximum strains) are quite sensitive to the temperature and moisture gradients within the pavement, which in turn can be quite sensitive to the details of the weather history.[36] Zuo et al. also found that the averaging period for weather data (hourly versus daily versus monthly) had a

significant effect; as would be expected, longer averaging periods reduced the impact of the peak conditions when disproportionate pavement distress may occur.

Superpave Binder Specification

The Superpave performance grade (PG) binder specification requires as input the annual minimum and the annual maximum 7-day average pavement temperature. The Superpave PG specification recommends a corresponding high and low temperature binder grade to ensure that the binder has suitable viscoelastic stiffness and creep properties at the expected high and low pavement temperatures and target reliability level.

LTPPBind (http://www.fhwa.dot.gov/pavement/ltpp/ltppbind.cfm) is a software tool developed by LTPP to help highway agencies select the appropriate Superpave PG for a particular site. LTPPBind features a database of air temperatures (minimum, mean, maximum, standard deviation, and number of years) for nearly 8,000 U.S. and Canadian weather stations.

Enhancements to the Superpave PG specification are currently under active consideration by the FHWA Binder ETG and other groups to address fatigue cracking resistance under immediate temperature conditions. These discussions may lead to additions/changes in the climate inputs for the Superpave PG specification.

HIPERPAV®

The HIPERPAV® analysis software (http://www.hiperpav.com/) assesses the influence of pavement design, concrete mix design, construction methods, and environmental conditions on the early-age behavior of Portland cement concrete (PCC) pavements. The service life of concrete pavements is highly dependent on curing behavior during the first 72 hours following placement. Stresses in concrete develop from the combined effects of curling and warping and the restraint of movements along the slab-subbase interface. These stresses may be of sufficient magnitude to cause cracking while the concrete strength is still relatively low. Prediction and/or monitoring of the stresses during this time is extremely important because problems during curing may lead to loss of long-term pavement performance.

Environmental inputs required by the HIPERPAV® software include hourly temperature, wind speed, humidity, and cloud cover for the first 72 hours after placement; minimum and maximum air temperatures during the critical curing period, defined as after 72 hours to first traffic application; minimum and maximum air temperatures for the duration after the critical curing period; and typical monthly rainfall for a 12-month period.

HIPERPAV® implicitly requires solar radiation input for the heat balance equations at the pavement surface. Solar radiation is estimated internally in the software from latitude, elevation, and percent cloud cover.

Good comparisons have been found between HIPERPAV® predicted and actual measured temperatures.[37] Although HIPERPAV® is targeted specifically at concrete pavements, stresses versus strength gain as the concrete matures is an issue for all concrete structures. These include bridge decks, bridge columns and abutments, and many other transportation infrastructure components.

Bridge Management

Bridge deterioration should logically depend on climate factors as well as many other variables. For example, bridge decks and structural elements in northern tier states with freeze–thaw cycles and use of deicing salts can be expected to deteriorate more rapidly than those in warmer climates. Expansion joints in locales that have large temperature swings can be expected to deteriorate more quickly than those in more temperate locales.

Pontis is the AASHTO bridge management system used by most U.S. transportation agencies for managing bridge inventories and making decisions about preservation and functional improvements for bridge structures. Pontis stores bridge inventory and inspection data, including detailed element conditions; supports network-wide preservation and improvement policies for use in evaluating the needs of each bridge in a network; makes project recommendations to derive maximum benefit from scarce funds; reports network and project-level results; and forecasts individual bridge lifecycle deterioration and costs.

Although bridge deterioration should logically depend on climate factors, the inclusion of climate data elements in the current version of Pontis is very limited and qualitative. Pontis has four climate conditions defined as Benign, Fair, Moderate, and Severe. The appropriate climate condition is not based on any specific environmental/climate/weather data elements but is simply selected by the user.

In April 2008, FHWA launched the Long-Term Bridge Performance (LTBP) Program, a major new strategic initiative designated as a flagship research project. The LTBP Program is intended to be a 20-year undertaking. Its major objective is to compile a comprehensive database of quantitative information from a representative sample of bridges nationwide, looking at every element of a bridge. By taking a holistic approach and analyzing all of the physical and functional variables that affect bridge performance, the study will provide a more detailed and timely picture of bridge health and better bridge management tools. The LTBP Program completed a pilot study on seven bridges to validate protocols for assessment, data collection, and management. Data collection in two clusters in mid-Atlantic States began in March 2013 after completion of the pilot study.

Climate data for the LTPB are being extracted from the Clarus weather station network (described further in the next section) and online from Weather Underground (www.wunderground.com). Key data elements include humidity, temperature, and number of snowfalls greater than 1 inch. Current temporal frequency for climate data is low. However, future deterioration models may require more frequent data, e.g., to model thermal stresses in bridges with frozen bearings. Some QC checks of the climate data are performed in Clarus and others by LTBP.

Summary of Existing Applications

It is now increasingly possible to perform complex thermodynamic modeling of the influence of climate and other environmental considerations on infrastructure performance. However, the data needs for these models often exceed what has been required (or available) in the past. New/ emerging pavement modeling tools such as the MEPDG and HIPERPAV® require more and

finer-grained (e.g., hourly) climate data as inputs than do older techniques (e.g., 1993 AASHTO).[8] These finer-grained climate data are available in the current LTPP database only for the relatively small number of AWS locations.

A common development arc for modeling is to start with very complex models that take into account second- and third-order interactions. Exercising these models helps identify the important controlling factors that dominate the intended use of the model so that the model can subsequently be simplified. This philosophy can be paraphrased as "You have to make things complicated before you can make them simple." High-quality, finer-grained climate data are essential to this process.

In addition to the uses of climate data in infrastructure performance prediction, climate monitoring during infrastructure construction can also be highly beneficial. This monitoring can help to optimize closure times or times to initiation of the next construction phase based on climate-material interaction considerations.

CONVENTIONAL SOURCES OF CLIMATIC DATA

NOAA is the principal U.S. scientific agency focused on the conditions of the oceans and the atmosphere of the planet. NOAA's NCDC is the world's largest active archive of weather data. The NCDC has more than 150 years of data on hand with 224 gigabytes of new information added each day. The NCDC archives contain more than 320 million paper records, 2.5 million microfiche records, and more than 1.2 petabytes of digital data. Data are received from a wide variety of sources, including satellites, radar, automated airport weather stations, NWS cooperative observers, aircraft, ships, radiosondes, wind profilers, rocketsondes, solar radiation networks, and NWS forecast/warnings/analyses.

NCDC also manages NOAA's Regional Climate Centers (RCC). The RCCs provide access to essential climate variables through the Applied Climate Information System, a part of NCDC's National Virtual Data System.

Additional local climatic data are available from State climatologist offices. Forty-seven States and Puerto Rico currently have State climatologists. They work closely with NCDC, the RCCs, and the NWS to provide improved climate services through greater integration of data quality control and improved communication and coordination.

The Canadian National Climate Data and Information Archive (CNCDIA) operated by Environment Canada contains the official climate and weather observations for Canada. The CNCDIA includes climate elements such as temperature, precipitation, relative humidity, atmospheric pressure, wind speed, wind direction, visibility, cloud types, cloud heights and amounts, soil temperature, evaporation, solar radiation and sunshine and occurrences of thunderstorms, hail, and other weather phenomena.[38]

The Clarus Initiative is a collaborative effort of the FHWA Road Weather Management Program and the Intelligent Transportation Systems Joint Program Office to reduce the impact of adverse weather conditions on surface transportation users.[39] To achieve this goal, a robust data assimilation, quality checking, and data dissemination system needed to be created so that near real-time atmospheric and pavement observations could be provided. By working in partnership

with agencies, Clarus connects existing sensors into a nationwide network. The Clarus system data can be used to support transportation operations resources such as Enhanced Road Weather Forecasting, Seasonal Weight Restriction Decision Support Tool, Non-Winter Maintenance and Operations Decision Support Tool, Multi-State Control Strategy Tool, and Enhanced Road Weather Content for Traveler Advisories. New quality checking algorithms have recently been implemented to enhance the capabilities of the current Clarus system.

Clarus consolidates data from existing sensors operated by a network of different agencies. As a consequence, the available data vary significantly by location/agency. There are currently approximately 75 different observation types collected by 140 sensor systems operated by the various agencies.

METAR, which roughly translates from French as Aviation Routine Weather Report, is the international standard for reporting hourly meteorological data.[40] METAR reports wind, visibility, runway visual range, present weather, sky condition, temperature, dew point, and altimeter setting. METAR reports are provided by the NWS, the Federal Aviation Administration (FAA), and others via the Automated Weather Observing System, Automated Surface Observing System (ASOS), and Automated Weather Sensor System.[41] METAR data and the related Terminal Aerodrome Forecasts data are available at http://weather.noaa.gov/weather/coded.html.

For the purpose of tracking climate change, NOAA has developed the USCRN. The USCRN consists of 120+ research-grade stations collecting high-quality climate data, including temperature and precipitation, solar radiation, surface skin temperature, surface winds, relative humidity, and (in the future) soil moisture and soil temperature at five depths.[42] The USCRN program will collect data for 50 years to track climate change. Figure 6 shows the coverage of the USCRN stations.

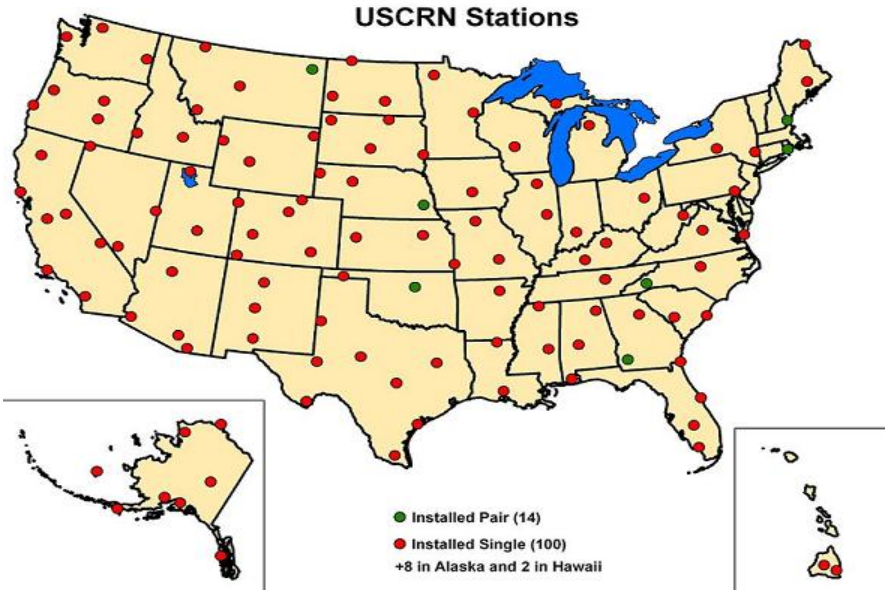

Source: NOAA

Figure 6. Map. U.S. Climate Research Network stations.[42]

Automated Surface Observing System (ASOS)

ASOS is a network of first-order climate stations operated cooperatively by the NWS, the FAA, and the Department of Defense. These data are available through the NCDC in NOAA. ASOS is the Nation's primary surface weather observing network. Observations from ASOS are updated every minute, 24 hours a day, 365 days a year. The following weather elements are reported by ASOS:[(43)]

- Sky condition: cloud height and amount (clear, scattered, broken, overcast) up to 12,000 ft.
- Visibility (to at least 10 statute mi).
- Basic present weather information: type and intensity for rain, snow, and freezing rain.
- Obstructions to vision: fog, haze.
- Pressure: sea-level pressure, altimeter setting.
- Ambient temperature, dew point temperature.
- Wind: direction, speed, and character (gusts, squalls).
- Precipitation accumulation.
- Selected significant remarks, including variable cloud height, variable visibility, precipitation beginning/ending times, rapid pressure changes, pressure change tendency, wind shift, and peak wind.

Although there are roughly 1,000 ASOS located throughout the United States, there are vast areas without coverage.

Road Weather Information Systems (RWIS)

Many States maintain RWIS equipment as part of their safety management for roadways. A key component of the RWIS is an Environmental Sensor Station (ESS) that measures atmospheric, surface and/or hydrologic conditions using one or more sensors. There is no standardized ESS sensor configuration. An individual ESS may include a wind sensor, camera, solar radiation sensor, temperature/dew point sensor, precipitation sensor, visibility sensor, and snow depth sensor on a tower. Sensors located away from the tower may include road surface temperature, subsurface temperature, flooding water level, and precipitation accumulation sensors.

Solar Radiation Data

Solar radiation data are a principal input to thermodynamics-based climate-structure interaction models for predicting temperature and/or moisture distributions in pavements and other

transportation infrastructure systems. Unfortunately, the LTPP OWS CLM data module does not contain any solar radiation data, not even indirect measures such as percent cloud cover.

Measured hourly solar radiation data are available from the 42 LTPP AWS sites, and this information is stored in the offline AWS climate tables. All of the LTPP AWS climate data are located near LTPP SPS test sites. Additional AWSs are located at sites included in the SMP program. However, the LTPP AWS monitoring measurements have been terminated. None of the AWS solar radiation data have ever been compared and/or measured against other data sources, nor has solar radiation data from other data sources been assessed for widespread inclusion in the LTPP program.

The amount of publically available solar radiation data from ground stations has increased over the past 20 years. The NCDC has made available historic solar radiation databases from the 1952 to 1976 period and now has online the updated National Solar Radiation Data Base (NSRDB) for the 1991 through 2010 time period. The updated NSRDB contains hourly solar radiation (including global, direct, and diffuse) and meteorological data for 1,454 stations, up from the 239 stations in the earlier 1961 through 1990 NSRDB. The update includes the conventional time series for NSRDB ground stations as well as a 0.1-degree gridded dataset that contains hourly solar records for 8 years (1998 through 2005) for the United States (except Alaska above 60 degrees latitude) at about 100,000 pixel locations (nominal 10- by 10-km pixel size). The National Renewable Energy Laboratory (formerly the Solar Energy Research Institute) in Golden, CO, also maintains a database of solar radiation data.

Newer satellite-based solar radiation sensors are a potential replacement for ground-based sensors in determining local solar radiation inputs for infrastructure performance models. High-quality solar radiation data are readily available from Geostationary Operational Environmental Satellites (GOES) operated by NOAA's National Environmental Satellite Data and Information Service. Two geostationary satellites, one over the eastern and another over the western United States, provide complete coverage for most of the contiguous United States and much of southern Canada. Data for more northern locations can be obtained from polar orbit satellites by request from NOAA.

Access to these data (http://www.atmos.umd.edu/~srb/gcip/) is an outgrowth of the ongoing activity at the Department of Atmospheric and Oceanic Science, University of Maryland, to develop and validate an operational model for deriving surface and top of the atmosphere shortwave radiative fluxes from GOES in support of the Global Continental International Project activities and regional weather prediction models. Instantaneous, hourly, daily, and monthly mean information on surface downwelling shortwave, top of the atmosphere downwelling and upwelling radiative fluxes, photosynthetically active radiation, cloud amount, and surface skin temperature are provided for an area bounded by 70 to 125 degrees W longitude and 25 to 50 degrees N latitude. Validation results against ground truth are also available. Historical data at a 0.5 degrees (approximately 37.3 mi) spatial resolution are available from 1996 onward. The historical data are currently being reprocessed at a 0.125 degrees (approximately 9.3 mi) spatial resolution; these reprocessed data are currently available for 1996 through 2000.

MERRA

A promising new source of hourly climate data, which became known to the study team in spring 2012, is MERRA. MERRA contains reprocessed atmospheric observations from 1979 to the present using the National Aeronautics and Space Administration (NASA) Goddard Earth Observation System Version 5 (GEOS-5). This represents a merger of physics-based modeling with satellite, airborne, ship, radiosonde, and buoy measurements. More than 4 million observations are assimilated into the MERRA models every 6 h. MERRA can provide a continuous record of hourly values for all inputs to current advanced infrastructure models. The basis for MERRA as well as QC, data availability, evaluation of MERRA data for use in pavement and other infrastructure applications, and benefits of MERRA data are discussed in the following chapters.

CHAPTER 4. MODERN ERA RETROSPECTIVE-ANALYSIS FOR RESEARCH AND APPLICATIONS (MERRA)

The MERRA product from NASA is a new alternative for obtaining high-quality atmospheric and surface weather history data.[44,45] MERRA is a physics-based reanalysis model that combines computed model fields (e.g., atmospheric temperatures) with ground-, ocean-, atmospheric-, and satellite-based observations that are distributed irregularly in space and time. The result is a uniformly gridded dataset of meteorological data derived from a consistent model and analysis system over the entire data history. MERRA improves on earlier generations of reanalysis models such as those developed by NOAA's National Center for Environmental Prediction, the European Centre for Medium-Range Weather Forecasts, and the Japan Meteorological Agency.[46,47,48]

Distribution of MERRA data is funded by NASA's Science Mission Directorate. The data are not copyrighted and are open to all for both commercial and noncommercial uses. NASA uses MERRA to help verify seasonal climate forecasting systems, generate climate data records, serve as input to satellite retrieval algorithms, and provide atmospheric forcings for hydrologic and land surface process studies.[49] In addition, MERRA is regularly evaluated and validated to ensure continuity and consistency because the data product is produced in near real-time.

MERRA data are provided at an hourly temporal resolution and a 0.5-degree by 0.67-degree (latitude/longitude) spatial resolution from 1979 to the present. Figure 7 illustrates graphically the spatial density of MERRA grid points over the continental United States; MERRA spans the entire globe at this spatial resolution. For contrast, figure 8 shows the spatial distribution and density (computed as the number of ASOS stations per MERRA grid pixel) of first-order ASOS ground-based weather stations over the continental United States; the ASOS coverage is limited to the United States. The ASOS OWSs are the primary source of climate data for the MEPDG weather database. The higher spatial resolution and larger geographic scope of the MERRA data are clear. In addition, NASA is currently upgrading MERRA to a 0.62- by 0.62-mi horizontal resolution.

The merger of the GEOS-5 model with observations is based on the Grid-Point Statistical Interpolation (GSI), which is a three-dimensional variational data assimilation analysis algorithm. Prior to assimilation, the available observations undergo a sophisticated QC/quality assurance (QA) procedure. Only observations that pass the QC/QA procedure are used during assimilation. For a given 6-h assimilation window, the GEOS-5 model first predicts the background (predictor) states over which the GSI analysis is computed (figure 9). Next, an incremental analysis update (IAU) procedure is conducted during which the analysis correction is applied to the forecast model gradually over the 6-h assimilation window. In essence, the IAU serves to move the model forecast toward closer agreement with the assimilated observations without introducing abrupt discontinuities or physical inconsistencies into the model dynamics. Once the IAU procedure has completed the given 6-h assimilation window, the model advances forward in time to the next 6-h window. This process is repeated over the course of the more than 30-year observation record. More than 4 million observations (mostly satellite-derived) are typically ingested during a 6-h assimilation cycle. For more details on the GEOS-5 model and the GSI procedure, the reader is referred to Rienecker et al.[44]

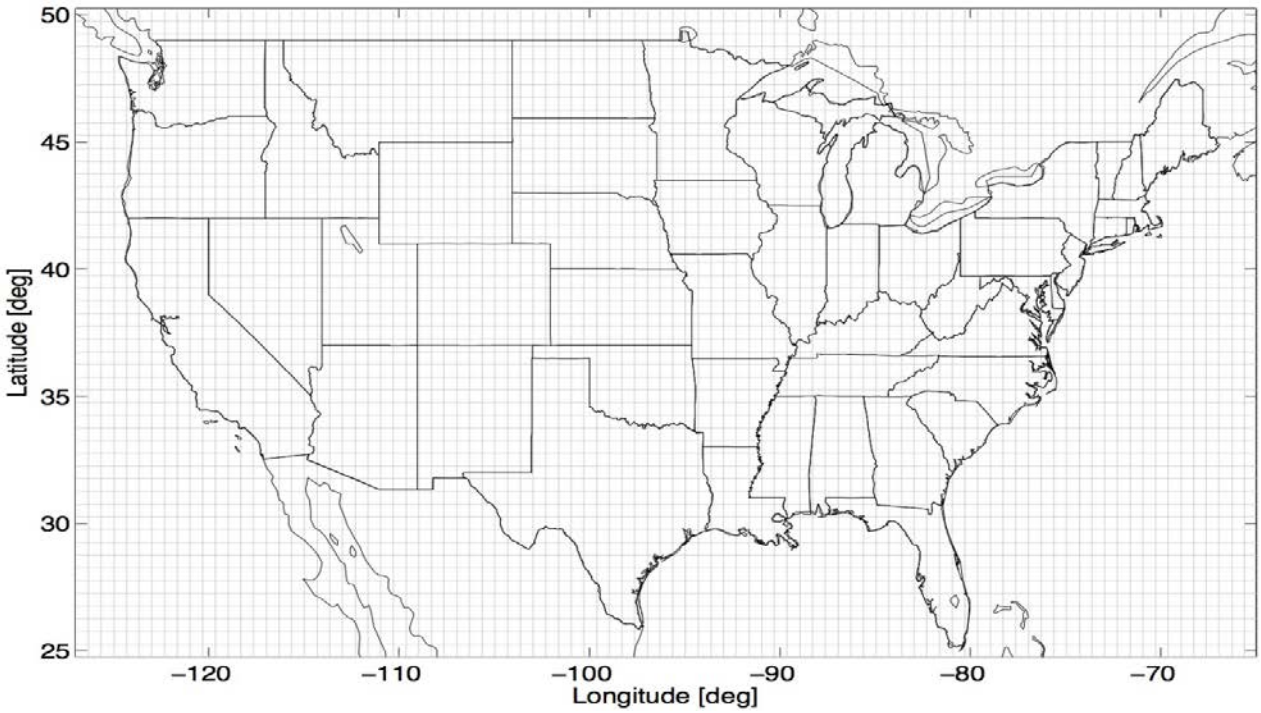

Figure 7. Map. Map of MERRA grid points over the continental United States where each grid point is approximately 31.1 by 37.3 mi at mid-latitudes.

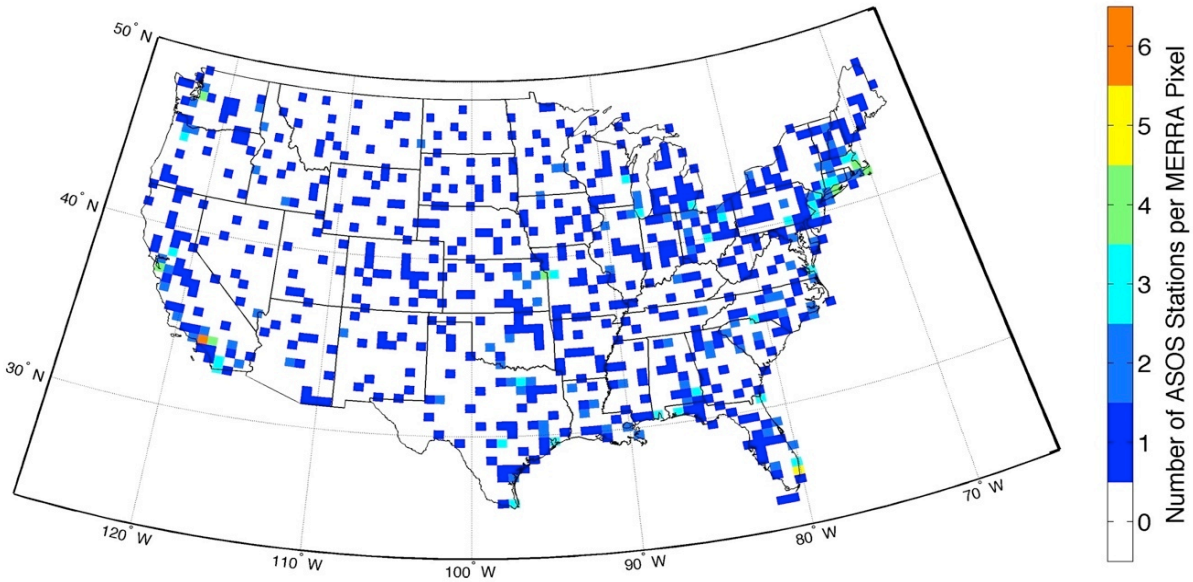

Figure 8. Map. Spatial distribution and density of first-order ASOS stations over the continental United States.

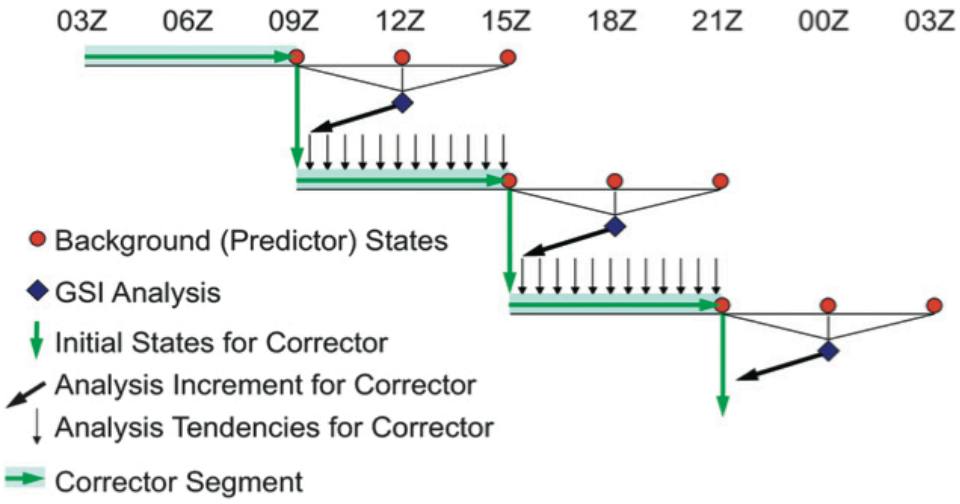

Source: M.M. Rienecker et al.

Figure 9. Illustration. Schematic of the IAU procedure in MERRA (from Rienecker et al.) shown in Greenwich Mean Time.[44]

MERRA is capable of providing all of the weather history inputs required by the MEPDG and other current infrastructure applications. Table 2 contains the MERRA data elements used to develop MEPDG weather history inputs. In addition, MERRA contains additional data elements useful for enhancements of current infrastructure applications and/or for support of future applications. Samples of available data elements are provided in table 3. A complete listing of all MERRA data elements can be found at http://gmao.gsfc.nasa.gov/products/documents/MERRA_File_Specification.pdf.

Table 2. MERRA data elements available to develop MEPDG weather history inputs.[45]

Element	Description	Units
CF	Total cloud fraction	fraction
PPT	Precipitation flux incident upon the ground surface	kg H_2O m^2 s^{-1}
PS	Surface pressure at 2 m above ground surface	Pa
Q	Specific humidity at 2 m above ground surface	kg H_2O kg^{-1} air
Rsw	Shortwave radiation incident upon the ground surface	W m^{-2}
Rtoa	Shortwave radiation incident at the top of atmosphere	W m^{-2}
T	Air temperature at 2 m above ground surface	K
U	Eastward wind at 2 m above ground surface	m s^{-1}
V	Northward wind at 2 m above ground surface	m s^{-1}

Table 3. Examples of other MERRA data elements of potential interest for transportation infrastructure applications.(45)

Element	Description	Units
T	Air temperature at 10-meters above ground surface[1]	K
U	Eastward wind at 10-meters above ground surface[1]	m s^{-1}
V	Northward wind at 10-meters above ground surface[1]	m s^{-1}
PRMC	Total profile soil moisture content	m^3 m^{-3}
RZMC	Root zone soil moisture content	m^3 m^{-3}
SFMC	Top soil layer soil moisture content	m^3 m^{-3}
TSURF	Mean land surface temperature (including snow)	K
TSOIL	Soil temperature in layer (available for 6 soil layers)	K
PRECSNO	Surface snowfall	kg m^{-2} s-1
SNOMAS	Snow mass	kg m^{-2}
SNODP	Snow depth	m
EVPSOIL	Bare soil evaporation	W m^{-2}
EVPTRNS	Transpiration	W m^{-2}
EVPSBLN	Sublimation	W m^{-2}
QINFIL	Soil water infiltration rate	kg m^{-2} s^{-1}
SHLAND	Sensible heat flux from land	W m^{-2}
LHLAND	Latent heat flux from land	W m^{-2}
EVLAND	Evaporation from land	kg m^{-2} s^{-1}
LWLAND	Net downward longwave flux over land	W m^{-2}
SWLAND	Net downward shortwave flux over land	W m^{-2}
EMIS	Surface emissivity	fraction
ALBEDO	Surface albedo	fraction

[1]Also available at approximately 100 m and other elevations.

MERRA is freely available to all research agencies and universities through the NASA Modeling and Assimilation Data and Information Services Center (MDISC) at http://disc.sci.gsfc.nasa.gov/daac-bin/DataHoldings.pl. Subsets of the MERRA data at an hourly resolution as a function of time and space can be requested from MDISC, including specification of the desired data element(s). Once the timeframe, region of the globe, and MERRA data elements of interest are selected, the data files are retrieved by NASA in Hierarchical Data Format (HDF) or Network Common Data Form (NetCDF) format. The HDF and NetCDF supercomputer data formats are the only data formats currently supported by NASA to keep storage of the large dataset sizes tractable. Once NASA retrieves the requested data files, they are posted to a public FTP server for access by the user. A number of computing languages (e.g., C++, FORTRAN, IDL, and MATLAB®) contain HDF and NetCDF libraries that can be employed to open the MERRA data files, extract the relevant locations in space and time, and prepare the data for subsequent use in MEPDG or any other infrastructure application of interest.

CHAPTER 5. EVALUATION OF MERRA FOR USE IN PAVEMENT AND OTHER INFRASTRUCTURE APPLICATIONS

INTRODUCTION

A series of analyses were performed to evaluate the suitability of using MERRA for pavement and other infrastructure applications. Because the MEPDG is the most demanding current application in terms of climate inputs as well as a major focus of many LTPP and other research efforts, the evaluation of MERRA focuses on its suitability for use in predicting pavement performance using the MEPDG. The following three sets of evaluation analyses have been performed:

- A systematic quantitative evaluation of the sensitivity of MEPDG distress predictions to fundamental climate parameters. This evaluation, which has not been done before, is essential for establishing which elements of climate data are most important to pavement infrastructure performance (according to the MEPDG). This provides a context for the subsequent analyses described in this chapter.

- A statistical comparison of climate parameters from MERRA versus ground-based OWS and AWS instruments.

- A quantitative comparison of the pavement performance predicted by MEPDG using MERRA versus ground-based OWS and AWS weather histories.

SENSITIVITY OF MEPDG PERFORMANCE PREDICTIONS TO CLIMATE PARAMETERS

The analysis methodology developed in the AASHTO MEPDG and accompanying software places great emphasis on the influence of climate on pavement performance.[3] Hourly measured values of air temperature, precipitation, wind speed, percentage sunshine, and relative humidity over multiple years are required as climate inputs. Data from more than 800 OWSs across the United States were obtained for this purpose from the NCDC and incorporated into a weather station database that accompanies the MEPDG software.

Current understanding of the sensitivity of MEPDG predicted pavement performance to environmental factors is limited. Zaghloul et al., in a study of the New Jersey Turnpike, found that MEPDG predictions were surprisingly sensitive to the subset of weather stations used to derive the project-specific VWS data.[9] Tighe et al. used the MEPDG to quantify the impacts of climatic change on low traffic flexible pavement performance in southern Canada and found that rutting (asphalt, base, and subbase layers) and both longitudinal and alligator cracking are exacerbated by climate change, with transverse cracking becoming less of a problem.[50] Li et al. made a rudimentary attempt to systematically evaluate the influence of climate on MEPDG predictions by studying the effects of changes in average temperature and monthly precipitation on the performance of a flexible and rigid pavement section for Arkansas conditions.[29] They found that the increase in average temperature increased asphalt rutting significantly and rigid pavement faulting slightly. The increase in average monthly precipitation increased rigid pavement faulting slightly but had a nearly negligible effect on flexible pavement rutting.

Systematic sensitivity studies of flexible and rigid pavement performance have found that material environmental properties (e.g., thermal conductivity, hydraulic conductivity) generally have only a small influence on predicted performance; the exception is the high sensitivity of nearly all predicted performance to surface shortwave absorptivity. (See references 51 through 54.)

The objective of this evaluation was to quantify systematically the sensitivity of MEPDG pavement performance predictions to specific characteristics of the climate inputs. The pavement performance measures considered included longitudinal cracking, alligator cracking, asphalt concrete (AC) rutting, total rutting, and international roughness index (IRI) for flexible pavements and faulting, slab cracking, and IRI for rigid jointed plain concrete pavements (JPCP). The characteristics of the climate inputs examined in the study were the average annual temperature, average annual temperature range, average daily temperature range, wind speed, percent sunshine (or cloud cover), precipitation, and relative humidity. Pavement scenarios were examined for three generic climate conditions (cold-wet, hot-dry, and temperate) and three traffic levels (low, medium, and high) to assess sensitivity over a broad domain. More than 300 MEPDG (v1.100) runs were conducted for this study. The procedures and the results of the sensitivity analyses described in this study provide guidance on the conditions under which the various climate properties significantly influence pavement performance.

Sensitivity Analysis Methodology

Formalized rigorous approaches for sensitivity analyses of complex models have evolved substantially in recent years. Recent surveys of many of the sensitivity analysis techniques can be found in Cacuci, Saltelli et al.,, and elsewhere.[55,56] Most sensitivity studies of the MEPDG to date have focused largely on confirmation that the model is a realistic simulation of pavement system performance—i.e., to verify that the model is fundamentally sound. Most of these past studies have employed a “one at a time” (OAT) methodology in which one or more baseline cases are defined, and each input (e.g., average annual temperature) is then varied individually for each case to evaluate its effect on the output (e.g., quantity of fatigue cracking). Only the sensitivities around the reference input values for the baseline cases are evaluated—i.e., the evaluation is only for very small regions of the overall solution space. This provides only a “local” as opposed to a “global” sensitivity evaluation. Although global sensitivity analyses are more appropriate for complex nonlinear models with many inputs, local OAT evaluations are suitable for exploratory analyses and/or for simpler models having relatively few input parameters.[52] The local OAT sensitivity analysis approach has been adopted for the present exploratory study.

Sensitivity Metrics

A wide variety of metrics have been used to quantify sensitivity of model outputs to model inputs. These include coefficients from multivariate linear regressions, correlation coefficients (Pearson linear and Spearman rank), and a variety of partial derivative formulations.[52]

Although no individual metric is “perfect,” the best for interpreting the OAT analysis results in this study was a “design limit” normalized sensitivity index S_{jk}^{DL} as shown in figure 10.

$$S_{jk}^{DL}\left(\frac{\Delta Y_j}{DL_j}\right)\Big/\left(\frac{\Delta X_k}{X_k}\right)$$

Figure 10. Equation. Design limit normalized sensitivity index.

Where:

X_k = baseline value of design input *k*.
ΔX_k = change in design input *k* about the baseline.
ΔY_j = change in predicted distress *j* corresponding to ΔX_k.
DL_j = design limit for distress *j*.

This design limit normalized sensitivity index was notated more simply as *NSI*. The *NSI* always used the design limit as the normalizing factor for the predicted distress. *NSI* can be interpreted as the percentage change in predicted distress relative to the design limit caused by a given percentage change in the design input. The sensitivity of NSI follows: Hypersensitive, $NSI > 5$; Very Sensitive, $1 < NSI < 5$; Sensitive, $0.1 < NSI < 1$; and Non-Sensitive, $NSI < 0.1$. For example, consider total rutting as the predicted distress with a design limit of 0.75 inches. An *NSI* of -0.25 for the sensitivity of total rutting to average wind speed implies that a 10-percent reduction in average wind speed will increase total rutting ΔY_j by $NSI*(\Delta X_k/X_k)*DL_j$ = -0.25*-0.1*0.75 = 0.01875 inches.

Base Cases

The sensitivity analysis was conducted for a wide range of the model inputs and outputs. However, not all the combinations of model input values are physically plausible. For example, a thin asphalt layer on a thin granular base layer subjected to high traffic volume does not represent a realistic scenario likely to be encountered in practice. Therefore, a set of base cases were developed to cover the ranges of commonly encountered climatic conditions and traffic levels with associated surface layer and base layer thickness. A total of nine base cases encompassing three climatic zones, and three traffic levels were developed for each of the flexible pavement scenarios and the rigid pavement scenarios.

The three climatic zones used for base cases were cold-wet, hot-dry, and temperate. Table 4 summarizes the specific locations and the weather stations used to generate the reference climate files for each of the three climatic zones.

Table 4. Climate categories for base cases.

Climate Category	Location	Weather Station
Cold-Wet	Portland, ME	PORTLAND INTL JETPORT ARPT
Hot-Dry	Phoenix, AZ	PHOENIX SKY HARBOR INTL AP
Temperate	Los Angeles, CA	LOS ANGELES INTL AIRPORT

The three traffic levels analyzed are summarized in table 5. The ranges of average annual daily truck traffic (AADTT) values span the low (< 5,000), medium (5,000–10,000), and high (> 15,000) truck volume categories in Alam et al.[57] To put these traffic volumes into a more familiar context, estimates of the approximate numbers of equivalent single axle loads are also

included in table 5. The surface layer and base layer thicknesses for each traffic category are also listed. Higher traffic levels require correspondingly thicker surface and base layers.

Table 5. Traffic and pavement layer thickness for base cases.

Traffic Properties	Traffic Level		
	Low Traffic	**Medium Traffic**	**High Traffic**
Nominal AADTT[1]	1,000	7,500	25,000
Flexible ESALs (millions)[2]	1.79	9.82	29.77
AC Thickness	6.5	10	12.5
Base Thickness	6	7	9
Rigid ESALs (millions)[2]	4.69	25.78	78.13
JPCP Thickness	8	10	12
Base Thickness	4	6	8

[1]Based on MEPDG Interstate Highway TTC4 Level 3 default vehicle distribution.
[2]Based on design life of 15 years for flexible pavements/25 years for rigid pavements.
AADTT = Average Annual Daily Truck Traffic
ESAL = Equivalent Single-Axle Load
AC = Asphalt Concrete
JPCP = Jointed Plain Concrete Pavement

Table 6 and table 7 summarize the values of the major pavement design inputs required by the MEPDG. All analyses were performed using v1.100 of the public domain MEPDG software. Note that reliability was set at 50 percent, which means the mean predictions of pavement distresses from the MEPDG were directly used without any adjustments.

Table 6. Pavement design properties for base cases.

Input Parameter	Value
Design Life	15 years for flexible pavements/25 years for rigid pavements
Construction Month	August 2006
Reliability	50 percent for all distresses
AADTT Category	Principal Arterials—Interstate and Defense Rout
TTC	4
Number of Lanes in Design Direction	2 for low traffic/3 for medium and high traffic
Truck Direction Factor	50
Truck Lane Factor	75 for low traffic/55 for medium traffic/50 for high traffic
Default Growth Rate	No growth
First Layer Material Type	HMA for flexible pavements/ PCC for flexible pavements
Second Layer Material Type	Granular Base
Subgrade Material Type	Soil
Base Resilient Modulus	25,000
Base Poisson's Ratio	0.35
Subgrade Resilient Modulus	15,000
Subgrade Poisson's Ratio	0.35

AADTT = Average Annual Daily Truck Traffic
HMA = Hot Mix Asphalt
PCC = Portland Cement Concrete
TCC = Truck Traffic Classification

Table 7. Surface layer properties for base cases.

Material	Properties	Baseline Value
Hot Mix Asphalt (HMA)	Surface Shortwave Absorption	0.85
	Endurance Limit	100 με
	HMA Unit Weight	149.9 lb/ft^3
	HMA Poisson's Ratio	0.35
	HMA Thermal Conductivity	0.67 Btu/(ft)(fr)(ºF)
	HMA Heat Capacity	0.23 Btu/(lb)(ºF)
	Delta in HMA Sigmoidal Curve	2.83
	Alpha in HMA Sigmoidal Curve	3.90
	Effective Binder Content in HMA	10.1 percent
	Air Void in HMA	6.5 percent
	Tensile Strength at 14 ˚F	500 psi
	Aggregate Coefficient of Contraction in HMA	5E-6 (1/ºF)
	Design Lane Width	12 ft
Portland Cement Concrete (PCC)	Joint Spacing	15 ft
	Dowel Diameter	Various
	Edge Support—LTE	5 (no support)
	Edge Support—Widened Slab	12 (no support)
	Erodibility Index	3
	Surface Shortwave Absorption	0.85
	PCC Unit Weight	150 lb/ft^3
	PCC Poisson Ratio	0.15
	PCC Coefficient of Thermal Expansion	5.0E-6 1/ºF
	PCC Thermal Conductivity	1.25 Btu/(ft)(fr)(ºF)
	PCC Cement Content	500 lb/yd^3
	PCC W/C	Various
	PCC 7-Day MOR	572 psi
	PCC 7-Day E	3,650,255 psi

LTE = Load Transfer Efficiency
W/C = Water to Cement
MOR = Modulus of Rupture
E = Modulus of Elasticity

Weather Data Inputs

A total of three weather stations in the MEPDG were selected to represent the three different climatic zones. Details for the selected weather stations are summarized in table 8. All of the weather stations have more than 9 years of continuous climate data.

The EICM in the MEPDG requires five climate elements at hourly intervals: air temperature, percent sunshine, wind speed, precipitation, and relative humidity. These hourly values are directly adjusted in the climate input files in the sensitivity analyses. Seven climate characteristics were considered in the sensitivity analyses: average annual temperature, average annual temperature range, average daily temperature range, percent sunshine, wind speed, precipitation, and relative humidity. Hourly percent sunshine, wind speed, precipitation, and relative humidity values were varied by a fixed percentage across the entire weather history. Changes in average annual air temperature were implemented by shifting each hourly temperature value by a prescribed offset across the entire weather history. In addition to average air temperature, the amplitudes of the daily and annual temperature variations can also influence pavement performance. Consequently, the average daily and annual temperature ranges were

included in the sensitivity analyses. For each day/year, the average temperature values were first calculated. Then a fixed small percentage variation was applied to the difference between each hourly value and the average value for that day/year. In other words, the daily/annual air temperature variations were extended or shrunk by a defined percentage relative to the center of the variation. Table 9 summarizes the manipulations of climate inputs used in the sensitivity analyses.

Table 8. Details of weather stations in MEPDG.

Weather Station	Portland International Jetport Airport	Phoenix Sky Harbor International Airport	Los Angeles International Airport
Climatic Zone	Cold-Wet	Hot-Dry	Temperate
Associated .hcd file	14764.hcd	23183.hcd	23174.hcd
Data starts at	19960701	19960701	19970301
Data ends at	20060228	20060208	20060228
Location	Portland, ME	Phoenix, AZ	Los Angeles, CA
Elevation (ft)	72	1,106	326
Latitude	43.38	33.26	33.56
Longitude	70.18	111.59	118.25
Months available data	116	116	108

Table 9. Climate property inputs and treatments.

Climate Property Input	Treatments
Average Annual Temperature	5 percent of the average temperature over the entire weather history is added to/subtracted from each hourly value
Average Annual Temperature Range	The difference between each hourly value and the annual average value is varied by ±5 percent
Average Daily Temperature Range	The difference between each hourly value and the daily average value is varied by ±10 percent
Percent Sunshine	Each hourly value is varied by ±5 percent
Wind Speed	Each hourly value is varied by ±5 percent
Precipitation	Each hourly value is varied by ±5 percent
Relative Humidity	Each hourly value is varied by ±5 percent

Because there is no direct way to vary these climate property inputs in the MEPDG, the systematic changes in the climate characteristics were incorporated by modifying the MEPDG climate data input file for a given weather station using the following procedures:

- The .hcd file representing a particular weather station of interest was first found from the hcd folder in MEPDG installation directory (e.g., 14764.hcd for the PORTLAND INTL JETPORT ARPT for the Cold-Wet condition).

- All the values contained in the .hcd file were loaded into a MATLAB® calculation script.

- Modifications to the numbers were processed according to table 9 (e.g., all the hourly precipitation values are increased by 5 percent).

- The modified values were exported into another .hcd file with the same format as the original file (e.g., 14764_Prep_P.hcd with the same format as 14764.hcd).

- The filename of the newly created file was changed to the original filename so MEDPG would read the file and provide pavement performance predictions based on the modified condition (e.g., change 14764_Prep_P.hcd to 14764.hcd and let the MEPDG read it as PORTLAND INTL JETPORT ARPT to get pavement performance prediction for the climate condition in which hourly precipitation values have been increased by 5 percent).

Results and Interpretation

The design limit normalized sensitivity index values for each distress and climate parameter combination as computed from the OAT analysis results are shown in figure 11 for the flexible pavement cases. The following abbreviations are used because of space limitations: longitudinal cracking (LC), alligator cracking (AC), AC rutting (AR), TR total rutting (TR), and international roughness index (IRI). The results are based on three climatic zones and three traffic levels. Each column of subplots represents one climatic factor of interest, e.g., precipitation, and each row represents one traffic level. Note that relative humidity is not included in these plots, because it is used neither in the EICM nor in the distress models for flexible pavements. The different climate zones are represented by the different bars in each subplot. For example, the highest grey bar in the subplot in row 3 and column 5 means that the NSI of AC rutting to average annual temperature is slightly greater than 5 (hypersensitive) for the hot-dry climatic zone and high traffic condition.

Key observations from the flexible pavement sensitivity analysis results were as follows:

- Pavement performance is most sensitive to average annual temperature and average annual temperature range. This was most pronounced for AR but also significant for LC and TR. The normalized sensitivity index (NSI) values were all positive, which means that increasing annual average temperature and annual temperature range increase pavement distress. This observation, which matches engineering intuition, may have relevance to the evaluation of potential effects of climate change on pavement infrastructure.

- Percent sunshine and wind speed were consistently the next most sensitive climate parameters. As for temperature, this was most pronounced for AR but also significant for LC and TR. Percent sunshine affects the amount of upper atmosphere solar radiation that reaches the pavement surface and is available for heating the asphalt layer; AR sensibly increases as percent sunshine increases (positive NSI value). Wind speed had negative NSI values for all distresses, which means that pavement distresses decreased as wind speed increased; this was consistent with the inverse relationship between wind speed and pavement temperature.

- Flexible pavement performance had only a low sensitivity to average daily temperature range.

- The sensitivity of performance to precipitation was negligibly small. This was expected because the EICM does not include the effects of surface precipitation and infiltration in its modeling of temperature and moisture within the pavement.

- With regard to overall climate zone, the highest sensitivity values were generally found for the hot-dry climate condition.

The OAT sensitivity analysis results for JPCP rigid pavements are shown in figure 12. Again, these results are based on three climatic zones and three traffic levels. Similar to figure 11, each column of subplots represents one climatic factor of interest, each row of subplots represents one traffic level, and the bars represent the different climate zones. The rigid pavement distress abbreviations are F for faulting, SC for slab cracking, and IRI for international roughness index.

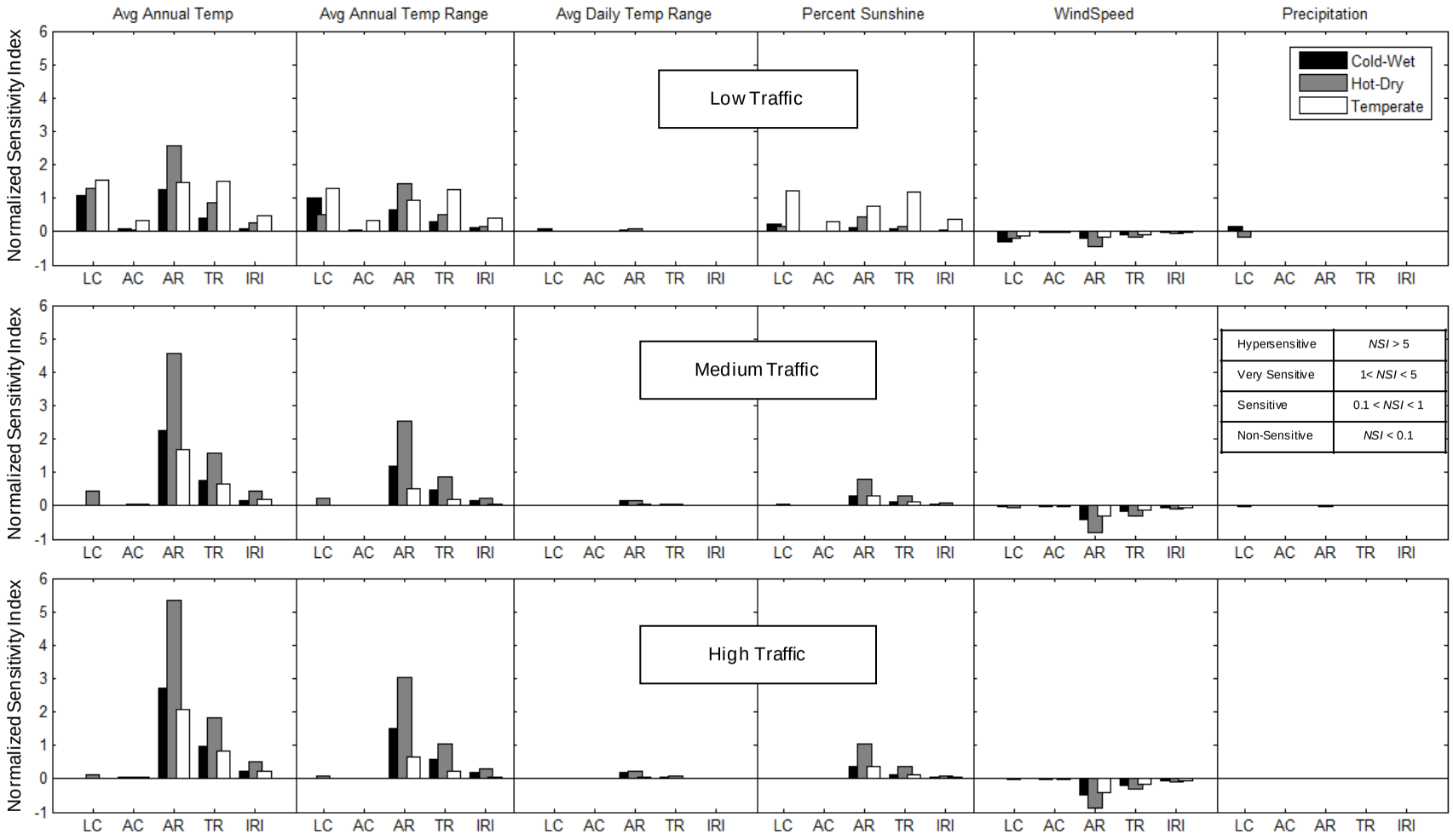

Figure 11. Graph. Sensitivity analysis results for flexible pavements.

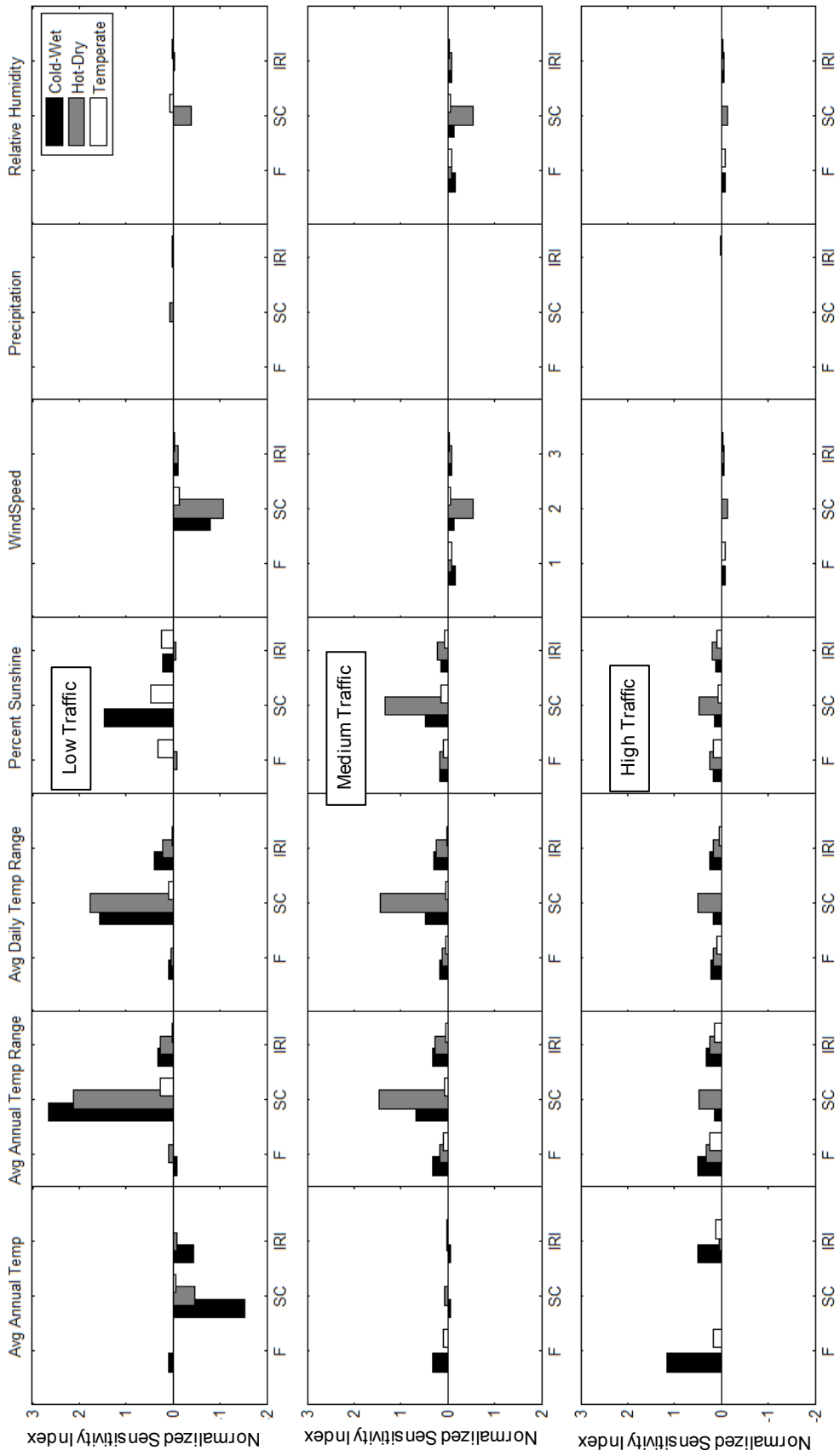

Figure 12. Graph. Sensitivity analysis results for rigid pavements.

Key observations from the JPCP rigid pavement analyses are as follows:

- Average annual and daily temperature ranges exhibited the highest sensitivity values, followed closely by percent sunshine. The NSI values for these climate parameters were all positive, meaning that increases in annual or daily temperature ranges or percent sunshine cause increased F, SC, and IRI. These trends were sensible, especially for average daily temperature range because this directly affects the amount of diurnal thermal curling.

- The sensitivities of the rigid pavement distresses to annual average temperature were moderately large but inconsistent. As design traffic and slab thickness increased, the NSI values increased for F, become decreasingly negative for SC, and changed sign for IRI. Annual average temperature thus had mixed effects on rigid pavements depending on the thickness of the slabs.

- The rigid pavement distresses were only moderately sensitive to wind speed and relative humidity. The NSI values for both climate characteristics were negative for all distresses, meaning that higher wind speed or relative humidity produced less pavement distress.

- The sensitivity of rigid pavement performance to precipitation was negligibly small. Again, this was expected given that the EICM does not include the effects of surface precipitation and infiltration in its modeling of temperature and moisture within the pavement.

- Overall, slab cracking was the JPCP distress that was consistently most sensitive to climate effects.

- The NSI values tended to be larger for thinner slabs. This implies that heavily trafficked rigid pavements having thicker slabs were relatively less sensitive to climate effects.

- In general, the NSI values tended to be smaller in the temperate climate zone.

Sensitivity Analysis Conclusions

The sensitivity of MEPDG pavement performance predictions to key climate characteristics was systematically and quantitatively evaluated. Three climate zones and three traffic levels were considered to assess sensitivity over an extended MEPDG problem domain. Sensitivity of predicted pavement distress to change in climate characteristic was quantified in terms of NSI that relates the change in distress relative to its design limit to the percentage change in the climate characteristic from its baseline value. Key conclusions from the results include the following:

- Average annual temperature and average annual temperature range were the most sensitive climate characteristics for both flexible and rigid pavements. Average daily temperature range also had a very significant influence on JPCP slab cracking but

almost no effect on flexible pavement performance. The sensitivity of JPCP slab cracking to percent sunshine was also very high.

- Percent sunshine and wind speed were moderately important climate characteristics for both flexible and rigid pavements. Percent sunshine affects the amount of upper atmosphere solar radiation that reaches the pavement surface and is available for heating. Wind speed had negative NSI values for all distresses, which means that pavement distresses decreased as wind speed increased; this was consistent with the inverse relationship between wind speed and pavement temperature.

- Precipitation had negligible influence on either flexible or rigid pavement performance. This was sensible given that the EICM does not include the effects of surface precipitation and infiltration in its modeling of temperature and moisture within the pavement.

- Asphalt rutting, total rutting, and longitudinal cracking were the flexible pavement distresses that were most sensitive to climate characteristics.

- Slab cracking was the rigid pavement distress most sensitive to climate characteristics.

STATISTICAL COMPARISON OF MERRA VERSUS AWS/OWS WEATHER DATA

Hourly weather histories were obtained from three different data sources: MEDPG OWSs, LTPP AWSs, and MERRA. Statistical evaluations of the MEPDG-related climate inputs from these three sources provided an initial assessment of their similarities and differences and helped identify any potential data issues. The MEPDG hourly climate inputs are air temperature, wind speed, percent sunshine, relative humidity, and precipitation.

MEPDG OWS

The hourly weather data in the MEPDG OWS files are based on first-order ASOS climate stations described previously in chapter 3. Most of the MEPDG climate data are obtained from the Unedited Local Climatological Data (ULCD) product, which covers the period of July 1996 through December 2004. Only minimal quality checks have been performed by the NCDC for most of these historical data. As described later, additional quality checking of the MEDPG OWS data was performed as part of this study. Beginning in January 2005, data are available from the Quality Controlled Local Climatological Data (QCLCD) product (http://www.ncdc.noaa.gov/land-based-insitu-station-data/quality-controlled-local-climatological-data-qclcd).

The MEPDG requires a minimum of 24 months of actual weather station data; for many of the 800 OWSs in the MEPDG database, there is approximately 10 years of data. Pavement performance prediction periods longer than the weather time series length are accommodated by "recycling" the weather history—i.e., once the end of the weather time series is reached, it is repeated again from the start.

LTPP AWSs

LTPP collected hourly weather data from AWSs at SPS sites (1994 through 2008) and SMP sites (1993 through 2004) across the United States. Most AWSs have hourly weather series longer than 10 years. Significant quality checks are applied to the AWS data before they are uploaded into the LTPP database. However, as described later, data gaps and time misalignments are not rare, and these issues can create problems when trying to use AWS data as weather inputs to the MEDPG.

One weather input required by the MEPDG, percent sunshine, is not collected by the LTPP AWS; instead, the actual incoming shortwave solar radiation is measured and recorded. Although solar radiation is more directly relevant to daytime pavement temperature modeling than percent sunshine, estimation of net longwave radiation fluxes requires percent sunshine information (or percent cloudiness at night, where percent cloudiness is the complement of percent sunshine). To address this data limitation, synthetic percent sunshine data were generated by using the shortwave radiation regression equation incorporated in the MEPDG as shown in figure 13.[58]

$$Q_i = R * \left[A + B_{100}^{S_c}\right]$$

Figure 13. Equation. Shortwave radiation regression equation.

Where:

Q_i = incoming shortwave radiation received at ground level.

R^* = shortwave radiation incident on a horizontal surface at the top of the atmosphere; this depends on the latitude of the site and the seasonally varying solar declination.

A, B = empirical constants that account for diffuse scattering and adsorption by the atmosphere; the values of A and B incorporated in the MEPDG, which are based on data for the upper Midwest and Alaska, equal 0.202 and 0.539, respectively.[58]

S_c = average percent sunshine.

The Q_i values from the LTPP AWS data and the R^* values provided by MERRA can be used in the equation in figure 13 to solve for S_c. The average percent cloudiness at night is assumed equal to the average percent cloudiness during the day, computed as $100 - S_c$.

Note that R^* could also be estimated using the algorithms and data incorporated in the EICM. These estimates are generally close to the measured values from MERRA; this is discussed further later.

MERRA

The MERRA data were obtained electronically from the servers at NASA. The hourly MERRA data are provided at 0.5 degrees (latitude) by 0.67 degrees (longitude) horizontal spatial grid point resolution (approximately 31.1 by 37.3 mi at mid-latitudes) and at 72 atmospheric

elevations, including the ground surface. In this study, MERRA data were obtained from the surface grid point closest horizontally to the corresponding AWS or OWS location. The raw MERRA data were used to define the hourly temperature, wind speed, percent sunshine, precipitation, and relative humidity values. If there is a difference between MERRA grid point elevation and the target ground-based meteorological station, the MERRA air temperature is adjusted using the adiabatic lapse rate, defined as the rate of temperature change with respect to elevation. If the weather station elevation is greater than the MERRA elevation, the lapse rate is assumed to equal -8.0 °C/km—i.e., the MERRA temperature values are adjusted downward. Conversely, if the weather station elevation is lower than the MERRA elevation, the ambient lapse rate is assumed to equal 6.5 °C/km—i.e., the MERRA temperature values are adjusted upward.[59] The difference between the two lapse rates accounts for the possibility of condensation during adiabatic cooling with increasing elevation. Adiabatic air temperature adjustments were typically small (less than 33.8 °F) because the majority of locations used in this study had elevation differences smaller than 328 ft. However, a few study locations in complex terrain contained elevations differences upwards of 1,640 ft, which can result in temperature adjustments as large as 39.2 °F.

Data Quality Checks

All data were subjected to extensive quality checks prior to performing the comparison analyses.

OWS From MEDPG Database

Data quality checks for the MEPDG OWS weather files included the following:

1. Gaps in the time history—i.e., missing hourly data records.
2. Missing data values for any record.
3. Incorrect data formats—e.g., non-numerical "*" to designate missing data.
4. Physically irrational data values—e.g., negative wind speed, negative precipitation, percent sunshine less than 0 or greater than 100, relative humidity less than 0 or greater than 100.
5. Inconsistent temperatures, defined arbitrarily as adjacent hourly temperature values that differed by more than 50 °F.
6. Inadequate duration, defined as less than 8 years of continuous and complete weather data.

Any OWS file that failed any of these data quality checks was eliminated from further consideration. All of the 851 OWS weather files in the MEPDG database were checked, and only 21 stations passed all quality checks. Figure 14 summarizes the distribution of data quality errors in the MEPDG OWS files.

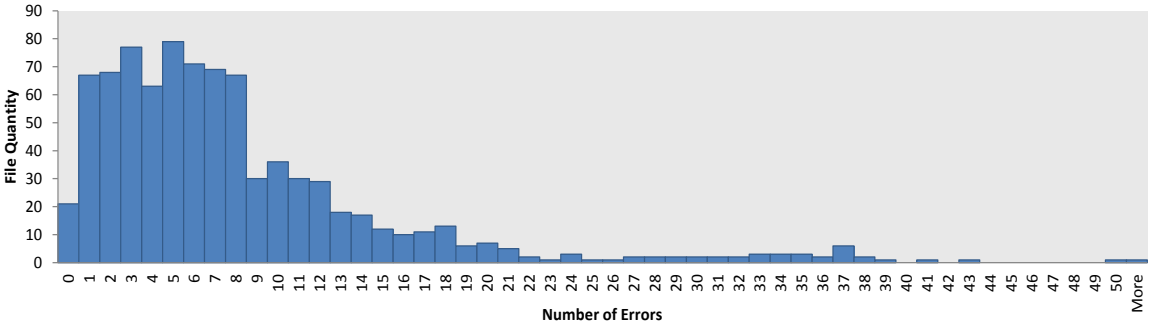

Figure 14. Graph. Data quality error distribution for OWS climate files in MEPDG database.

AWS From LTPP Database

The weather data from the LTPP AWSs are time-referenced using the local time at each site. All of the AWS weather files had problems accommodating the change to/from daylight savings time (DST) properly. When DST starts each year and the local time jumps forward from 2:00 a.m. to 3:00 a.m., no 2:00 a.m. data are stored in the database. When DST ends each year and the local time jumps backward from 2:00 a.m. to 1:00 a.m., there should be a duplicate 1:00 a.m. weather record. However, because the date and time fields in the LTPP database are key fields that prohibit duplicate values, only one of the 1:00 a.m. data records can be stored. This was corrected by shifting all DST records back to standard time and inserting the missing data values at the end of DST by interpolating adjacent records.

In addition to the DST issues, time gaps ranging from several hours to several days were found in many AWS weather files. These may be the result of equipment malfunctions or routine maintenance. Corrections were applied where possible. The time period for the analyses was selected to minimize the number of record gaps. One AWS site had to be dropped from consideration because of excessive record gaps.

MERRA Data

No quality-related issues were found in the MERRA data when the OWS and AWS quality checks were applied.

Weather Sites for the Study

A total of 12 sites were selected for the study after all quality checks and possible corrections to weather files were applied. Figure 15 shows the site locations. Table 10 summarizes the coordinates and other identifying information for each station. The stations beginning with “M” are OWSs from the MEPDG software. All other stations are AWSs from the LTPP database.

These stations spanned a range of topographical conditions. For example, sites 300800, 490800, and 040200 were located in topographical challenging mountainous locations while sites M94982, 530200, and M93817 were in more benign flat topography far from major water bodies.

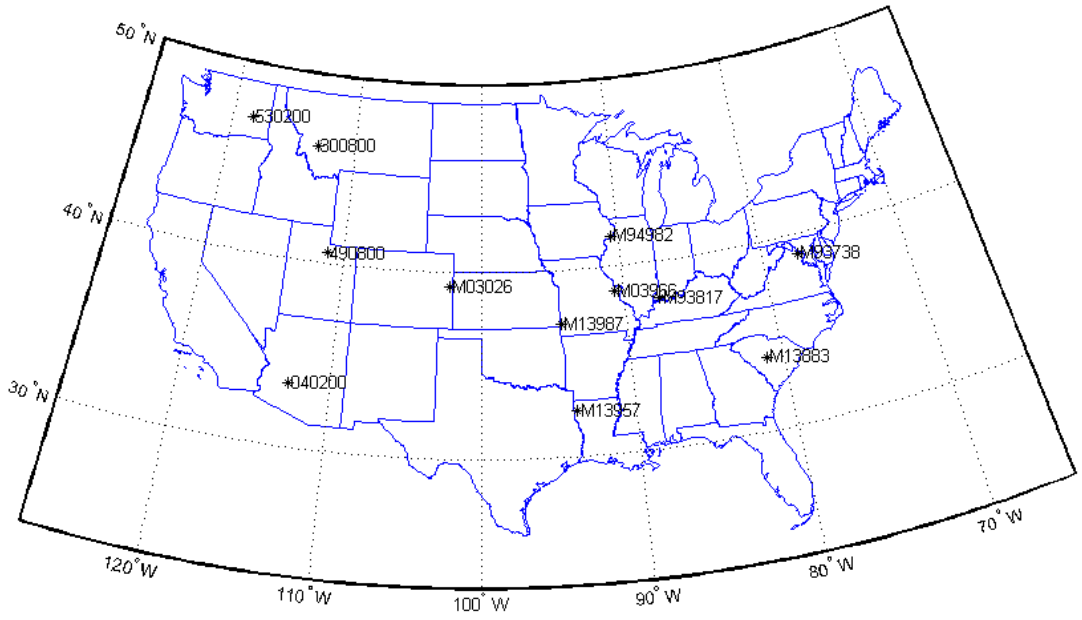

Figure 15. Map. Locations of ground-based weather stations investigated in this study.

Statistical Comparisons

Hourly weather histories for congruent time periods were selected from MERRA and the AWS and/or OWS at each site. Two sets of MEPDG runs were then performed for each site, one using the weather history from MERRA and the other using either the AWS or OWS data for the site. Each set of analyses contained one flexible and one rigid pavement scenario. The MEPDG predicted results at the end of design life (20 years for flexible pavements and 25 years for rigid pavements) were recorded and compared. Details of the MEPDG analyses are presented later. The overall agreement between the predicted MEDPG distresses using the MERRA versus AWS/OWS data was categorized as good, fair, or poor. The sites in each category were as follows:

- Good: AWS 530200; OWS M13987, M93817, M94982.
- Fair: AWS 040200, 300800; OWS M03026, M93738.
- Poor: AWS 490800; OWS M03966, M13883, M13957.

Table 10. Details of ground-based weather stations.

Site ID	Latitude	Longitude	Elevation (ft)	Weather Sources	Ground-Based Weather Station Location
M93738	38.95	-77.45	312	OWS, MERRA	DULLES ITL AIRPORT, VA
040200	33.43	-112.70	1096	AWS, MERRA	BUCKEYE MUNICIPAL AIRPORT, AZ
300800	46.14	-112.89	4006	AWS, MERRA	near ANACONDA, MT
490800	40.56	-111.13	6486	AWS, MERRA	near WOODLAND, UT
530200	47.12	-118.38	1811	AWS, MERRA	near RITZVILLE, WA
M03026	39.23	-102.28	4199	OWS, MERRA	KIT CARSON COUNTY AIRPORT, CO
M03966	38.67	-90.67	492	OWS, MERRA	SPIRIT OF ST LOUIS AIRPORT, MO
M13883	33.93	-81.12	243	OWS, MERRA	COLUMBIA METROPOLITAN ARPT, SC
M13957	32.45	-93.82	276	OWS, MERRA	SHREVEPORT REGIONAL ARPT, LA
M13987	37.15	-94.50	984	OWS, MERRA	JOPLIN REGIONAL AIRPORT, MO
M93817	38.03	-87.53	420	OWS, MERRA	EVANSVILLE REGIONAL ARPT, IN
M94982	41.62	-90.58	751	OWS, MERRA	DAVENPORT MUNICIPAL AIRPT, IA

Statistical analyses of hourly air temperature, wind speed, percent sunshine, precipitation, and relative humidity were performed for each of the weather history datasets. Example frequency distributions and comparisons of means and standard deviations are given in figure 16 through figure 25 and figure 26 through figure 35 for the respective sites having good (Evansville, IN, M93817) and poor (Shreveport, LA, M13957) agreement in MEPDG distresses using the different weather data time series. The differences in the weather statistics between these two sites were generally small except for wind speed and percent sunshine. The differences in MEPDG predicted distresses using MERRA versus OWS weather histories were most probably the consequence of the differences in the wind speed and percent sunshine in the two datasets. Examination of the similar figures at the other 10 sites confirms that the agreement between MERRA and AWS/OWS weather statistics is consistently quite close for temperature, precipitation, and relative humidity, and relatively larger for wind speed and percent sunshine.

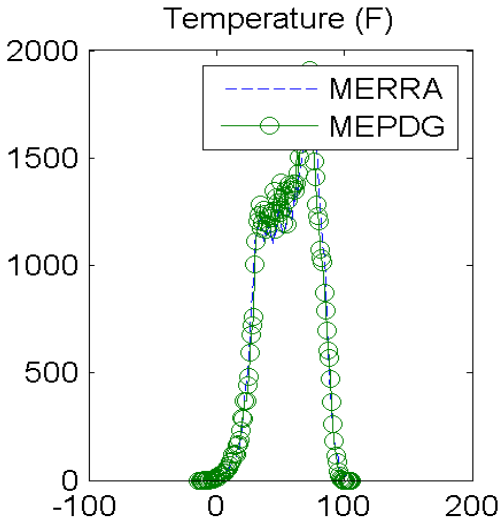

Figure 16. Graph. Site M93817 (Evansville, IN) with good agreement in MEPDG predicted distresses: distributions of hourly temperature.

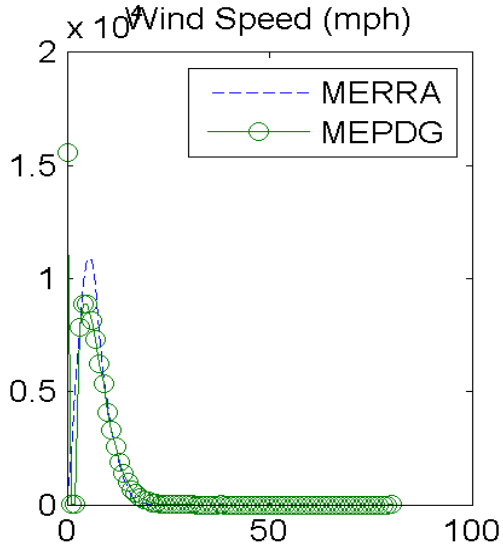

Figure 17. Graph. Site M93817 (Evansville, IN) with good agreement in MEPDG predicted distresses: distributions of hourly wind speeds.

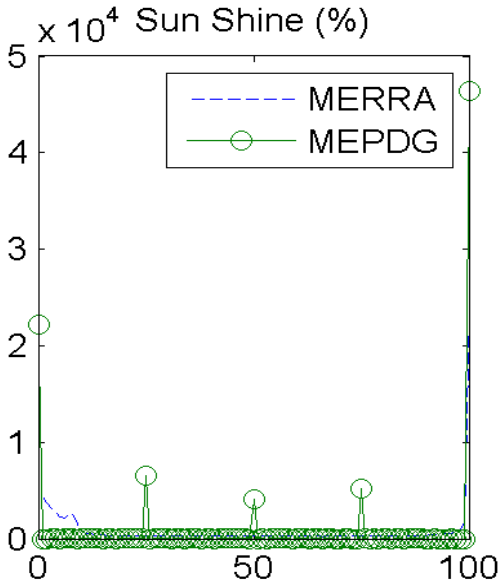

Figure 18. Graph. Site M93817 (Evansville, IN) with good agreement in MEPDG predicted distresses: distributions of hourly percent sunshine values.

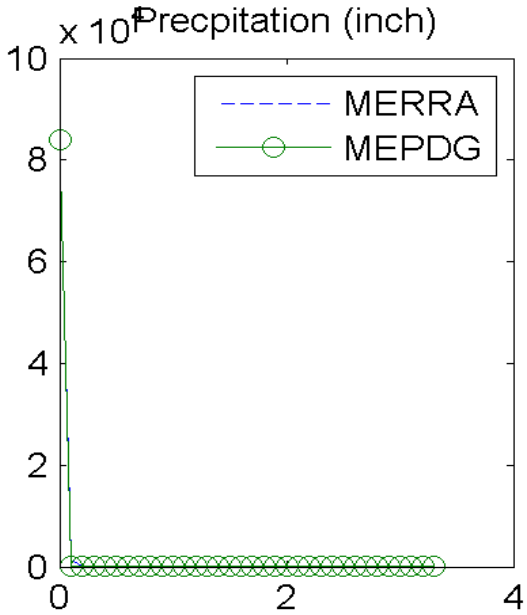

Figure 19. Graph. Site M93817 (Evansville, IN) with good agreement in MEPDG predicted distresses: distributions of hourly precipitation.

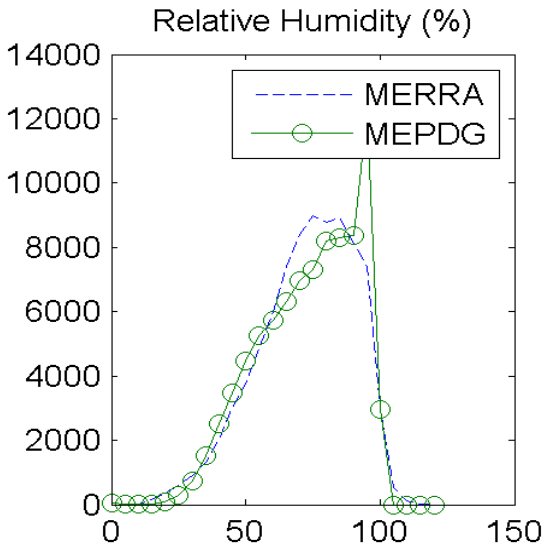

Figure 20. Graph. Site M93817 (Evansville, IN) with good agreement in MEPDG predicted distresses: distributions of hourly relative humidity values.

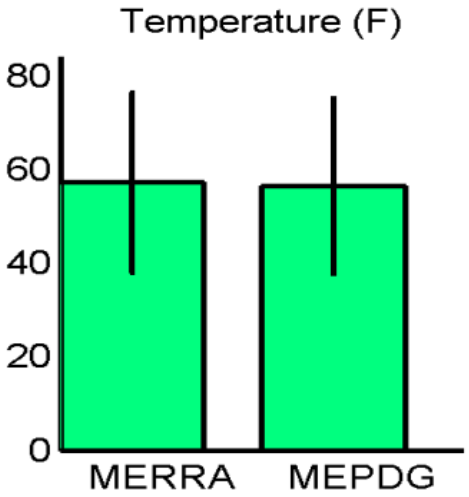

Figure 21. Graph. Site M93817 (Evansville, IN) with good agreement in MEPDG predicted distresses: hourly temperature means and standard deviations.

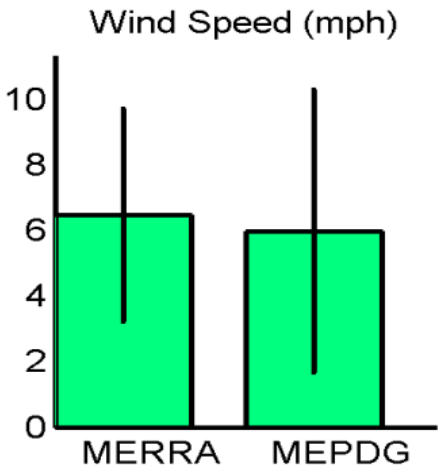

Figure 22. Graph. Site M93817 (Evansville, IN) with good agreement in MEPDG predicted distresses: hourly wind speed means and standard deviations.

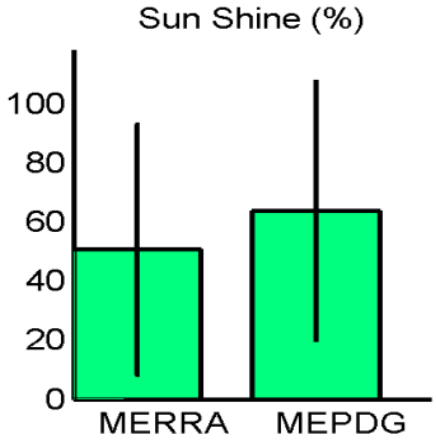

Figure 23. Graph. Site M93817 (Evansville, IN) with good agreement in MEPDG predicted distresses: hourly percent sunshine means and standard deviations.

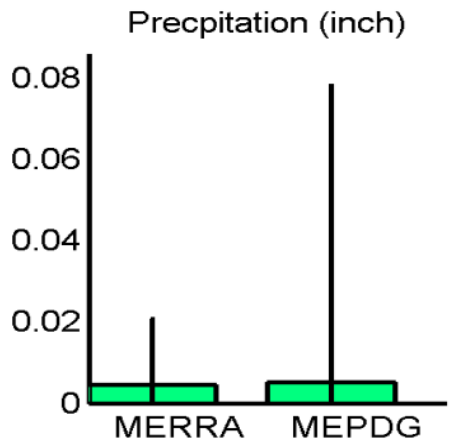

Figure 24. Graph. Site M93817 (Evansville, IN) with good agreement in MEPDG predicted distresses: hourly precipitation means and standard deviations.

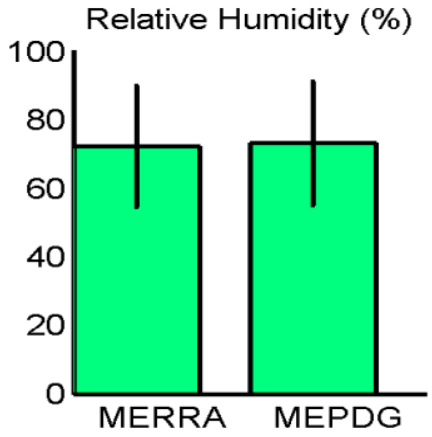

Figure 25. Graph. Site M93817 (Evansville, IN) with good agreement in MEPDG predicted distresses: hourly relative humidity means and standard deviations.

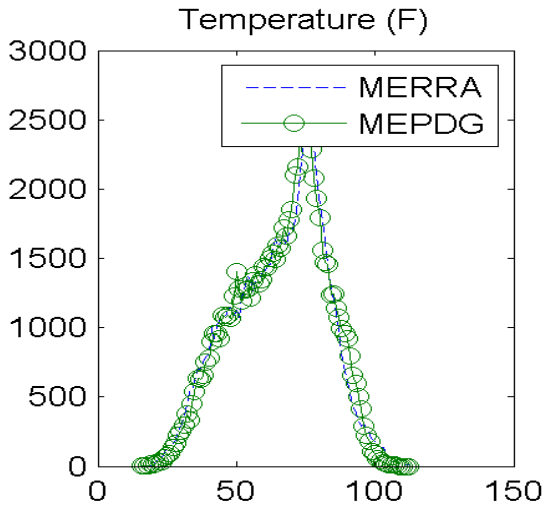

Figure 26. Graph. Site M13957 (Shreveport, LA) with poor agreement in MEPDG predicted distresses: distributions of hourly temperatures.

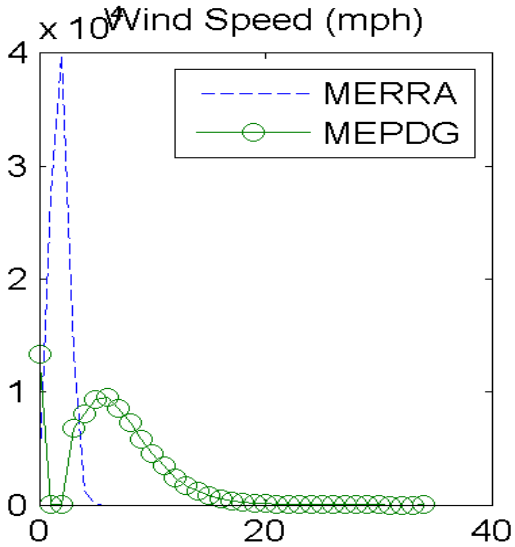

Figure 27. Graph. Site M13957 (Shreveport, LA) with poor agreement in MEPDG predicted distresses: distributions of hourly wind speeds.

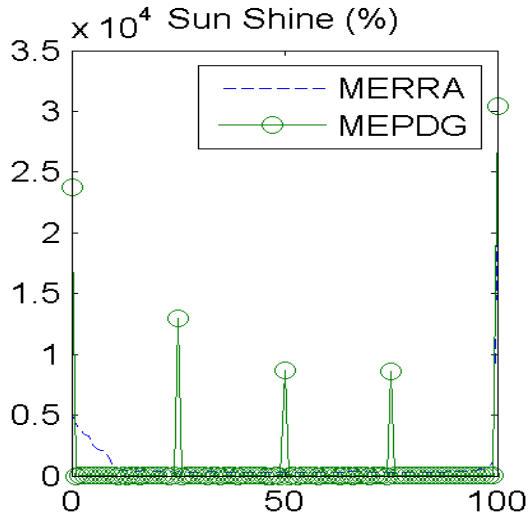

Figure 28. Graph. Site M13957 (Shreveport, LA) with poor agreement in MEPDG predicted distresses: distributions of hourly percent sunshine values.

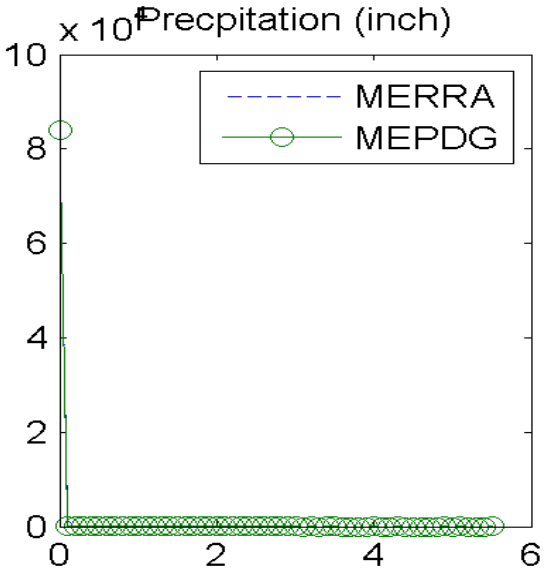

Figure 29. Graph. Site M13957 (Shreveport, LA) with poor agreement in MEPDG predicted distresses: distributions of hourly precipitation.

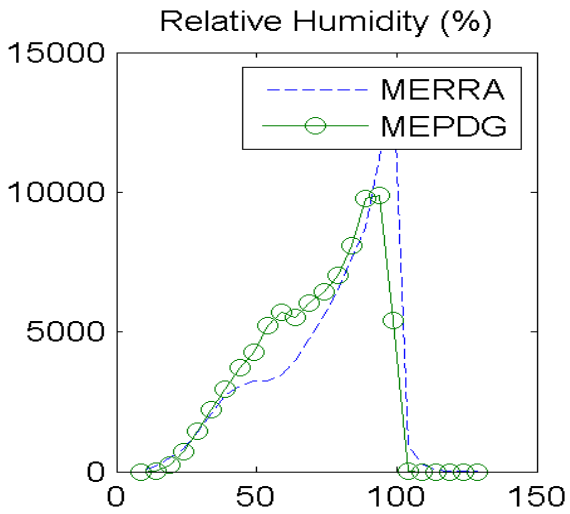

Figure 30. Graph. Site M13957 (Shreveport, LA) with poor agreement in MEPDG predicted distresses: distributions of hourly relative humidity.

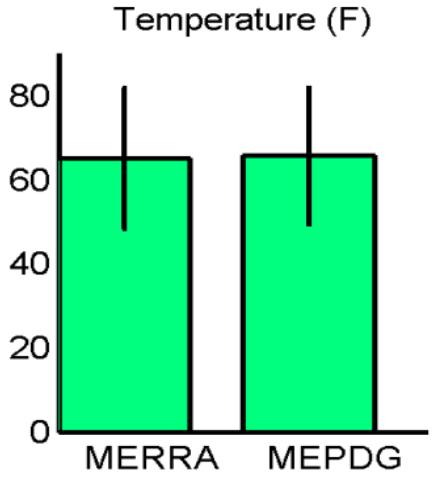

Figure 31. Graph. Site M13957 (Shreveport, LA) with poor agreement in MEPDG predicted distresses: hourly temperature means and standard deviations.

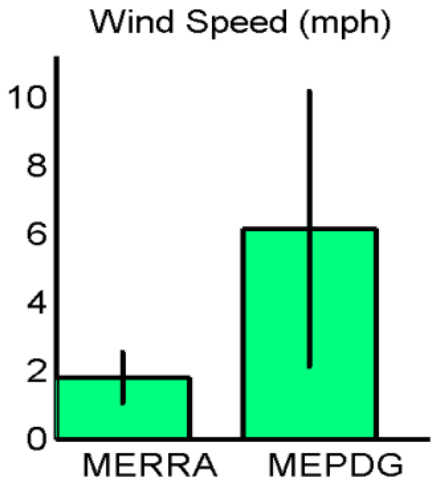

Figure 32. Graph. Site M13957 (Shreveport, LA) with poor agreement in MEPDG predicted distresses: hourly wind speed means and standard deviations.

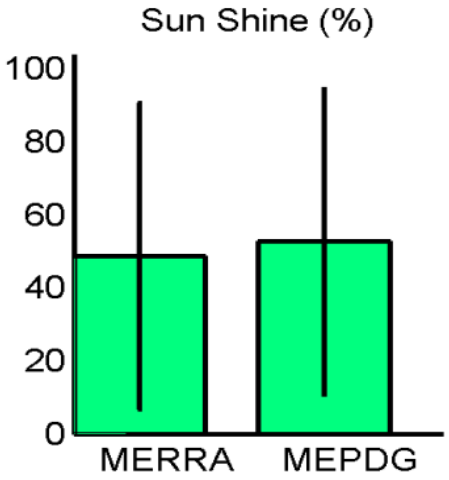

Figure 33. Graph. Site M13957 (Shreveport, LA) with poor agreement in MEPDG predicted distresses: hourly percent sunshine means and standard deviations.

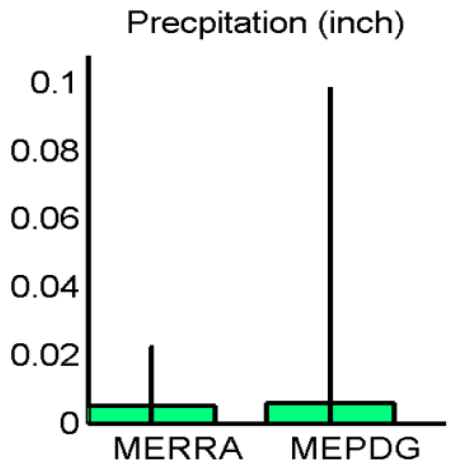

Figure 34. Graph. Site M13957 (Shreveport, LA) with poor agreement in MEPDG predicted distresses: hourly precipitation means and standard deviations.

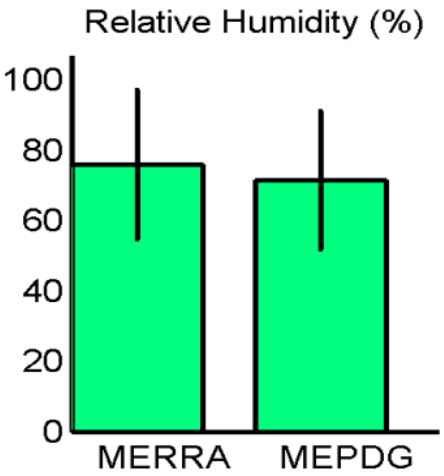

Figure 35. Graph. Site M13957 (Shreveport, LA) with poor agreement in MEPDG predicted distresses: hourly relative humidity means and standard deviations.

The discrepancies in hourly wind speed and percent sunshine values merited further evaluation. In general, mean wind speeds from the MERRA data tended to be lower than from AWSs/OWSs. The frequency distributions of hourly wind speed data from the MERRA and AWS/OWS data sources provided additional insights. Hourly wind speed frequency distributions are shown in figure 17 for site 93817 in Evansville, IN, and figure 27 for site 13957 in Shreveport, LA. These respectively had very good and very poor agreement in the MEDPG predicted distresses using the MERRA versus AWS/OWS weather data. The frequency distributions in figure 17 show very similar wind speed frequency distributions and statistics for the site with good agreement in MEPDG predicted distresses. However, figure 27 for the poor distress agreement site shows a frequency distribution for the MERRA data that is smooth with a well-defined single peak while the distribution for the OWS data from the MEPDG database is bimodal and has almost zero measurements of wind speed in the range of about 1 to 3 mi/h. This

"dropout" in the OWS wind speed data corresponds to the exact location of the peak frequency in the MERRA data. This "dropout" is also reflected in the discrepancies in the wind speed mean and standard deviations as shown in the bar chart in figure 32. Further examination of all OWSs in the current MEPDG database revealed that nearly all OWS weather files have almost zero measurements over the wind speed range of about 1 to 3 mi/h. The reason for this is unknown and difficult to hypothesize.

There were also issues with the percent sunshine measurements in both the AWS and OWS data sources. As described previously, the AWSs do not measure percent sunshine and thus the values of percent sunshine (and cloud cover) must be inferred. Percent sunshine is measured on an hourly basis at the OWSs, but the values are recorded as five discrete categories of 0, 25, 50, 75, and 100 percent. This is clearly evident in the OWS percent sunshine frequency distributions in figure 18 and figure 28. The hourly MERRA percent sunshine values, on the other hand, are recorded on a continuous scale from 0 to 100 percent.

There is a second potential issue with the OWS percent sunshine values. The OWS data in the MEPDG database are obtained primarily from ASOS ground stations. The ASOS ground stations measure percent sky cover based on reflections from a laser beam ceilometer).[(60)] The processing of this reflection data to determine sky cover is complex, but the end result is a reporting of sky cover in one of five categories. The five sky condition categories reported in the ASOS data, the ranges of electronically measured sky cover corresponding to each, and the human equivalent in oktas (one of eight increments of visual sky cover) are summarized in table 11. The presumed MEPDG OWS percent sky cover values (computed as 100 minus the percent sunshine) corresponding to the five reported percent sunshine categories are also given in the last column of table 11. These MEPDG values are presumed because there is no relevant documentation available for the MEDPG OWS files, but it seems plausible that the five MEPDG percent sunshine categories correspond to the five ASOS sky condition categories. If this is true, the data in table 11 suggest that there is an inconsistent mapping between ASOS and MEPDG OWS percent sky cover values for the various categories, which may introduce biases into the MEDPG OWS percent sunshine data.

Table 11. ASOS sky condition categories.

Sky Condition Category	ASOS Measured Percent Sky Cover (Range)	ASOS Measured Percent Sky Cover (Midpoint)	Human Equivalent (Oktas)	MEDPG OWS Percent Sky Cover
Clear (CLR)	0 to ≤ 5	2.5	0	0
Few Clouds (FEW)	> 5 to ≤ 25	15	> 0 to ≤ 2/8	25
Scattered Clouds (SCT)	> 25 to ≤ 50	37.5	> 2/8 to ≤ 4/8	50
Broken Clouds (BKN)	> 50 to ≤ 87	68.5	> 4/8 to ≤ 8/8	75
Overcast (OVC)	> 87 to ≤ 100	93.5	8/8	100

Figure 36 summarizes comparisons of statistics on the differences of selected weather inputs for the four sites that had full sets of data from AWS, MERRA, and two or more nearby OWSs. VWS weather histories were also generated from the OWS data using the MEPDG interpolation algorithms. Although the MEPDG VWS algorithm is not documented, through reverse

engineering, it appears to be based on an inverse square distance relationship with an elevation temperature correction using a 0.00349 °F/ft lapse rate in both the upward and downward directions. For the purposes of these comparisons, the AWS data were regarded as ground truth, and the evaluation was in terms of how well the weather statistics for the other data sources agree with those from the AWS. The data in figure 36 confirmed the earlier observation of generally good agreement in hourly temperature statistics among the different weather data sources. Although not shown in figure 36, this observation applies to precipitation and relative humidity statistics as well. Bar heights indicates mean value of the differences in weather parameters, error bars indicate standard deviations of the differences. Mean and standard deviation values of zero imply complete agreement between datasets. The largest discrepancies were again in the statistics for daily wind speed and percent sunshine. However, there were no patterns in these discrepancies. The MERRA data agreed best with the AWS in some cases (temperature for site 490800; wind speed for sites 300800, 490800). In other cases, the MERRA data agreed best with the VWS/OWS statistics but none of these agree very well with the AWS (wind speed for 040200, 530200; percent sunshine for sites 300800, 530200). Examination of all of these results suggests that the match between MERRA and AWS data in overall terms was at least as good as the agreement between VWS/OWS and AWS data.

Influence of site terrain and latitude were investigated in a final attempt to find some systematic explanation for the effect of the weather data source on MEPDG distress predictions. Agreement of MEPDG distress predictions using MERRA versus OWS weather inputs was classified into the three categories of good, fair, and poor, as described previously. Site terrain is categorized as flat, varying elevation, or mountainous. Latitude represents how far north/south the site was located. Trends between the agreement of MEPDG distress predictions and site terrain and latitude are illustrated in figure 37. Although the trends were weak, the data in figure 37 suggest that good agreement of MEPDG distress predictions is more likely for flat terrain and northern sites while poorer agreement is more likely for varying/mountainous terrain and southern sites. The influence of latitude on MEPDG distress predictions is addressed further in a later section.

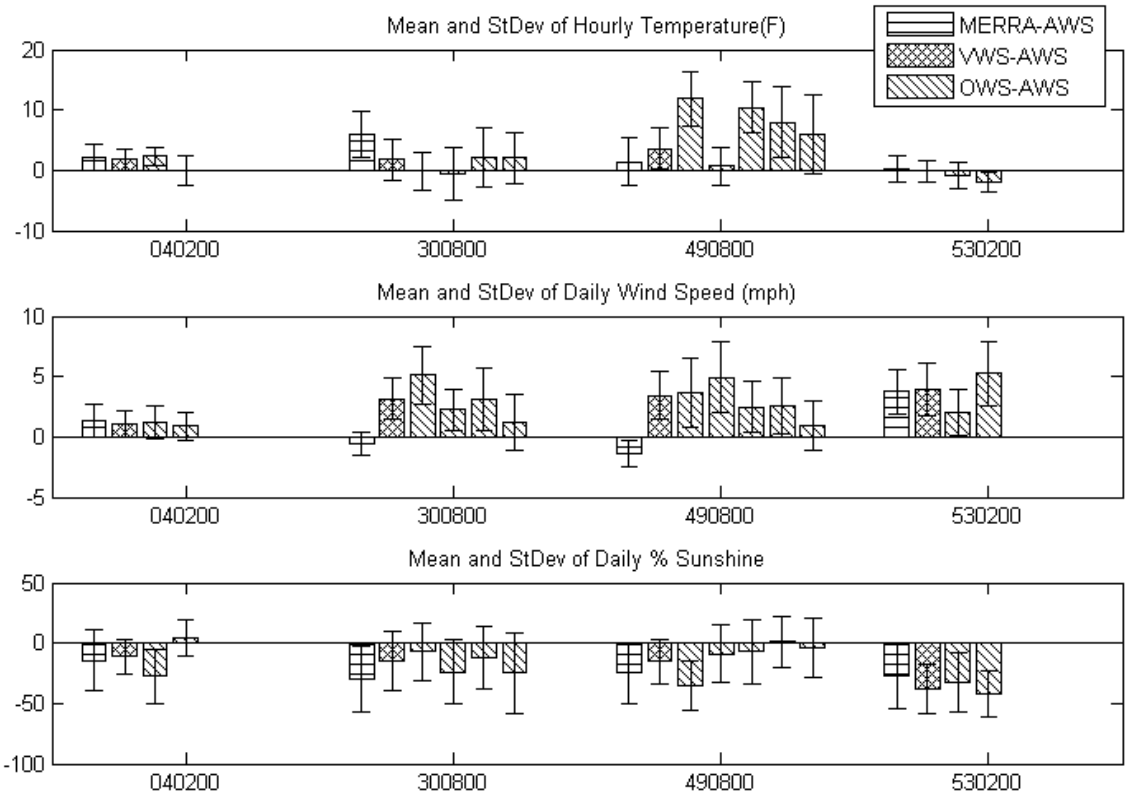

Figure 36. Graph. Comparison of key weather statistics: differences among MERRA versus AWS versus VWS versus OWS datasets.

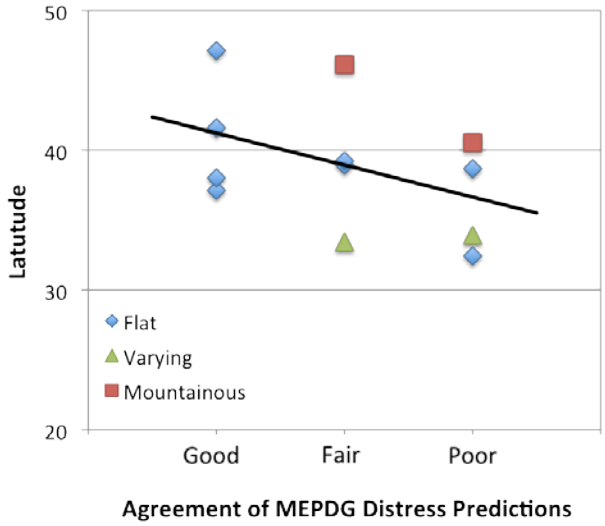

Figure 37. Graph. Influence of site terrain and latitude on agreement of MEPDG distress predictions using MERRA versus OWS weather inputs.

Statistical Comparison Conclusions

The following key conclusions were reached from the statistical comparison of MERRA versus AWS/OWS hourly weather data:

- There was generally good agreement in air temperature, precipitation, and relative humidity frequency distributions and statistics from all data sources.

- There was generally poorer agreement in percent sunshine and wind speed frequency distributions and statistics from the various data sources. These discrepancies may have been the result of the methods used to infer some data elements (percent sunshine for AWS), unexplained anomalies in the recorded data (wind speed for OWS), discrete versus continuous recording of data (wind speed), and potentially inaccurate mapping of cloud cover conditions (wind speed for OWSs).

- There were no systematic patterns in the discrepancies of MEPDG predicted distresses using AWS versus MERRA versus VWS versus OWS weather data sources. The results suggested that the match between MERRA and AWS data in overall terms was at least as good as the agreement between VWS/OWS and AWS data.

- There were weak trends in the differences in MEPDG distress predictions using MERRA versus OWS weather inputs, site terrain, and latitude. Good agreement of MEPDG distress predictions is more likely for flat terrain and northern sites while poorer agreement is more likely for varying/mountainous terrain and southern sites.

Overall, these conclusions support the use of MERRA as a source of weather data inputs for the MEPDG and other infrastructure applications.

COMPARISON OF MEPDG DISTRESS PREDICTIONS USING MERRA VERSUS OWS WEATHER DATA

The influences of different weather histories on MEPDG predicted distresses were examined in a preliminary statistical fashion previously. These influences are scrutinized from a more rigorously mechanistic perspective in this section. The suitability of MERRA as an alternative weather data source was evaluated by comparing the MEPDG prediction results using MERRA weather data inputs with predictions at the same location using conventional ground-based historical weather data. The ground-based historical weather data were obtained from the OWSs provided with the MEPDG software and the AWSs available in the LTPP database. Differences in absorbed solar energy at the pavement surface using these different weather history sources were examined as the possible cause for the differences in predicted distresses.

Enhanced Integrated Climate Model

Modeling of temperature and moisture conditions in the pavement structure in response to weather inputs is modeled in the MEDPG using the EICM. The EICM is a one-dimensional heat and moisture flow model that simulates pavement temperatures and moisture over depth and time in response to environmental inputs from the pavement surface. The analysis approach was

originally developed for the FHWA in the 1980s, revised in the 1990s, and then subsequently enhanced for implementation in the MEPDG. (See references 62, 63, 6, and 64.) The EICM requires the user to input the following weather data at hourly intervals over the entire design life of the project: air temperature, wind speed, percentage sunshine, relative humidity, and precipitation. The air temperature is used in the EICM heat balance equation for calculating longwave radiation and convective heat transfer. It is also used to define freeze–thaw periods, to determine the number of freeze–thaw cycles, and to estimate the TMI for setting the equilibrium saturation and matric suction conditions in the unbound layers. Wind speed is required for computing the convective heat transfer coefficient at the pavement surface. The percentage sunshine, along with latitude and date for computing solar declination, is needed for estimating the incoming solar radiation during the day and reflected longwave radiation at night. Relative humidity is used indirectly in the EICM to estimate net longwave radiation heat fluxes and in the MEPDG empirical distress models to compute the drying shrinkage of JPCP and continuously reinforced concrete pavement (CRCP) and also to determine the crack spacing and initial crack width in CRCP. Precipitation was required in early versions of the EICM to compute infiltration through the surface. However, infiltration modeling is disabled in the current version of the EICM, and any influence of surface moisture on surface heat flux is also neglected.

Although the MEPDG requires weather data inputs on an hourly basis, these values are interpolated and/or aggregated in different ways during the pavement prediction calculations. Hourly air temperatures are interpolated to the 0.1-h actual time interval used internally in the EICM finite difference integrations. Hourly wind speed is aggregated to a daily average value. Hourly percent sunshine (or its complement, percent cloud cover) is converted to average daytime and nighttime values. Relative humidity is converted to a daily average for estimating the longwave radiation heat losses from the pavement surface and to a monthly average for use in the MEPDG JPCP and CRCP distress models. Precipitation is not used in the current version of the EICM, but the hourly input values are converted to annual averages for use in the MEPDG distress models to determine the IRI site factor for flexible pavements and the erosion/loss of base support for rigid pavements.

MEPDG Prediction Results

Pavement distresses for the 12 sites identified previously in table 10 were predicted using the MEPDG and the MERRA and AWS/OWS weather histories. Both flexible and rigid pavement scenarios were investigated. The flexible pavement section consisted of 8 inches of asphalt concrete over 8 inches of A-1-a granular base layer over a semi-infinite A-6 subgrade layer. Traffic was set at an initial AADTT of 1,500 with 95 percent of trucks in the design lane and a compound traffic growth rate of 4 percent. The binder PG grade was selected using the LTPPBind program for the climate conditions at each site. The rigid pavement section consisted of 10 inches of JPCP over an A-2-4 granular base over an A-7-5 semi-infinite subgrade. Traffic was set at an initial AADTT of 7,500 with 55 percent of truck in design lane and no traffic growth.

A total of eight distresses (five for flexible pavements, three for rigid JPCP) were predicted by the MEPDG. For the flexible pavement scenario, AR was found to be the dominant distress, while slab cracking was the dominant distress for the rigid pavement scenario. Consequently, the subsequent discussion focuses on just these two distresses.

A design limit normalized difference (DLND) was used to present the differences of distress predictions between AWSs/OWSs and MERRA. The DLND is expressed in figure 38:

$$DLND_i^s = \frac{D_{i,MERRA}^s - D_{i,AWS\ /OWS}^s}{DL_i}$$

Figure 38. Equation. Design limit normalized difference.

Where:

$DLND_i^s$ = design limit normalized difference of distress *i* for site *s*.

$D_{i,MERRA}^s$ = predicted value of distress *i* for site *s* when using weather history from MERRA.

$D_{i,AWS/OWS}^s$ = predicted value of distress *i* for site *s* when using weather history from AWSs or OWSs.

DL_i = design limit for distress *i*—0.25 inches for AR and 15 for percent slab cracking.

The DLND represents the size of the differences in predicted distress using MERRA versus AWS/OWS weather data compared with the respective distress design limit. For example, if the DLND of AR is 0.5, this means that the MERRA data gave a predicted AR value that was higher than the predicted AR value using AWSs/OWSs by an amount equal to 0.5 times the design limit of AR, i.e., 0.5*0.25 inches = 0.125 inches.

Figure 39 summarizes the differences in predicted distresses as well as the statistics of the hourly weather input data for all sites. From left to right in figure 39 are 12 sets of bars, with each set corresponding to one site. The first row shows the DLND for AR and slab cracking at each station. The subsequent rows show the means and standard deviations for key weather parameters from each data source. Precipitation is not included because it is not an influential factor in the current EICM model. The DLND generally increases from left to right in the figure; in other words, the differences in predicted distress using MERRA weather data versus AWS or OWS data increases when going from left to right. The OWS in the legend represents the ground-based weather station, which in the context of the discussion in this section can be either AWS or OWS.

Noteworthy observations from figure 39 include the following:

- About a third of sites exhibited generally good agreement between the MERRA- and AWS/OWS-based distress predictions.
- The means and standard deviations of air temperature were consistently similar for the MERRA and AWS/OWS data.
- The differences between the MERRA and AWS/OWS mean daily wind speed increases in general from left to right—i.e., in parallel with the differences between predicted distresses.

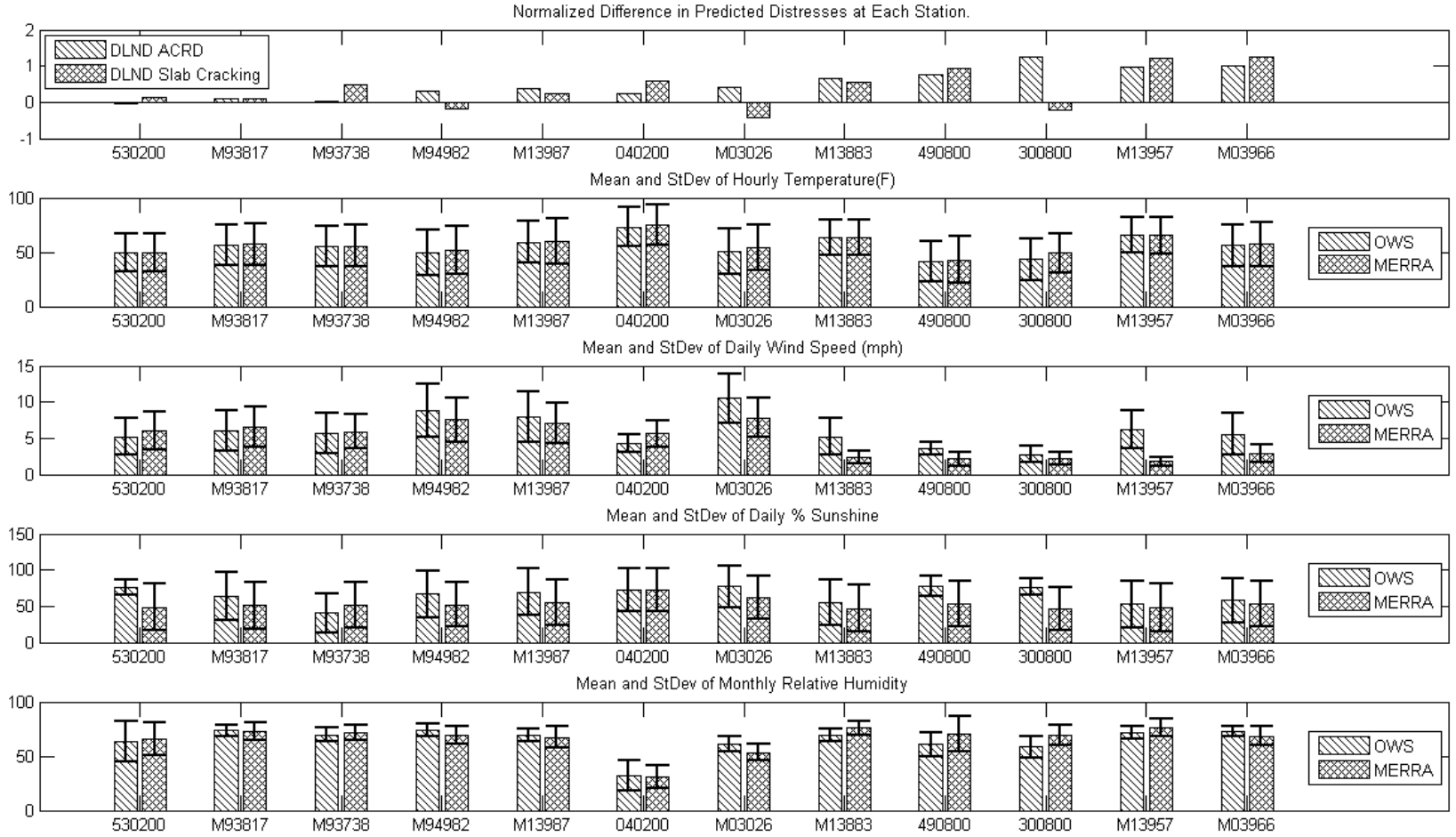

Figure 39. Graph. Summary of analysis results.

- Although the differences in the statistics for percent sunshine can be sizable, there is no obvious systematic trend moving from left to right as is the case for wind speed.

- The relative humidity statistics for the MERRA and AWS/OWS were similar at all sites.

The results in figure 39 were insufficient to explain the differences between the MERRA- and AWS/OWS-based distress predictions even for the cases where these differences were substantial. The results are also insufficient to establish which weather data source is more "correct." A more detailed examination of distress prediction agreement versus the weather data from the alternative sources is required. This additional analysis was completed and discussed in chapter 6.

Temperature

Although the air temperature mean and standard deviation values for the MERRA and AWS/OWS data generally agreed quite well, there were some exceptions. As shown in figure 39, sites M03026 and 300800 exhibited the largest temperature differences between MERRA and AWS/OWS data and also had moderate to large differences in predicted AR and slab cracking. Both of these sites are located in topographically challenging mountainous regions. Even though the MERRA air temperatures are corrected for elevation differences between the MERRA grid point and the AWS/OWS location, this was not sufficient to match the ground-based weather station data. More than just elevation varies rapidly over short distances in mountainous terrain; for example, the MERRA grid point might be on one side of a ridge and the AWS/OWS on the other side in a different microclimate. This will always be an issue in these types of terrain and will also plague ground-based weather data from stations that are not collocated with the pavement site. In other words, the only source for truly accurate weather data at pavement sites in topographically challenging areas is an onsite OWS.

Wind Speed

In general, mean wind speed from the MERRA data tended to be lower than from AWS/OWS data. As described previously, the frequency distributions for the MERRA data tend to be smooth with well-defined single peaks while the distributions for the OWS data from the MEPDG database are frequently bimodal with almost zero measurements of wind speed in the range of about 1 to 3 mi/h (figure 27 and figure 32). This "dropout" in the OWS wind speed data corresponds to the exact location of the peak frequency in the MERRA data.

Figure 40 and figure 41 depicts the trends of DLND for AR and slab cracking versus the difference between MERRA and AWS/OWS average hourly wind speeds, respectively. The different shapes of the data points correspond to the level of prediction agreement (good, fair, and poor). Overall, DLND decreases with increasing difference in average wind speed (in an absolute value sense). This is more pronounced for AR than for slab cracking. Although the R^2 values are low, the trends nevertheless suggest that biases in wind speed will produce biases in the MEPDG pavement predictions. Given the dropout in low wind velocities in the OWS data (figure 27 and figure 32), it would appear that the ground-based wind speed data are more suspect.

One additional note regarding wind speed: The wind speed used in the convection boundary condition for the EICM is defined at an elevation of 6.5 ft above the ground surface.[65] The MERRA data wind speed data are reported at this 6.5-ft elevation, but the precise elevations for OWS measurements are not known.

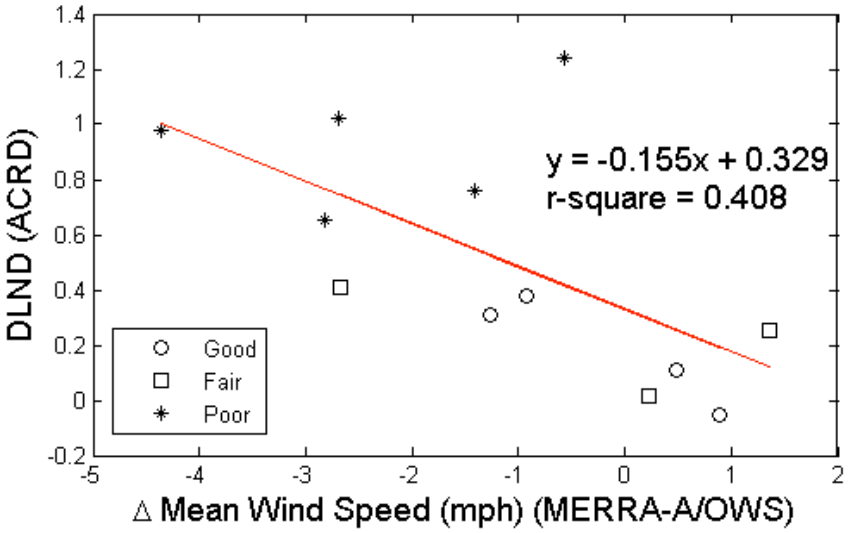

Figure 40. Graph. DLND in predicted asphalt concrete rut depth (ACRD) versus mean hourly wind speed difference.

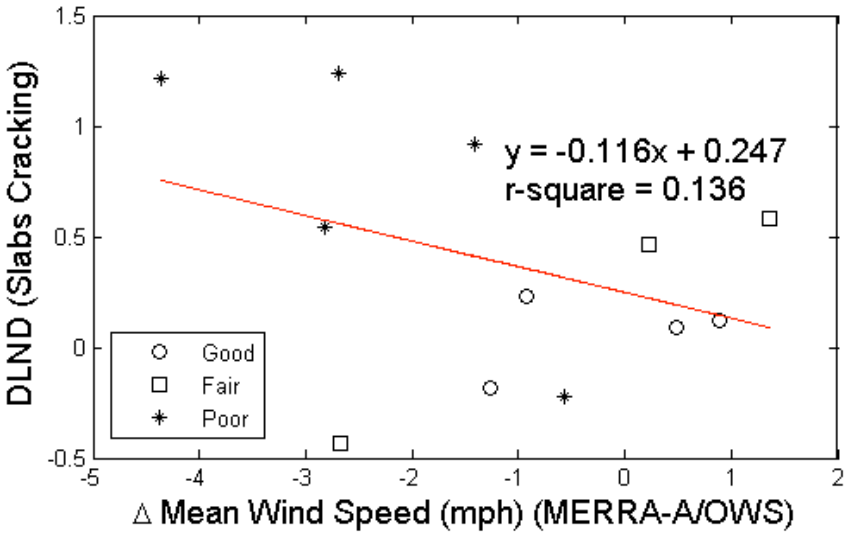

Figure 41. Graph. DLND in predicted slab cracking versus mean hourly wind speed difference.

Percent Sunshine

As described earlier, there were issues with the percent sunshine measurements in both the AWS and OWS data sources. The AWSs do not measure percent sunshine and thus the values of percent sunshine (and cloud cover) must be inferred. Percent sunshine is measured on an hourly

basis at the OWS, but the values are recorded as five discrete categories (0, 25, 50,75, and 100 percent—see figure 18 and figure 28), and there is some question whether these categories are mapped correctly from the underlying ASOS categories (table 11). The hourly MERRA percent sunshine values are recorded on a continuous scale from 0 to 100 percent.

Figure 42 and figure 43 depicts the trends of DLND for AR and slab cracking versus the difference between MERRA and OWS average percent sunshine, respectively. The meaning of the shapes of the points is the same as in figure 40 and figure 41. Censoring the one outlier on the far right, the results suggest that the differences in the MEPDG predicted distress are correlated quite strongly with the differences in the percent sunshine values in the weather data sets. Because there were issues with the AWS and OWS measurement of this parameter, these data would appear to be the most suspect.

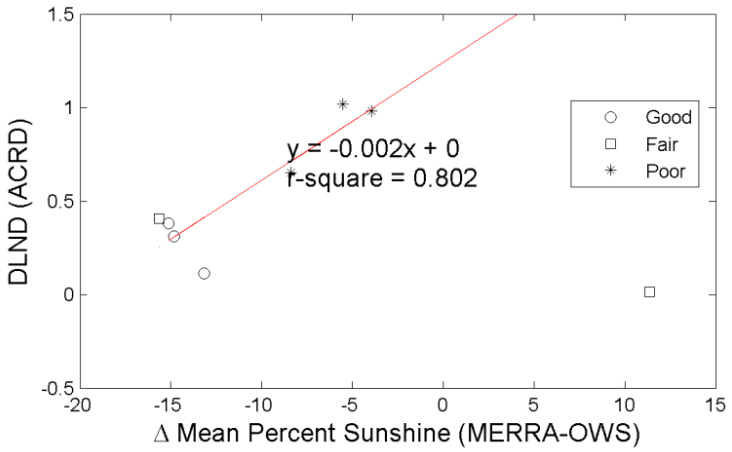

Figure 42. Graph. DLND in predicted ACRD versus mean hourly percent sunshine difference.

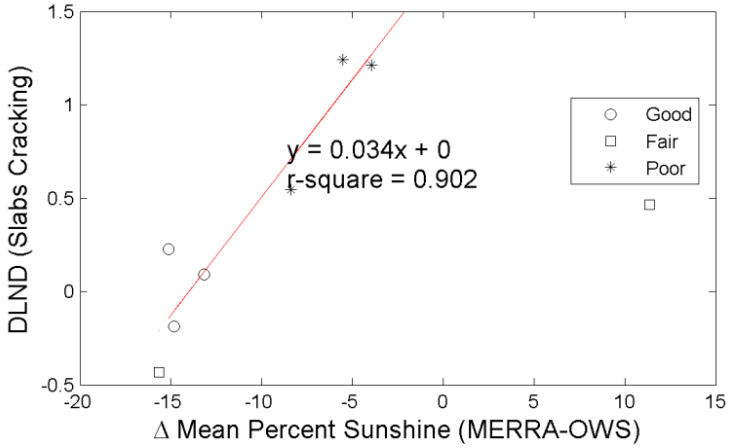

Figure 43. Graph. DLND in predicted slab cracking versus mean hourly percent sunshine difference.

Combined Effects of Wind Speed and Percent Sunshine

Wind speed and percent sunshine both have a strong influence on pavement temperature distributions and thus on AR and PCC slab cracking. Higher wind speed increases convective losses at the surface and thus decreases the solar radiation available to heat the pavement. Higher percent sunshine, on the other hand, increases the solar radiation reaching the pavement surface and thus increases pavement temperatures. As described in the preceding section, MERRA tended to have lower wind speeds and lower percent sunshine values than for ground-based weather data. Given the physics of the heat transfer at the pavement surface, these two trends will cancel each other to some unknown extent.

To evaluate the combined effects of wind speed and percent sunshine, the relevant components of the EICM formulation can be employed to evaluate the net energy absorbed by the pavement surface. The relevant equations are given in the NCHRP Project 1-37A final report.(6) The net heat flux available for absorption through the pavement surface Q_g is shown in figure 44.

$$Q_g = (Q_i - Q_r) + (Q_a - Q_e) - Q_h - Q_c$$

Figure 44. Equation. Net heat flux available for absorption.

Where:

Q_i = heat flux due to incoming shortwave radiation.
Q_r = heat loss due to reflected shortwave radiation.
Q_a = heat flux due to incoming longwave radiation.
Q_e = heat loss due to outgoing longwave radiation.
Q_h= heat loss due to transpiration, condensation, evaporation, and sublimation.
Q_c = heat loss due to convection.

Transpiration, condensation, evaporation, and sublimation heat losses are ignored in the EICM, i.e., $Q_h = 0$. All heat fluxes and losses are in units of energy per time and area, e.g., Btu/hr-ft^2. (Note on units: The derivations in this section are based on the NCHRP Project 1-37A documentation of the EICM. This documentation employs a variety of mixed and often inconsistent units. No attempt has been made here to remedy this.)

The net incoming shortwave solar radiation heat flux Q_i at the pavement surface is estimated indirectly in the EICM using the equation in figure 13, which is repeated here for convenience in figure 45.

$$Q_i = R * \left[A + B_{100}^{S_c}\right]$$

Figure 45. Equation. Shortwave radiation regression equation.

As before, R^* is the extraterrestrial radiation incident on a horizontal surface at the outer atmosphere; A and B are empirical coefficients that account for diffuse scattering and adsorption by the atmosphere; and S_c is the percent sunshine, equivalent to 100 minus the percent cloud cover. Values of A and B incorporated in the EICM are based on 10 years of data for the upper Midwest and Alaska and are equal 0.202 and 0.539, respectively.(58) Only EICM OWS data are considered here because the AWSs do not provide a direct measurement of S_c.

There are two choices for determining Q_i in MERRA. The first, similar to what is done in the EICM, is to estimate it from the equation in figure 45 using S_c values derived from the MERRA cloud cover data. However, MERRA also provides a direct measure of incoming shortwave heat flux as the R_{sw} data element in units of W/m^2. This latter approach, which eliminates the need for the empirical *A* and *B* parameters in the equation in figure 45, was employed for the present analyses.

The net incoming shortwave radiation heat flux Q_s after subtracting reflected radiation, is calculated from the OWS data as shown in figure 46:

$$Q_s = (Q_i - Q_r) = a_s R \left[A + B \frac{S_c}{100}\right]$$

Figure 46. Equation. Shortwave radiation heat flux from OWS data.

Q_s can also be calculated from the MERRA data as (after appropriate unit conversions) using the equation shown in figure 47:

$$Q_s = (Q_i - Q_r) = a_s R_{sw}$$

Figure 47. Equation. Shortwave radiation heat flux from MERRA data.

Where a_s is the surface shortwave absorptivity (the complement of albedo) set equal to 0.85 for both asphalt and PCC surfaces and the other terms are as previously defined. Note that the Q_s values for the MERRA and OWS/EICM approaches will not be identical.

The incoming and outgoing longwave radiation heat fluxes are given in figure 48 and figure 49 respectively.

$$Q_a = Q_z \left(1 - \frac{NW}{100}\right)$$

Figure 48. Equation. Incoming longwave radiation heat flux.

$$Q_e = Q_x \left(1 - \frac{NW}{100}\right)$$

Figure 49. Equation. Outgoing longwave radiation heat flux.

Where:

N = cloud base factor; 0.9 to 0.8 for cloud heights of 1,000 to 6,000 ft.[(66)]
W = average cloud cover during day or night.
Q_z = heat flux due to incoming longwave radiation without correction for cloud cover.
Q_x = heat loss due to outgoing longwave radiation without correction for cloud cover.

Note that both the incoming and outgoing longwave radiation heat fluxes in the equations found in figure 48 and figure 49 are functions of the average cloud cover, which will in general be different for the MERRA and OWS weather histories.

The uncorrected incoming longwave radiation heat flux Q_z is computed in figure 50:

$$Q_z = \sigma_{sb} T_{air}^4 \left(G - \frac{J}{10^{\rho p}} \right)$$

Figure 50. Equation. Uncorrected incoming longwave radiation heat flux.

Where:

σ_{sb} = Stefan-Boltzman constant, 0.172×10^{-8} Btu/(hr-ft^2-°F^4).
T_{air} = air temperature in degrees Rankine (°R).
G = 0.77.
J = 0.28.
ρ = 0.074.
p = vapor pressure of the air (1 to 10 mm Hg), which is related to relative humidity.

The uncorrected outgoing longwave radiation heat loss Q_x is computed in figure 51:

$$Q_x = \sigma_{sb} \varepsilon T_s^4$$

Figure 51. Equation. Uncorrected outgoing longwave radiation heat loss.

Where:

ε = emissivity of the pavement, which depends on pavement color, texture, and temperature; a typical value is 0.93.

T_s = pavement surface temperature in °R.

The final term remaining in the equation in figure 44 is the convective heat loss Q_c, which is given by figure 52:

$$Q_c = H(T_{air} - T_s)$$

Figure 52. Equation. Convective heat loss.

Where T_{air} and T_s are as defined previously, and H is the convection heat transfer coefficient. The convective heat transfer coefficient depends on many variables and is thus difficult to define. The expression employed in the EICM is shown in figure 53:[(65)]

$$H = 122.93[0.00144T_m^{0.3}U^{0.7} + 0.00097(T_s - T_{air})^{0.3}]$$

Figure 53. Equation. Convection heat transfer coefficient.

Where:

T_s = pavement surface temperature, in °K.
T_{air} = air temperature, in °K.
T_m = average of surface and air temperatures, in °K.
U = average daily wind speed at an elevation of 2 m above the surface, in m/sec.

The EICM documentation recommends a maximum value for H of 3.0 Btu/(hr-ft^2-°F). Note that the average daily wind speed U will in general be different for the MERRA and OWS weather histories.

The equations in figure 44 through figure 53 enable comparisons of the net heat flux Q_g into the pavement for both the MERRA and OWS weather histories. This net heat flux, when integrated over time, gives the energy density absorbed into the pavement. To simplify these exploratory analyses, only the daily average values of the hourly air temperatures were used, and the difference between the pavement surface temperature and the air temperature was assumed constant at 30 °F.

Figure 54 through figure 59 illustrate the effect of absorbed energy density on predicted pavement performance. The daily absorbed energy densities over 1 year are summarized in the graph at the top of each figure; the frequency distribution of the daily absorbed energy density is given in the lower right; and the mean and standard deviation of daily absorbed energy density are given in the bar chart in the lower left. The daily absorbed energy densities predicted using the MERRA data agree well with those using the OWS weather histories for site M93817 (Evansville, IN) in figure 54. However, the agreement is not as good for site M13957 (Shreveport, LA) in figure 57; this can be seen most clearly in the mean and standard deviation comparisons in the lower left, where the mean daily absorbed energy density for the MERRA data is about 10 to 15 percent greater than the mean for the OWS weather history. Comparing these results with the differences in predicted distresses given at the top of figure 39 shows very good correlation between distress prediction agreement and absorbed energy agreement. Site M93187, which had the closest agreement in the absorbed energy densities using MERRA versus OWS, also had among the closest agreement in predicted distresses using the two weather data sources. Conversely, site M13957 had the worst agreement between absorbed energy densities and also had among the worst differences in predicted distresses using the MERRA versus OWS weather histories.

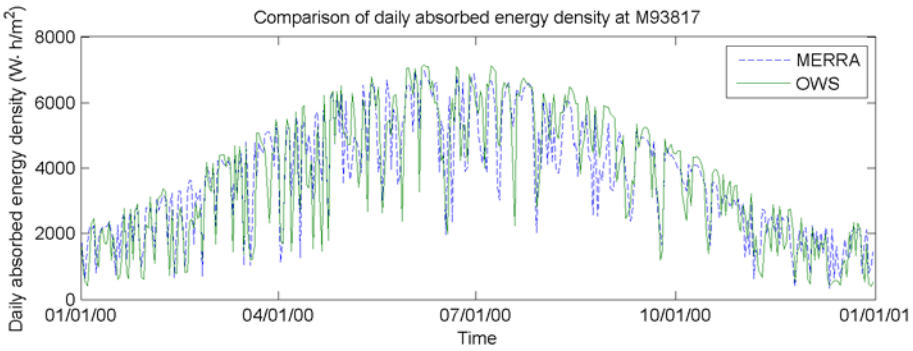

Figure 54. Graph. Absorbed energy density versus time during a typical day at site M93817 (Evansville, IN).

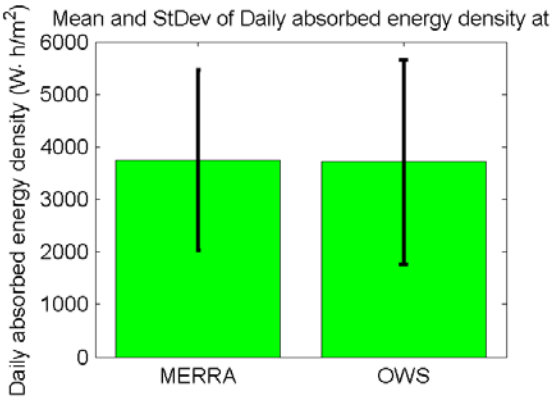

Figure 55. Graph. Mean and standard deviation of daily absorbed energy density at site M93817 (Evansville, IN).

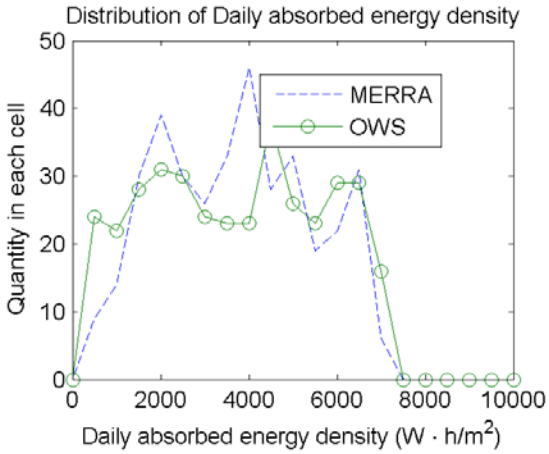

Figure 56. Graph. Distribution of daily absorbed energy density at site M93817 (Evansville, IN).

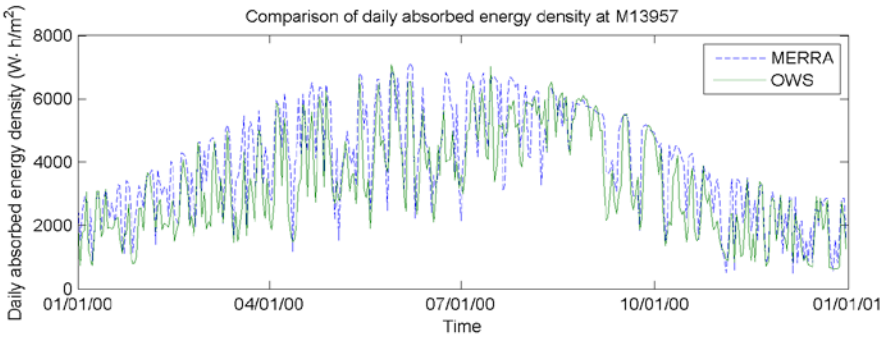

Figure 57. Graph. Absorbed energy density versus time during a typical day at site M13957 (Shreveport, LA).

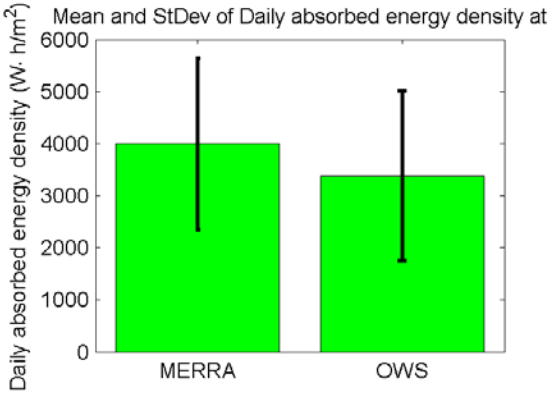

Figure 58. Graph. Mean and standard deviation of daily absorbed energy density at site M13957 (Shreveport, LA).

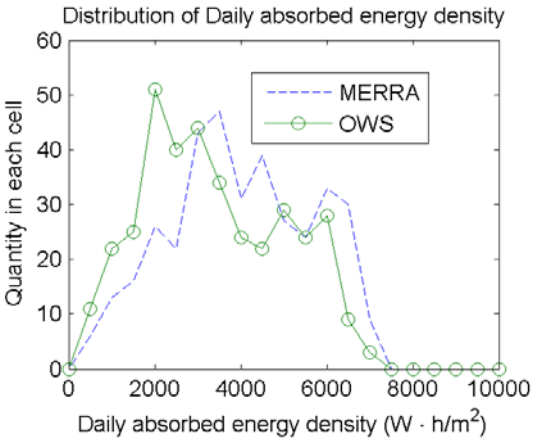

Figure 59. Graph. Distribution of daily absorbed energy density at site M13957 (Shreveport, LA).

Figure 60 and figure 61 depict the trend between DLND in predicted distresses (ACRD and slab cracking, respectively) and the mean daily absorbed energy density for all of the OWS sites analyzed. The prediction differences for both AR and PCC slab cracking consistently increase

with increased differences in the mean daily absorbed energy density from the MERRA versus OWS weather histories. These differences are due to the combined effects of differences in estimates of total incoming solar radiation and differences in measured wind speed and percent cloud cover (or conversely percent sunshine). The MERRA data for these parameters are judged to be the most reliable for the following reasons:

- Total incoming shortwave radiation is provided explicitly in the MERRA data while it must be determined indirectly from the OWS data using estimates of top-of-atmosphere incoming solar radiation, measured percent sunshine/cloud cover, and an empirical relation for atmospheric diffuse scattering and absorption.

- Many of the OWS histories have dropouts of low wind speeds in the 1 to 3 mi/h range while the MERRA wind speed data exhibit more physically plausible distributions.

- The OWS percent sunshine/cloud cover is reported as five discreet categories compared with the continuous reporting in the MERRA data. There is also a question of whether the mapping of cloud cover from the underlying ASOS data to the OWS categories is done correctly.

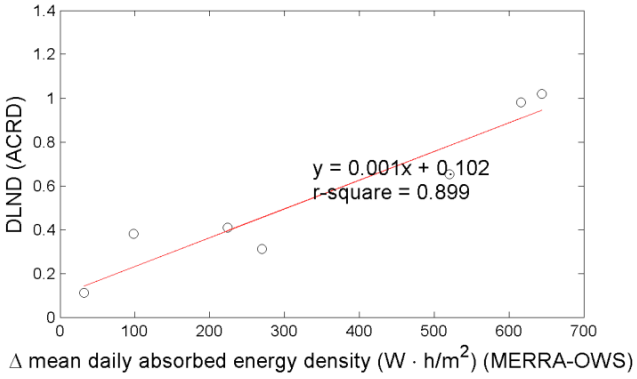

Figure 60. Graph. DLND in predicted ACRD versus absorbed energy differences.

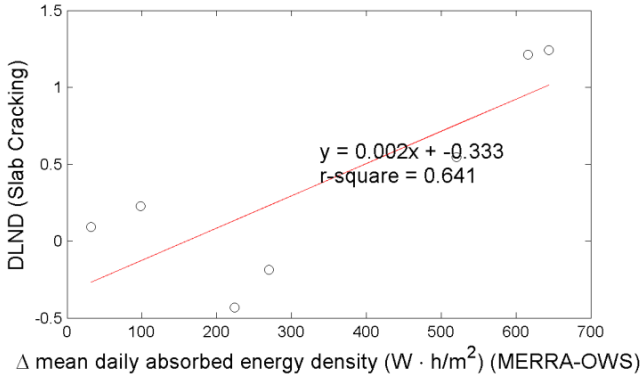

Figure 61. Graph. DLND in predicted slab cracking versus absorbed energy differences.

The first bullet point above supports the more qualitative observations made in the previous section. Figure 37 suggested that the discrepancies in MEPDG distress predictions tended to increase at lower latitudes—i.e., at more southerly site locations. The *A* and *B* calibration

coefficients in the empirical relation for atmospheric diffused scattering and absorption in equation in figure 45 are based on conditions in the northern continental United States (including Alaska). This calibration becomes less appropriate for southern States, which is consistent with the observed increased differences in absorbed energy density and consequent differences in MEPDG distress predictions for the MERRA versus OWS weather histories.

The next chapter provides details on a more in-depth statistical and pavement performance comparison than contained in this chapter.

CHAPTER 6. ADDITIONAL MERRA DATA VALIDATION

BACKGROUND AND OBJECTIVES

Initial evaluations of the MERRA data presented in the previous chapter suggest that they are as good as, and in many ways superior to, weather data time series from conventional surface-based OWSs. The recommendations from these initial evaluations were that LTPP should adopt MERRA as the data source for its next update to the climate data module and develop a tool to extract and use these data for engineering applications.

These recommendations were presented as a draft phase 2 report that was subsequently reviewed by the Transportation Research Board's ETG on LTPP Special Activities, FHWA experts, and LTPP staff.[(1)] The project team received and addressed 118 comments on the draft phase 2 report. Two primary comments necessitate additional analysis with the following primary objectives:

1. More extensive analysis of MERRA data.
2. Development of a tool to disseminate MERRA data.

This chapter addresses the first of these objectives. It can be broken down into the following set of specific study activities:

- If possible, establish an appropriate ground truth for climate data.
- Perform statistical comparisons of ground truth, OWS, and MERRA.
- Evaluate the correctness of MEPDG SSR calculations.
- Compare MEPDG pavement performance predictions using ground truth, OWS, and MERRA climate data.

CLIMATE DATA SOURCES

A variety of data sources were examined in this study. Ground-based climate data provided as part of the MEPDG serve as the standard input for flexible and rigid pavement simulations using the Pavement ME Design® software. Additional data sources employed for comparisons with the MEPDG climate files include the USCRN, the NWS Cooperative Observer Program (COOP), the Department of Energy Solar Infrared Radiation System (SIRS), and NASA's MERRA. Further details on MEPDG, USCRN, COOP, SIRS, and MERRA are provided below.

MEPDG

The MEPDG methodology is implemented in the Pavement ME Design® software product from AASHTO. The climate data files needed as inputs to the MEPDG methodology and supplied with the Pavement ME Design® software are derived from two data products provided by the NCDC: the ULCD for times prior to 1 January 2005 and the QCLCD for times after 1 January 2005. Many of the ULCD and QCLCD sites are part of the NWS ASOS. Despite the limited QC

incorporated in the QCLCD product and additional QC measures undertaken by the MEPDG model developers, these reference inputs still contain numerous measurement and/or data processing errors. However, a nonexhaustive review of the data found that the edited QCLCD data after 1 January 1, 2005, contains fewer processing errors than the unedited ULCD data prior to January 1, 2005. The QCLCD product includes hourly meteorological measurements for approximately 1,600 stations located across the United States.

The MEPDG climate data are the inputs to the EICM. The developers of MEPDG performed additional QC steps on the ULCD and QCLCD products for use with the EICM. Nonetheless, the climate data provided with the MEPDG still contain some measurement and data coding errors and time series gaps, albeit reduced as a result of the additional quality control steps.

Table 12 summarizes the meteorological data evaluated in this study, both from the MEDPG climate files and from the other climate data sources described in the subsequent sections.

Table 12. Variables employed from each measurement product for use during analysis.

Variable of Interest	QCLCD	MEPDG	USCRN	MERRA	COOP	SIRS
Air Temperature	X	X	X	X	X[4]	—
Dew Point Temperature[1]	—	—	—	—	X[5]	—
Specific Humidity[1]	X	X	X	X	—	—
Wind Speed	X	X	—	X	X[5]	—
Precipitation	X	X	X	X	X[5]	—
Shortwave Radiation	—	—	X	X	—	X
Cloud Cover Fraction[2]	—	X	—	X	—	—
Sky Condition[3]	X	—	—	—	—	—

[1]Dew point temperature and specific humidity provide equivalent information regarding humidity
[2]Cloud cover fraction serves as a proxy for shortwave radiation
[3]Sky condition serves as a proxy for cloud cover fraction, and hence, shortwave radiation
[4]Only daily maximum / minimum / average values are available to the public
[5]Only daily average values are available to the public
X = measurement/estimate is available at the majority of locations
— = Data not included in source
QCLCD = Quality Controlled Local Climatological Data
MEPDG = Mechanistic Empirical
USCRN = United States Climate Reference Network
MERRA = Modern-Era Retrospective Analysis for Research and Application
COOP = Cooperative Observer Program
SIRS = Solar Infrared Radiation System

USCRN

A summary describing the USCRN was provided in chapter 3. Observations collected by the USCRN were of particular interest in this study because they are derived from a minimum of three clustered sensors that are then averaged together prior to public distribution. The averaging of multiple measurements at each point in time serves to reduce measurement error and hence provides what is arguably the closest estimate of the ground truth. It is worth emphasizing here that all measurements inherently contain error. In addition, weather data are spatially variable, and measurements separated by even only a few hundred meters will be slightly different. However, for purposes of this study the USCRN measurements were considered as “reference” measurements of the true value of the meteorological data at the site.

COOP

Daily measurements of meteorological variables are available through the NWS COOP. COOP measurements collected from more than 570 individual station locations, were employed for use in this study. As opposed to the hourly (or shorter) measurements collected for the data products outlined in the preceding sections, COOP only provides daily averages and the daily range (i.e., maximum and minimum values) for certain meteorological variables. As a result, COOP data were used in this study to examine more closely the diurnal range of values from the hourly products in table 12 and to provide further insights regarding the fidelity of the different hourly products.

SIRS

Ground-based radiometer measurements from the SIRS program operated by the Atmospheric Radiation Measurement Program under the auspices of the United States Department of Energy were used for direct comparison against model estimates of shortwave radiation.(67) Only the USCRN and MERRA products contain estimates of downwelling shortwave radiation at the surface. MEPDG estimates of downwelling shortwave radiation are inferred from cloud cover conditions (fraction) by employing an empirical expression described later in this report. Using this approach, it was possible to compare different solar radiation estimates even though not all of the data products contained direct estimates of downwelling shortwave radiation at the surface.

MERRA

Meteorological inputs used to force the model were obtained from the MERRA product (http://gmao.gsfc.nasa.gov/merra/).(45) MERRA is provided at an hourly temporal resolution, 0.5 by 0.67 degrees (latitude/longitude) spatial resolution, and is available from 1979 to the present. Chapter 4 provides a summary description of MERRA.

The MERRA product results from the merger of a physically based model (i.e., the NASA GEOS-5 Version 5.2.0) with satellite, airborne, ship, and radiosonde observations of the atmosphere. NASA frequently uses the MERRA product to help verify seasonal climate forecasting systems, generate climate data records, serve as input to satellite retrieval algorithms, and provide atmospheric forcings for hydrologic and land surface process studies.(49) In addition, MERRA is regularly analyzed and validated to ensure continuity and consistency because the data product is produced in near real-time.

A major advantage of MERRA over ground-based climate data sources is the uniform spatial coverage. The ground-based ASOS stations that provide much of the MEPDG/ULCD/QCLCD climate data are mostly located at airports and therefore clustered along the east and west coasts of the United States and around major population centers.

Measurement Product Collocation

To compare measurements from one measurement network against those from another, it is first necessary to collocate the measurement networks in space prior to collocating the measurement sequences in time. The collocation process was conducted for the QCLCD station locations (and

hence the MEPDG station locations by association). That is, all computed distances treat the given QCLCD station as located at the center of the search area. Next, for a given QCLDC station, the horizontal distance was computed for every station in each of the measurement networks outlined above. A minimum separation distance of 0.5 degrees (approximately 31.1 mi at mid-latitudes) was specified. This was done so that each collocated set of measurement stations would be representative of the same local topographic and climate conditions. In addition, given the spatial resolution of the MERRA product, this guaranteed that at least one MERRA location (grid cell) would correspond to every QCLCD (and hence every MEPDG) station location. If at least one station location from each of the measurement networks outlined above was within 0.5 degrees of the given QCLCD measurement station, then those respective measurement stations from each measurement network were used during the statistical analysis discussed later.

Figure 62 through figure 64 show the histograms of the horizontal separation distances from the collocation procedure. As illustrated in figure 62, the MEPDG weather stations are derived directly from the QCLCD data set, and hence the separation distance is often equal to zero. Because there are many more QCLCD stations than MEPDG stations, sometimes more than one QCLCD station falls within the spatial threshold available for comparing against a given MEPDG station—this results in the occasional nonzero separation distances between QCLCD and MEPDG station locations. The MERRA data, as expected, showed the greatest range in separation distance (see figure 64).

Figure 65 shows the locations within the contiguous United States of the various climate data products examined in this study. A total of 354 combinations of USCRN, QCLCD, and MERRA data sites (diamond symbol) were collocated to within 0.5 degrees of horizontal separation.

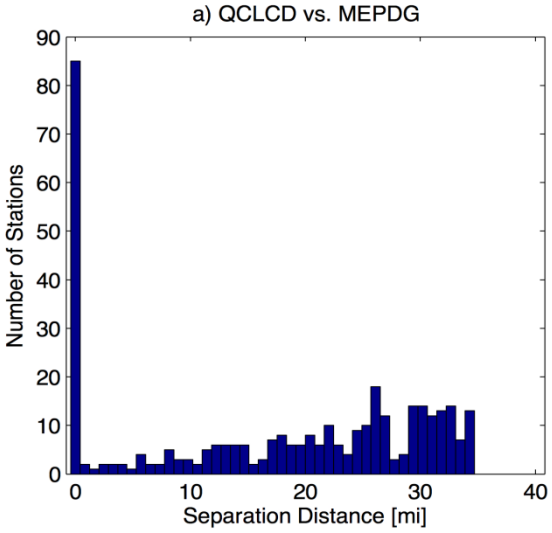

Figure 62. Histogram. Histogram of separation distances (in mi) relative to QCLCD for MEPDG stations.

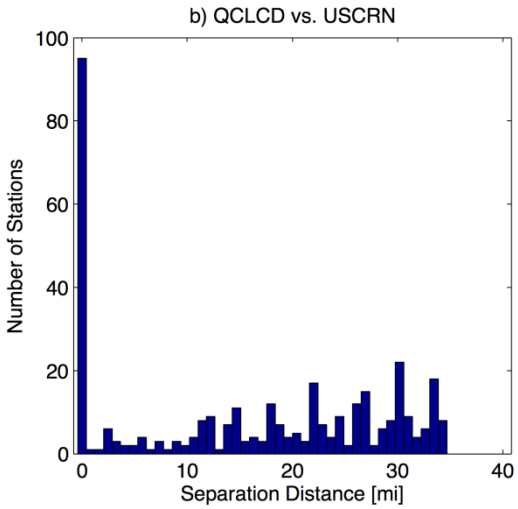

Figure 63. Histogram. Histogram of separation distances (in mi) relative to QCLCD for USCRN stations.

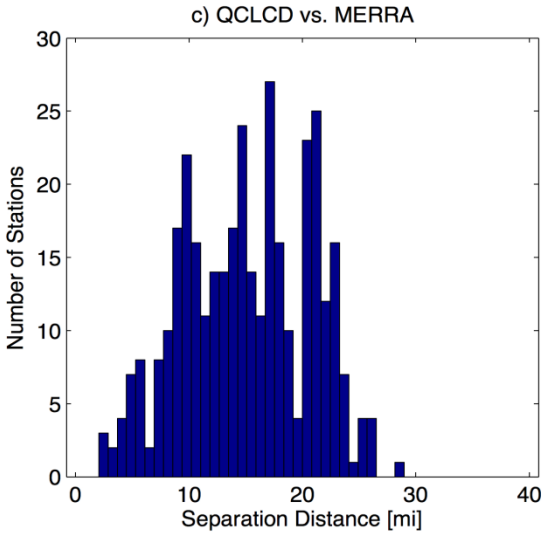

Figure 64. Histogram. Histogram of separation distances (in mi) relative to QCLCD for MERRA grid points.

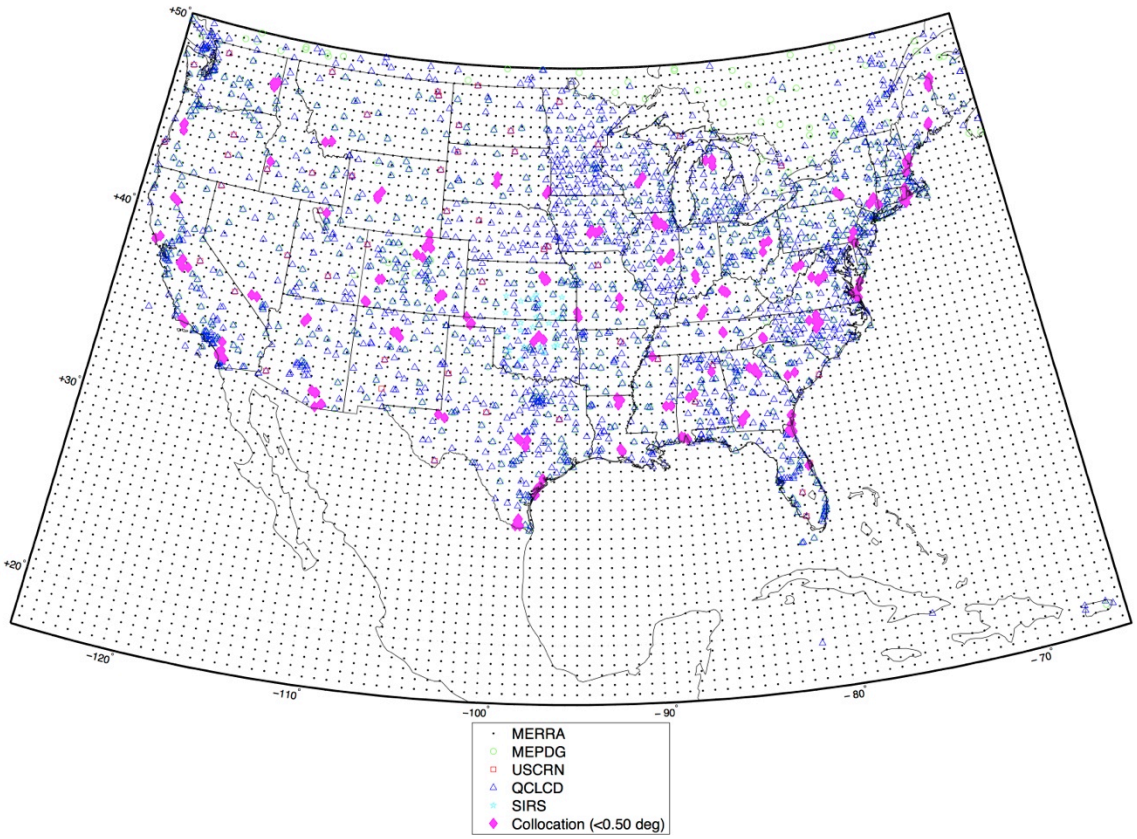

Figure 65. Map. Collocated USCRN, QCLCD, and MERRA data sets.

Elevation and Temperature Correction

Discrepancies in measurement elevation arise because not all collocated measurement locations are at precisely the same location in space. These discrepancies are greatest in regions of complex terrain (e.g., Rocky Mountains) and are less apparent in regions of low topographic relief. Because elevation differences can cause differences in air temperature, an air temperature correction was implemented to remove any systematic biases associated with elevation differences. The process was implemented in the MERRA product; it was not deemed necessary in the ground-based measurement products because most of the ground-based measurement stations are located in relatively flat terrain (e.g., at airports).

If differences exist between the land surface elevation at the MERRA grid point and the ground-based meteorological station, the MERRA air temperature is adjusted using an adiabatic lapse rate. If the elevation difference is positive (i.e., the ground station elevation is greater than the MERRA elevation), the ambient lapse rate is assumed to equal -8.0 °K/km. Conversely, if the elevation difference is negative (i.e., the station elevation is less than the MERRA elevation), the ambient lapse rate is assumed to equal -6.5 °K/km.[59] The difference between the two lapse rates accounts for the possibility of condensation during adiabatic cooling. Using the appropriate lapse rate, γ, the temperature correction is then computed as shown in figure 66:

$$T_{air,corrected} = T_{air} + \gamma \cdot \Delta z$$

Figure 66. Equation. Adiabatic lapse rate temperature correction equation

Where Δz is the elevation difference between the ground station and the nearest MERRA grid point and is defined as positive in the upward direction. Adiabatic air temperature adjustments were typically small (less than 1 °K) because the majority of locations used in this study had elevation differences less than 328 ft. However, a few study locations in complex terrain contained elevation differences upwards of 1,640 ft, which could result in temperature adjustments as large as 4 °K.

Statistical Comparisons of Data Sources

Statistical analyses were conducted between the different data sources relative to USCRN (i.e., USCRN treated as the reference measurement) for the approximately 17-year period of July 1, 1996, through September 1, 2013. This time period corresponds to the approximate temporal overlap of all of the available data sources used in this study. The emphasis of the statistical evaluation was on temperatures because prior studies had shown that pavement performance was most sensitive to these climate inputs.[1,2] Wind speed and cloud cover are the next most sensitive climate inputs; however, the USCRN data do not contain these data elements, and consequently, they could not be evaluated. Although the MEPDG in its current form assumes no infiltration of surface water into the pavement layers, precipitation data from the various climate data products were nevertheless compared. Cloud cover, wind speed, and humidity were also compared to a lesser extent. Cloud cover is important primarily because of its impact on incoming SSR at the ground surface. Although SSR is not a direct input in the MEPDG, it is the principal driver for pavement heating and cooling. To evaluate the SSR issue, SIRS observations were used to supplement the USCRN SSR observations. Hence, the following meteorological analyses were conducted in-depth: (1) near-surface air temperatures, (2) precipitation at the ground surface, and (3) shortwave radiation at the ground surface.

Comparisons of USCRN, QCLCD, and MERRA Hourly Data

Near-Surface Air Temperature

Hourly air temperatures were compared for QCLCD versus USCRN and MERRA versus USCRN data, where the USCRN data are the assumed ground reference values. (Note: Because MEPDG data are derived from QCLCD, MEPDG and QCLCD are used interchangeably here.) For a given collocated set of USCRN, QCLCD, and MERRA locations, only those portions of the air temperature time series that were present in all three records were used for the statistical analysis. Some of the spatially collocated datasets did not have any temporal overlaps. As a consequence, only 275 of the 354 spatially collocated data sets in figure 65 could be included in the statistical comparisons.

Figure 67 shows a typical comparison of the diurnal temperature variations from the MERRA and MEPDG/QCLCD datasets for a single site. Overall, the agreement is very good. Figure 68 shows a typical comparison of the hourly temperature frequency distributions from the MERRA and MEDPG/QCLCD datasets over the entire 17-year analysis period for a single site. Again, the overall agreement between the two datasets is very good.

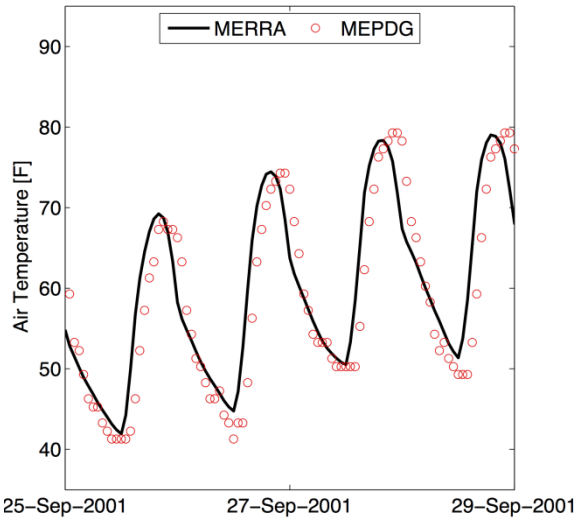

Figure 67. Graph. Typical comparison of diurnal temperature variations for MERRA versus MEPDG (QCLCD) data.

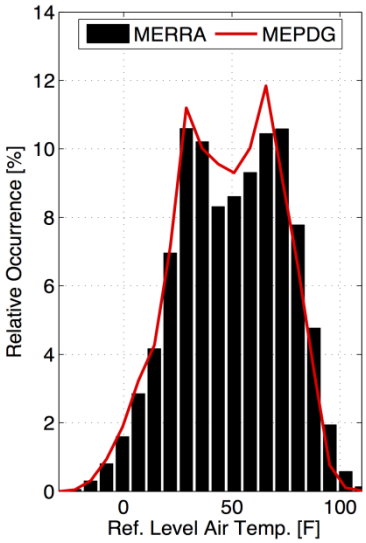

Figure 68. Graph. Typical comparison of hourly temperature frequency distributions for MERRA versus MEPDG (QCLCD) data.

The differences between QCLCD versus USCRN and MERRA versus USCRN hourly temperatures at coincident time points at a given location were used to compute bias and root mean squared error (RMSE). Figure 69 shows a typical frequency distribution for bias in the hourly temperatures for a single site located outside Chattanooga, TN. At this site, the MERRA data (average bias = 0.62 °F) compared better with the USCRN reference than did the QCLCD data (average bias = 2.00 °F), although the spread in the MERRA bias distribution was somewhat larger. At other sites, the QCLCD data compared better with the USCRN reference than did the MERRA data, but in most cases the average bias values were small—on the order of approximately 2 °F. Figure 70 is an example of a "worst-case" scenario for a site near Jacksonville, FL. Here the MERRA data (average bias = 5.52 °F) compared less well with the

USCRN reference than did the QCLCD data. This is not surprising for a location right on the coast where half of the MERRA grid cell may be over land and half over water.

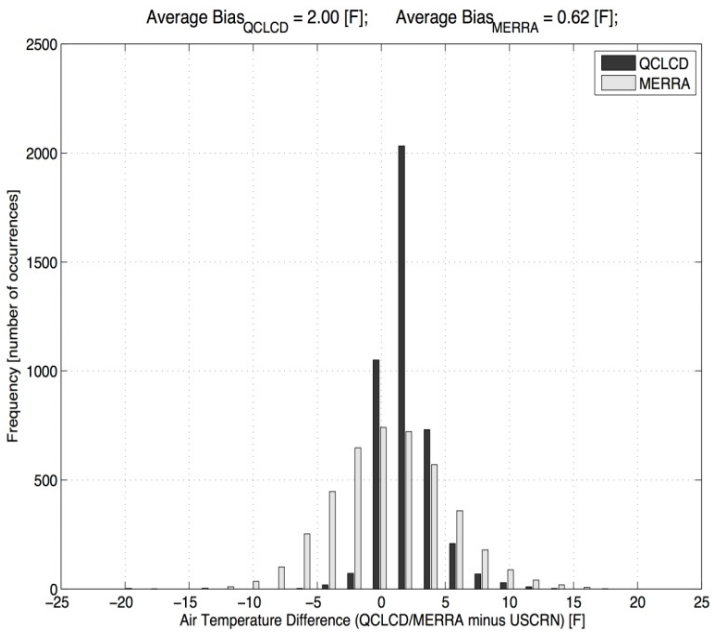

Figure 69. Graph. Frequency distribution of bias for QCLCD versus USCRN and MERRA versus USCRN hourly temperature values for a single site (outside Chattanooga, TN)—typical results.

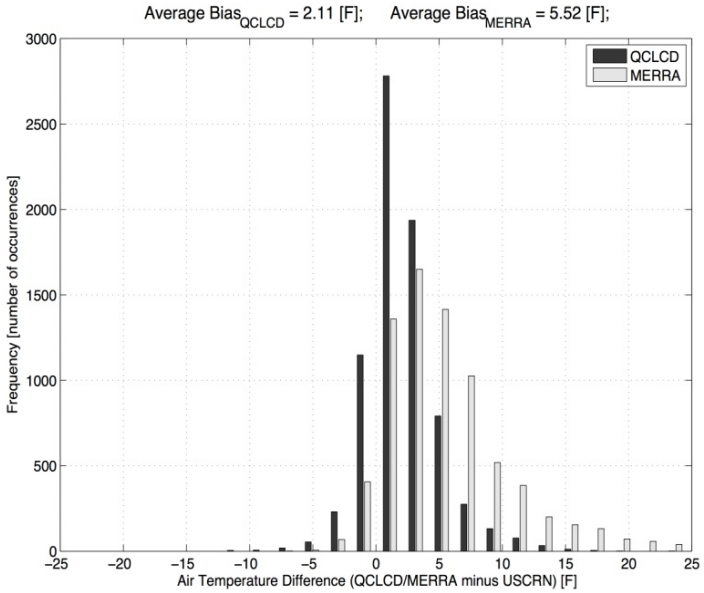

Figure 70. Graph. Frequency distribution of bias for QCLCD versus USCRN and MERRA versus USCRN hourly temperature values for a single site (near Jacksonville, FL)—worst-case results.

The calculations behind figure 69 and figure 70 were repeated at each of the other 273 collocated data sets to determine the average bias and RMSE in the QCLCD versus USCRN and MERRA

versus USCRN hourly temperature values at each site. The distributions of the average bias and RMSE values are illustrated in figure 71 and figure 72, respectively. The average of the average bias across all 275 data sets was 1.14 °F for QCLCD versus USCRN and 2.53 °F for the MERRA versus USCRN comparisons. The spread of the MERRA bias distribution is slightly broader than for the QCLCD data. The average RMSE values (figure 72) were 3.68 °F for the QCLCD versus USCRN and 5.91 °F for the MERRA versus USCRN comparisons. Overall, both the QCLCD and MERRA data were different and warmer than the USCRN reference values, with the MERRA data being slightly warmer and more variable.

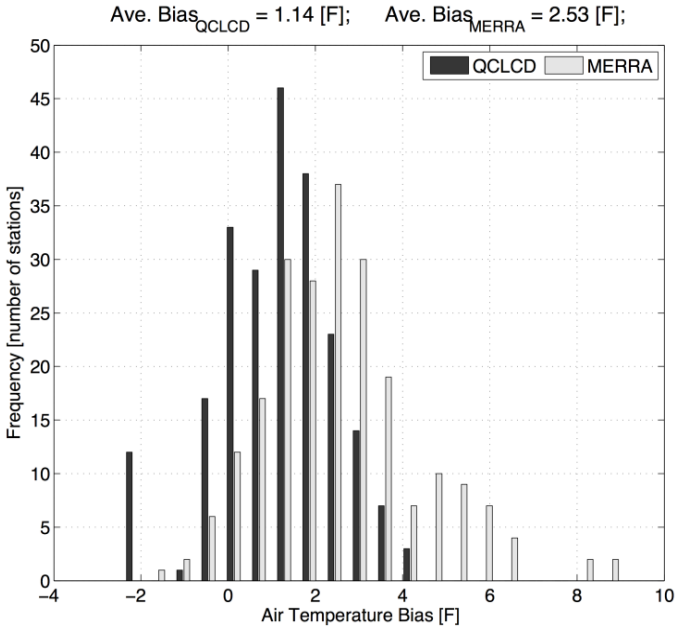

Figure 71. Graph. Frequency distribution of average hourly temperature bias across all sites for QCLCD versus USCRN and MERRA versus USCRN climate data.

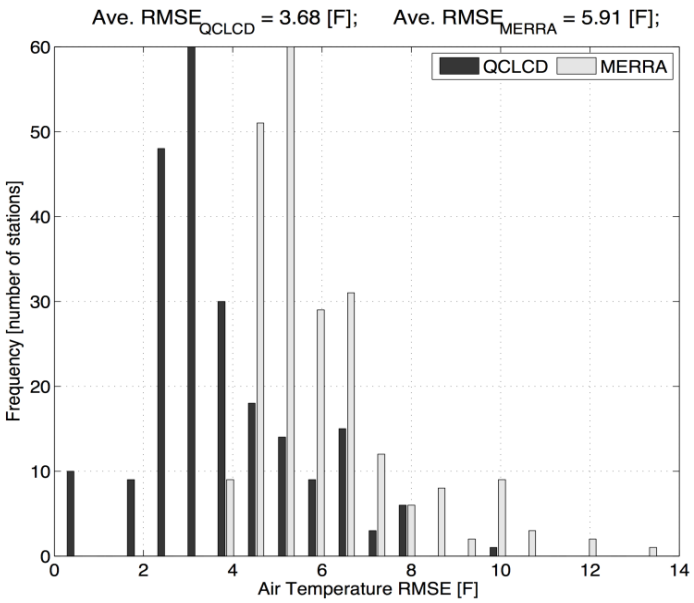

Figure 72. Graph. Frequency distribution of RMSE of QCLCD versus USCRN and MERRA versus USCRN hourly temperature values across all sites.

Precipitation at the Ground Surface

Analyses similar to those behind figure 71 and figure 72 were conducted for hourly precipitation rates for collocated USCRN, QCLCD, and MERRA stations. Only non-zero precipitation events were considered to better evaluate storm effects. More specifically, if at least one climate data source contained a non-zero hourly precipitation value, then that hour was included in the evaluation. If all of the data sources registered zero precipitation for an hour, then that hour was excluded. As shown in figure 73 and figure 74, both the QCLCD and MERRA data closely agree with USCRN precipitation measurements, but MERRA has 50 percent less average bias than does QCLCD (-0.00059 inches/h versus -0.00106 inches/h). Further, data from numerous QCLCD stations contain significant negative bias relative to USCRN, which is consistent with rain gauge "under catch," which is a known and pervasive problem with point-scale rain gauges.[(68)] The RMSE is also slightly lower in the MERRA estimates (0.032 inches/h versus 0.036 inches/h for QCLCD).

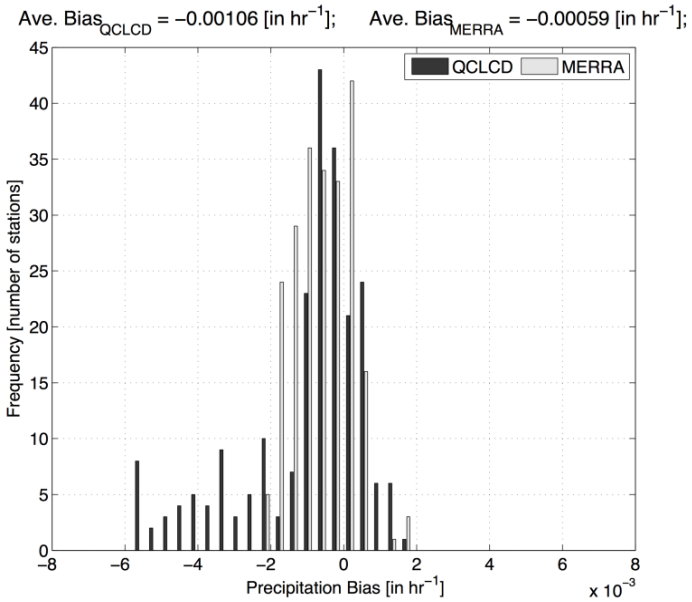

Figure 73. Graph. Frequency distribution of average hourly precipitation bias across all sites for QCLCD versus USCRN and MERRA versus USCRN climate data.

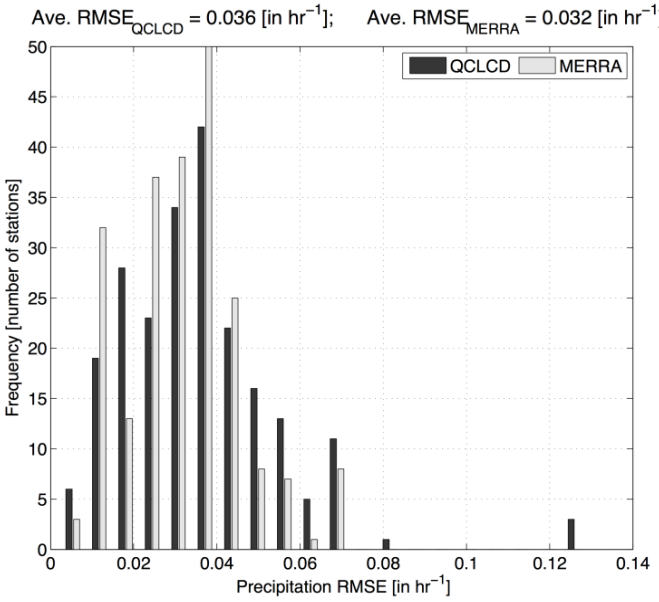

Figure 74. Graph. Frequency distribution of RMSE of QCLCD versus USCRN and MERRA versus USCRN hourly precipitation rates across all sites.

Comparisons of USCRN, COOP, and MERRA Daily Temperatures

The statistical analysis approach employed for hourly temperature data was repeated for daily mean, minimum, and maximum temperatures. The daily USCRN measurements were compared against daily values from the NWS COOP data as well as daily values derived from the original hourly MERRA estimates. Figure 75 shows the distribution of the collocated USCRN, COOP, and MERRA sites. The daily mean, minimum, and maximum temperatures from USCRN and MERRA were extracted from the original hourly temperature data. There was insufficient

temporal overlap of the data for some of the sets of collated sites to enable computation of meaningful statistics. Statistical comparisons were made only where a large (> 100) number of daily readings were available for comparison.

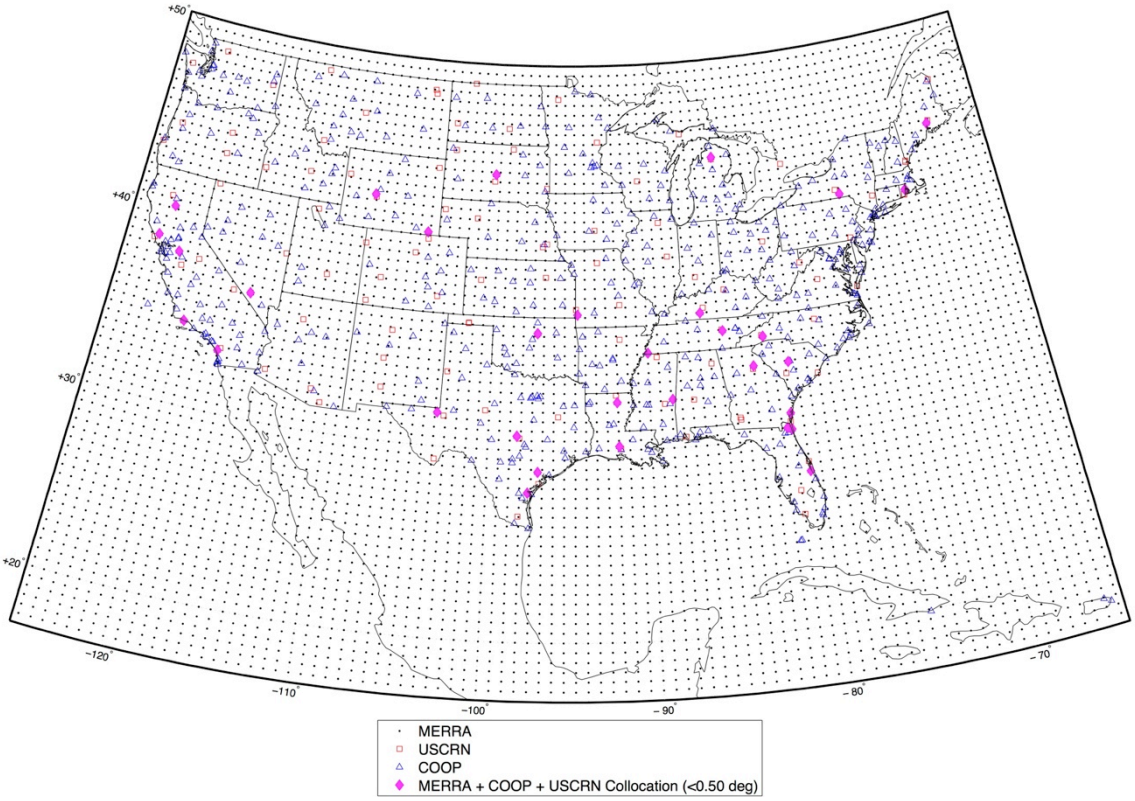

Figure 75. Map. Collocated USCRN, COOP, and MERRA data sets.

The average bias and RMSE for the COOP versus USCRN and MERRA versus USCRN daily mean temperature values were computed for each set of collocated sites. The distributions of these bias and RMSE values are illustrated in figure 76 and figure 77, respectively. The average of the average bias across all sites (figure 76) was 1.85 °F for COOP versus USCRN and 2.73 °F for the MERRA versus USCRN comparisons. The average RMSE values (figure 77) were 3.03 °F for the COOP versus USCRN and 4.20 °F for the MERRA versus USCRN comparisons. Overall, both the COOP and MERRA daily mean temperatures were different and warmer than the USCRN reference values, with the MERRA data being slightly warmer and more variable.

Figure 78 and figure 79 summarize the average bias and RMSE for the COOP versus USCRN and MERRA versus USCRN daily minimum temperature values. The average of the average bias across all sites (figure 78) was 0.68 °F for COOP versus USCRN and 3.61 °F for the MERRA versus USCRN comparisons. The average RMSE values (figure 79) were 3.34 °F for the COOP versus USCRN and 6.04 °F for the MERRA versus USCRN comparisons. These findings suggest COOP does a better job of capturing the lower range of the diurnal air temperature than does MERRA. This is likely due to the spatial mismatch between the point-scale observations (i.e., USCRN and COOP) and grid cell scale estimates produced by MERRA. The adiabatic air temperature correction for elevation differential may also contribute to these differences.

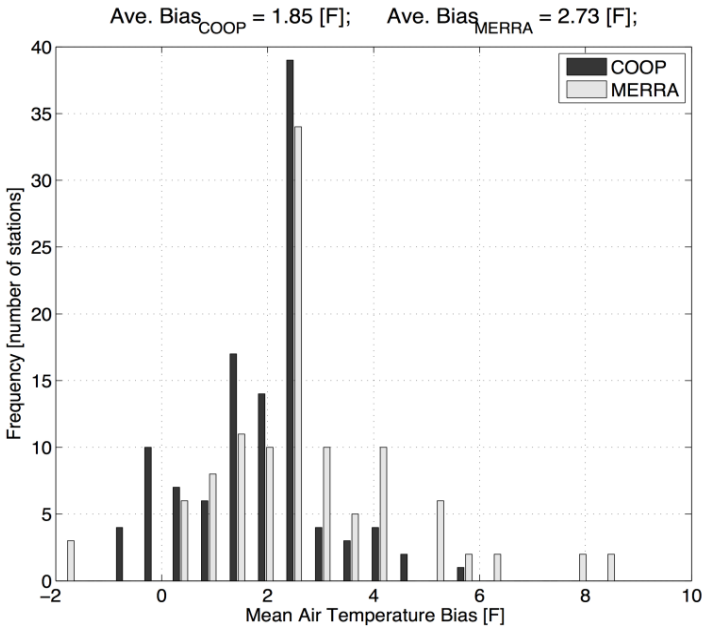

Figure 76. Graph. Frequency distribution of daily mean temperature bias across all sites for COOP versus USCRN and MERRA versus USCRN climate data.

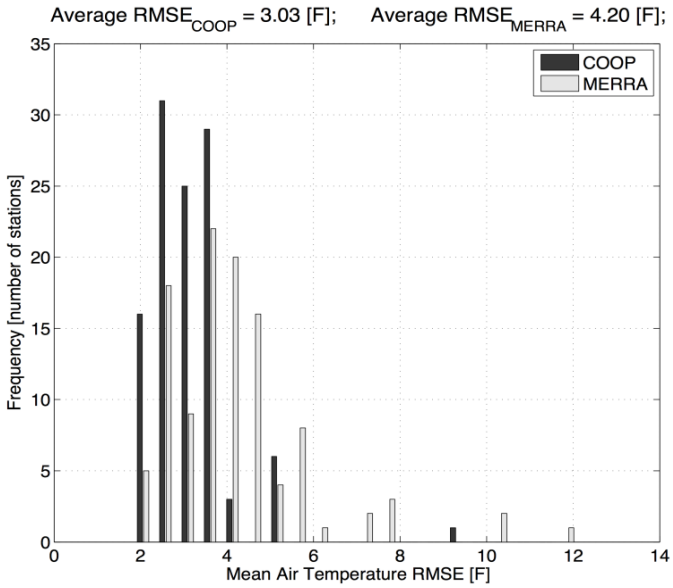

Figure 77. Graph. Frequency distribution of RMSE of COOP versus USCRN and MERRA versus USCRN daily mean temperature values across all sites.

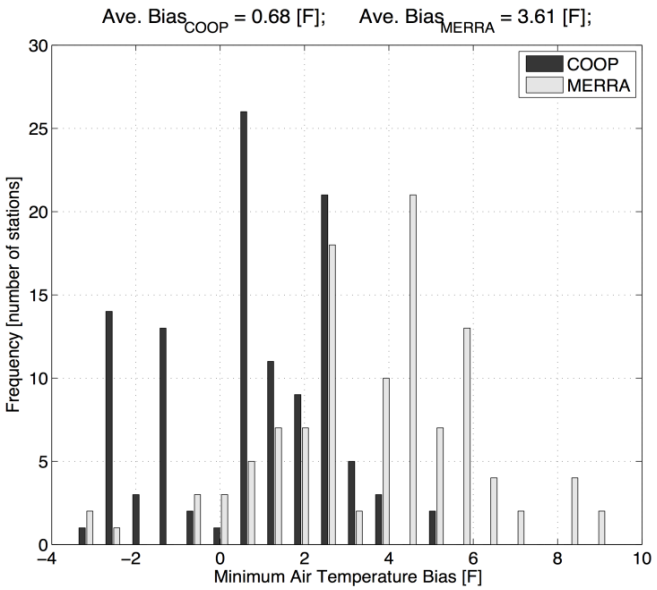

Figure 78. Graph. Frequency distribution of daily minimum temperature bias across all sites for COOP versus USCRN and MERRA versus USCRN climate data.

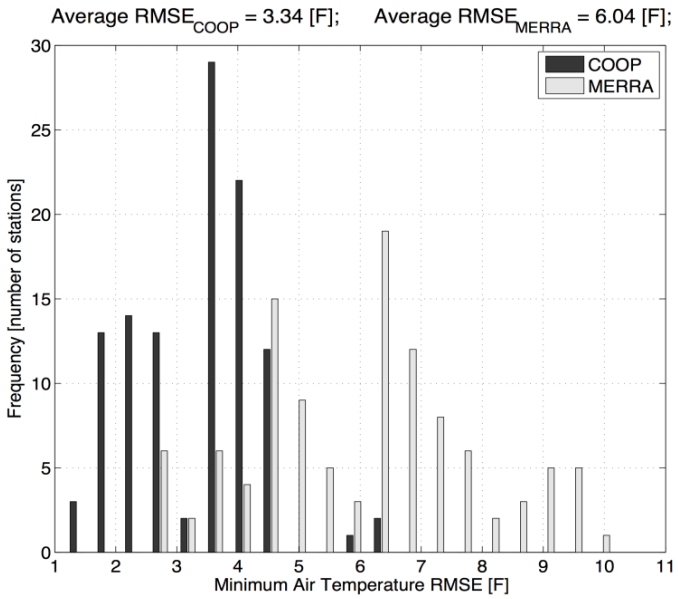

Figure 79. Graph. Frequency distribution of RMSE of COOP versus USCRN and MERRA versus USCRN daily minimum temperature values across all sites.

Figure 80 and figure 81 summarize the average bias and RMSE for the COOP versus USCRN and MERRA versus USCRN daily maximum temperature values. The average of the average bias across all sites (figure 80) was 2.46 °F for COOP versus USCRN and 2.88 °F for the MERRA versus USCRN comparisons. The average RMSE values (figure 81) were 3.46 °F for the COOP versus USCRN and 5.21 °F for the MERRA versus USCRN comparisons. Overall, both the COOP and MERRA daily maximum temperatures were different and warmer than the USCRN reference values, with the MERRA data being slightly warmer and more variable.

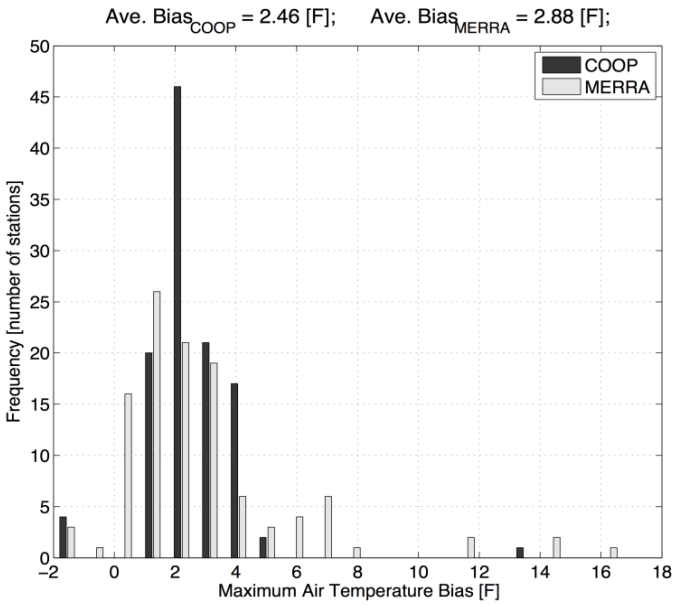

Figure 80. Graph. Frequency distribution of daily maximum temperature bias across all sites for COOP versus USCRN and MERRA versus USCRN climate data.

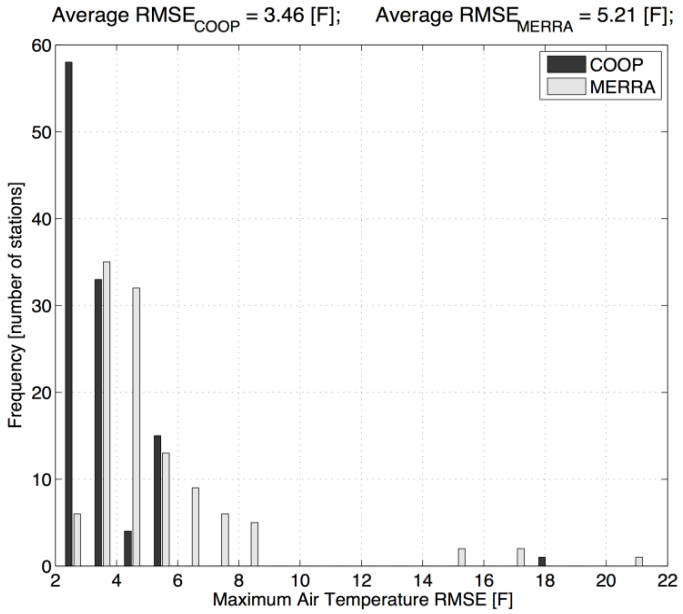

Figure 81. Graph. Frequency distribution of RMSE of COOP versus USCRN and MERRA versus USCRN daily maximum temperature values across all sites.

Comparisons of Hourly SIRS, QCLCD, and MERRA SSR

Although SSR is not a direct input in the MEPDG, it is the principal driver for pavement heating and cooling. Both USCRN and the SIRS were used as ground truth to evaluate the SSR issues.

The USCRN and SIRS stations use radiometers to directly measure the SSR at the site. The QCLCD sites (and, by association, the MEPDG weather station data) do not have radiometers and thus do not measure SSR. In the EICM calculations embedded in the MEPDG software, the

downwelling shortwave radiation is determined using an empirical equation that is a function of cloud cover as shown in figure 82:

$$Q_s = a_s R \left(A + B \frac{S_c}{100}\right)$$

Figure 82. Equation. Downwelling shortwave radiation.

Where Q_s downwelling (incoming) shortwave radiation, a_s is the surface shortwave absorptivity of the pavement, and *R* is the shortwave radiation at the top of the atmosphere that is a function of latitude and seasonally varying solar declination. The term S_c is the percentage of sunshine computed as $S_c=1–NW$, where *N* is a cloud base factor equal to 0.9 to 0.8 for cloud heights of 1,000 to 6,000 ft, and *W* is the average cloud cover during day or night.(66) The constants *A* and *B* are empirical terms that account for diffuse scattering and adsorption by the atmosphere; the values of *A* and *B* incorporated in the MEDPG, which are based on data for the upper Midwest and Alaska, equal 0.202 and 0.539, respectively.(58) This empirical expression is required only with the QCLCD measurements because USCRN, SIRS, and MERRA all provide direct measurement or estimates of downwelling shortwave radiation.

Figure 83 and figure 84 summarize the average bias RMSE for the QCLCD versus USCRN and MERRA versus USCRN SSR values across all collocated data sets. Recall that each point in figure 83 represents the average of the hourly SSR bias values over the entire duration of temporally matched data series at a single site. Each point in figure 84 represents the RMSE of the hourly SSR values at a single site. The average of the average bias across all sites (figure 83) was 20 W/m^2 for QCLCD versus USCRN and 51 W/m^2 for the MERRA versus USCRN comparisons. For perspective, these values can be compared against the maximum shortwave radiation at the top of atmosphere equal to 1,366 W/m^2; the bias values are less than 4 percent of this maximum. The average RMSE values (figure 84) were 176 W/m^2 for the QCLCD versus USCRN and 166 W/m^2 for the MERRA versus USCRN comparisons. Overall, both the QCLCD and MERRA SSR values were different and slightly higher than the USCRN reference values.

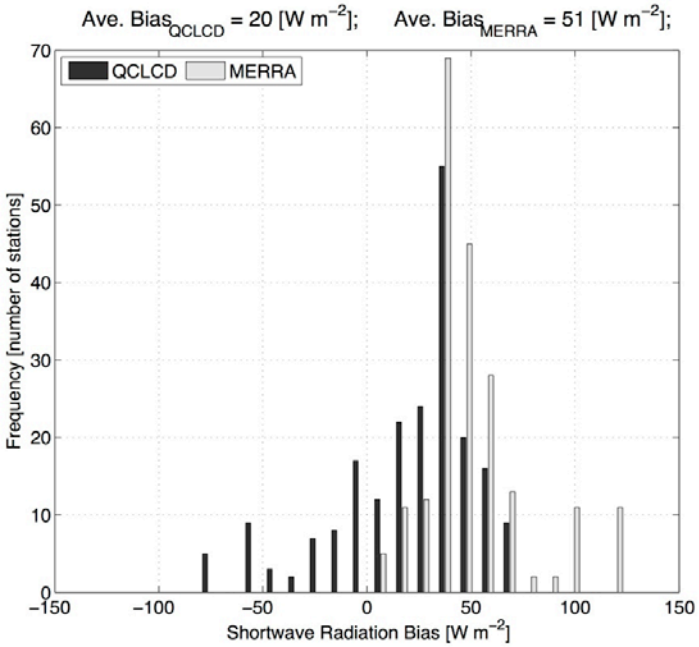

Figure 83. Graph. Frequency distribution of SSR bias across all sites for QCLCD versus USCRN and MERRA versus USCRN climate data.

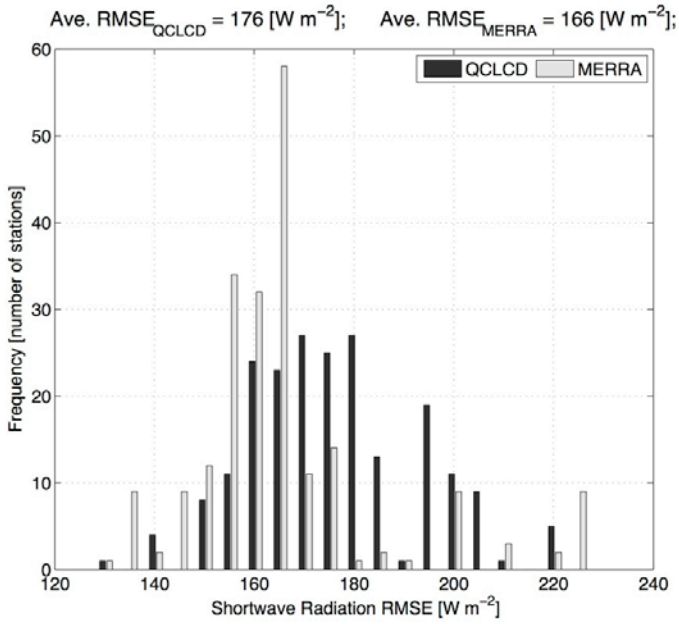

Figure 84. Graph. Frequency distribution of RMSE of QCLCD versus USCRN and MERRA versus USCRN SSR values across all sites.

Five SIRS sites were used for a more in-depth evaluation of SSR differences. The SIRS sites, which are all located in the southern Great Plains, were designed specifically for collecting SSR data using very sophisticated and accurate radiometers. Figure 85 and figure 86 summarize the bias and RMSE for QCLCD versus SIRS and MERRA versus SIRS climate data as a function of cloud cover. Several important insights can be drawn from these figures. During periods of low cloud cover—i.e., periods of maximum SSR and pavement heating—the QCLCD has high

positive biases and variability relative to MERRA. MERRA has a greater positive bias during periods of heavy cloud cover but these conditions generally do not correspond to the extremes for pavement performance.

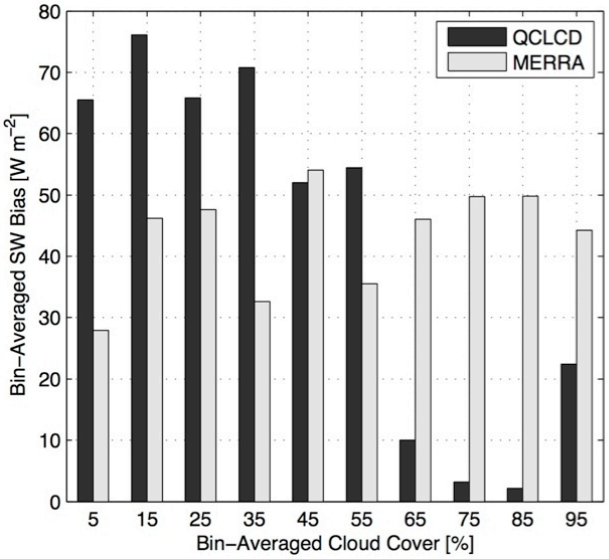

Figure 85. Graph. SSR bias as a function of cloud cover for QCLCD versus SIRS and MERRA versus SIRS climate data.

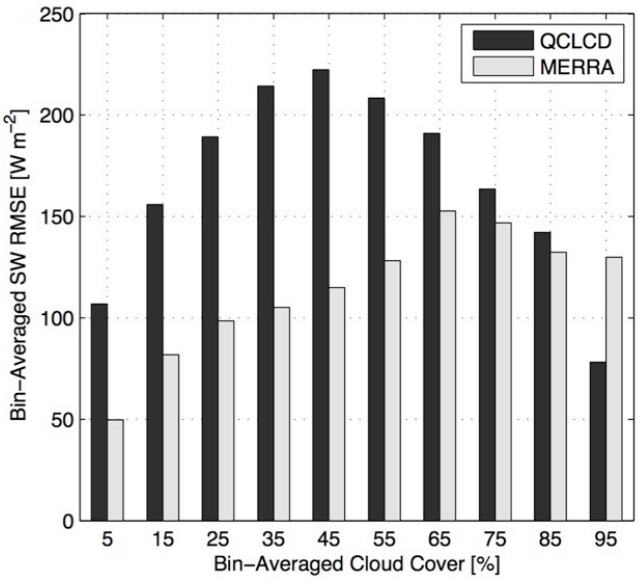

Figure 86. Graph. SSR RMSE as a function of cloud cover for QCLCD versus SIRS and MERRA versus SIRS climate data.

A complementary trend can be observed as a function of season. Figure 87 shows the bias in daily averaged SSR for QCLCD versus SIRS and MERRA versus SIRS for each month during the analysis period. The QCLCD data show much higher biases than MERRA during the summer months of May through September—the critical period of maximum pavement heating. Conversely, the MERRA data show higher biases during the later winter and spring months of

January through April; these are generally less critical periods for pavement heating and performance. The RMSE values for both sets of climate data are relatively similar (figure 88).

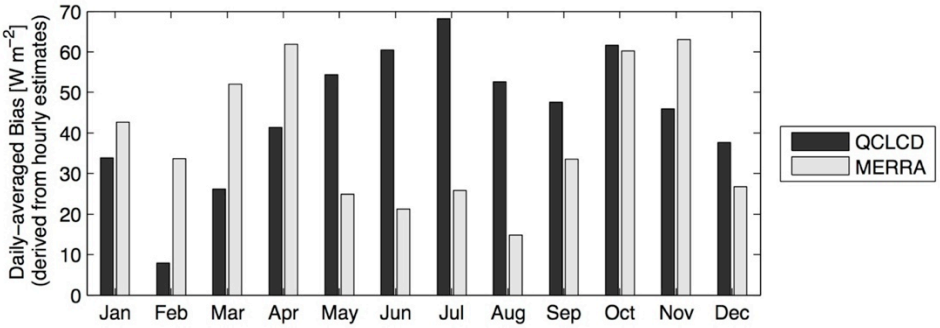

Figure 87. Graph. SSR bias as a function of season for QCLCD versus SIRS and MERRA versus SIRS climate data.

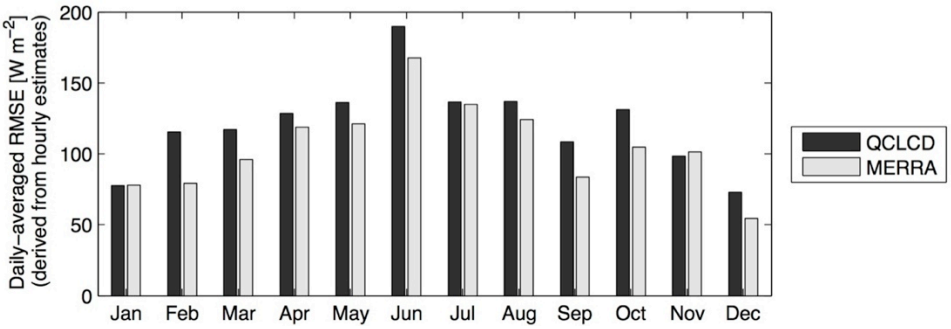

Figure 88. Graph. SSR RMSE as a function of season for QCLCD versus SIRS and MERRA versus SIRS climate data.

The overall conclusions drawn from these data are as follows. The SSR values from the QCLCD data estimated empirically using the equation in figure 82 and the values predicted by the MERRA approach show similar bias on an annual basis. However, when disaggregated into bias as a function of cloud cover and bias as a function of month of year, the QCLCD data tend to have higher positive biases during the critical extreme-temperature periods for the pavement—low cloud cover and summer months—compared with the MERRA data. This may be a consequence of the empirical relation used in the EICM to estimate SSR based on top-of-atmosphere radiation and cloud cover. Use of the MERRA direct SSR data eliminates the need for this type of empirical relationship.

Conclusions From Statistical Comparisons

The overall conclusions from the statistical comparisons of the various climate data sources can be summarized as follows:

- Although in concept, the USCRN data are the closest thing to ground truth, it is the opinion of the project team that the concept of ground truth does not truly exist for climate data. Given the expected measurement errors and the spatial variability of

weather data over even short distances, even two ground truth stations separated by only a few hundred meters will inevitably give slightly different climate data time series.

- The statistical comparisons of hourly data found that the QCLCD and MERRA data have small and roughly comparable differences from the USCRN values. The average bias and RMSE computed for the QCLCD and MERRA data compared with the USCRN reference for average hourly temperature are summarized in table 13. (Recall that temperature is the most sensitive climate data input for the MEPDG models.) The MERRA data are slightly warmer on average than the QCLCD values but only by slightly more than 1 °F in most cases.

- The statistical comparisons of daily temperature data found that the COOP and MERRA data have small but roughly comparable differences from the USCRN values. The average bias and RMSE computed for the COOP and MERRA data compared with the USCRN reference for mean, minimum, and maximum daily temperatures are summarized in table 14. The MERRA data are slightly warmer than the COOP values, but in most cases by less than 1 °F.

- The comparisons for MEPDG SSR calculations against predicted MERRA and measured SIRS values found that the bias was generally small in comparison to peak solar radiation values. However, the MEPDG values had higher positive bias and variability than MERRA during critical low percent cloud cover conditions and hot summer months, and lower positive bias during the less important late winter months. The project team recommends that the Pavement ME Design® Task Force explore the option of using SSR as a direct input rather than percent cloud cover.

Table 13. Summary of statistical comparisons of QCLCD versus USCRN and MERRA versus USCRN hourly climate data.

	Bias		RMSE	
	QCLCD	MERRA	QCLCD	MERRA
Average Hourly Temperature (°F)	1.14	2.53	3.68	5.91

Table 14. Summary of statistical comparisons of COOP versus USCRN and MERRA versus USCRN daily climate data.

	Bias		RMSE	
	COOP	MERRA	COOP	MERRA
Average Daily Mean Temp (°F)	1.85	2.73	3.03	4.20
Average Daily Min Temp (°F)	0.68	3.61	3.34	6.04
Average Daily Max Temp (°F)	2.46	2.88	3.46	5.21

COMPARISONS OF PREDICTED PAVEMENT PERFORMANCE

Pavement performance as predicted by the MEDPG models incorporated in the Pavement ME Design® software was evaluated using the MEPDG weather data files provided with the software (derived from the QCLCD and ULCD products from NCDC) and the MERRA climate data for collocated sites and congruent time series. A total of 20 sites were analyzed; their distribution across the contiguous United States is shown in figure 89.

It would have been ideal to evaluate MEPDG performance predictions using the USCRN ground truth data in addition to the MEDPG and MERRA weather time series. However, the USCRN data do not include the wind speed and cloud cover data required for the MEPDG models. Several attempts were made to synthesize these missing data from other sources but none was satisfactory.

Both new flexible pavements and new JPCP were analyzed. The pavement structures, traffic loads, material properties, and other inputs for the analysis correspond to the medium traffic cases for the sensitivity analyses described in Schwartz et al.[(1)] All analyses were performed using version 2.0 of the Pavement ME Design® software.

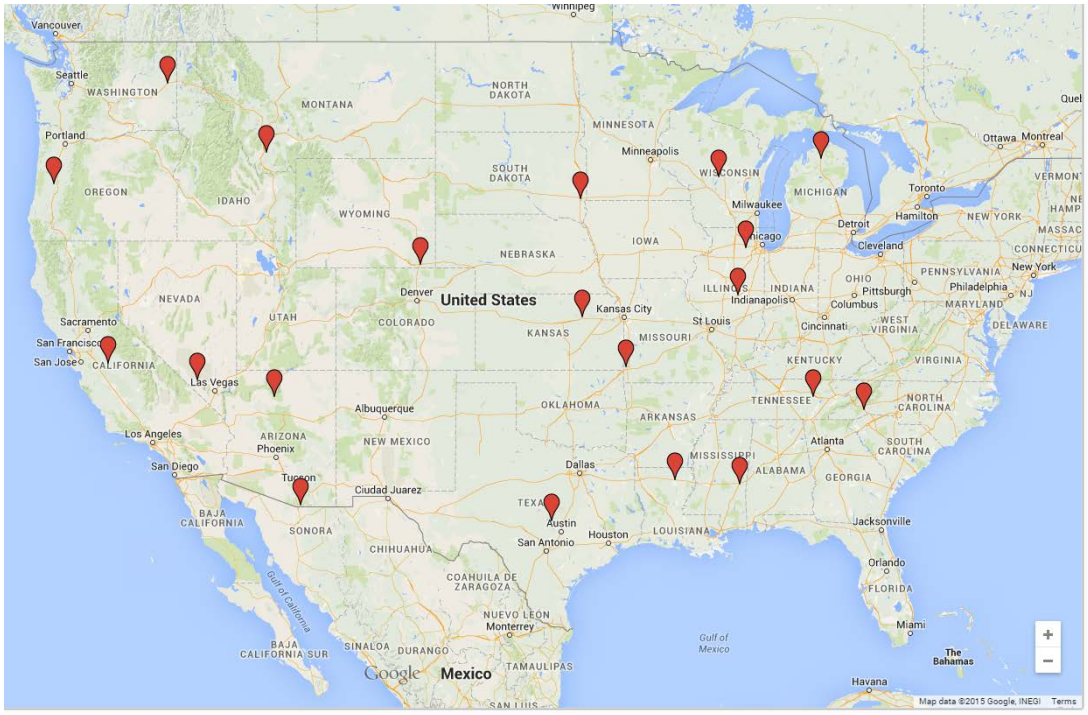

©2014 Google®

Figure 89. Map. Sites used for evaluation of MEPDG performance predictions using MEPDG and MERRA climate data.[(69)]

Comparisons of flexible pavement performance as predicted by the MEPDG using MERRA versus MEPDG weather data are shown in figure 90 for total rutting, figure 91 for AC rutting, figure 92 figure 92 for alligator fatigue cracking, figure 94 for top-down fatigue cracking, and figure 95 for roughness. In all cases, the predictions are clustered tightly although not perfectly

along the respective lines of equality. This is consistent with the close but not perfect agreement found among these climate data time series in the statistical comparisons described previously. The worst agreement in performance predictions is for top-down fatigue cracking (figure 94). However, this model is also generally viewed as unreasonably sensitive and unrealistic; a replacement for the current top-down fatigue cracking model is currently being developed in NCHRP Project 1-52.

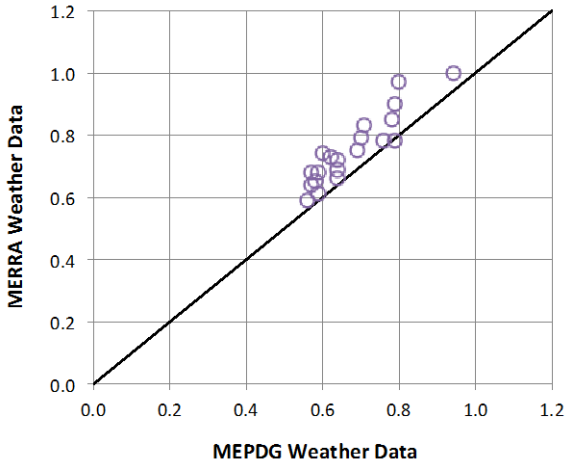

Figure 90. Graph. Comparison of MEPDG total rutting predictions (inches) using MERRA versus MEPDG weather data.

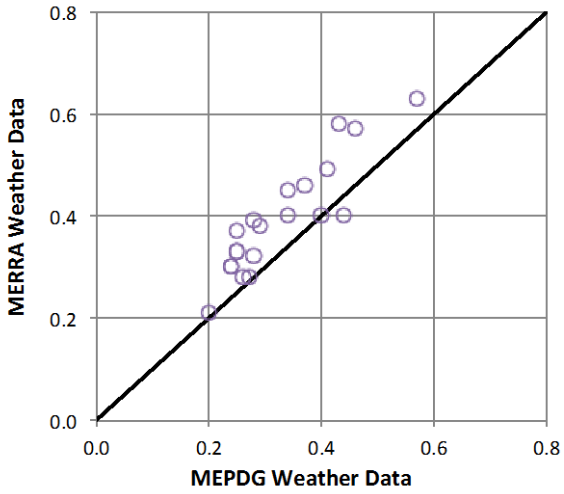

Figure 91. Graph. Comparison of MEPDG AC rutting predictions (inches) using MERRA versus MEPDG weather data.

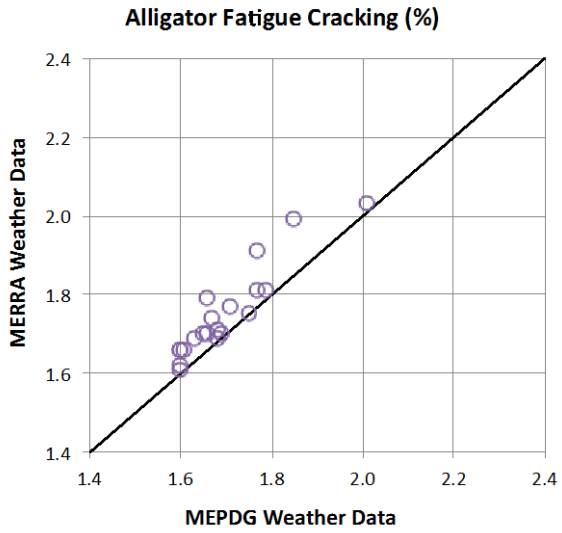

Figure 92. Graph. Comparison of MEPDG alligator fatigue cracking predictions using MERRA versus MEPDG weather data.

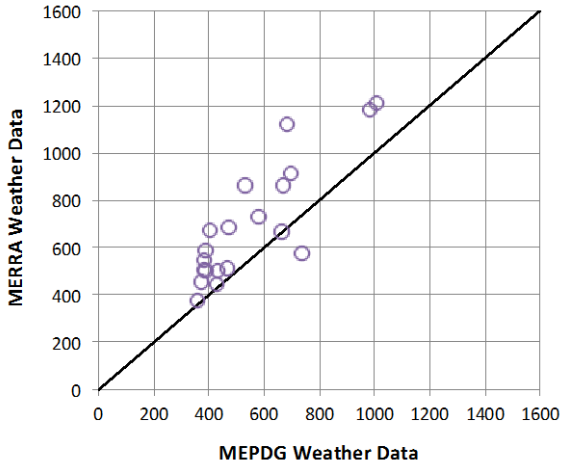

Figure 93. Graph. Comparison of MEPDG top-down fatigue cracking predictions (ft/mi) using MERRA versus MEPDG weather data.

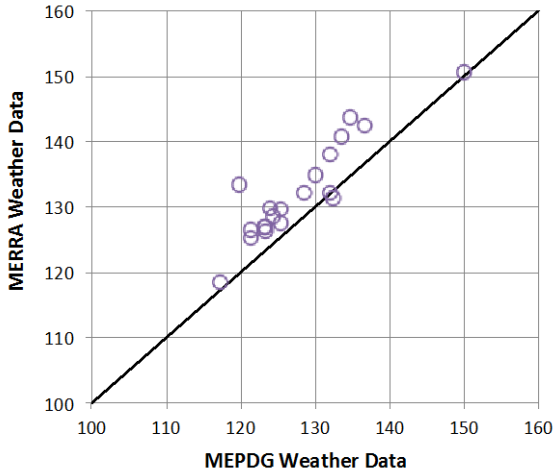

Figure 94. Graph. Comparison of MEPDG flexible pavement IRI predictions (inches/mi) using MERRA versus MEPDG weather data.

Comparisons of rigid JPCP pavement performance as predicted by the MEPDG using MERRA versus MEPDG weather data are shown in figure 95 for transverse cracking, figure 96 for joint faulting, and figure 97 for roughness. In all cases, the predictions are clustered tightly although not perfectly along the respective lines of equality. This is consistent with the close but not perfect agreement found among these climate data time series in the statistical comparisons described previously. The agreement between the MERRA versus MEPDG weather data cases for rigid pavement performance is somewhat less than for flexible pavements. However, this is consistent with the fact that rigid pavement performance is more sensitive to shorter term (e.g., diurnal) temperature variations and thus to the differences between MERRA versus MEPDG weather data over short time periods.

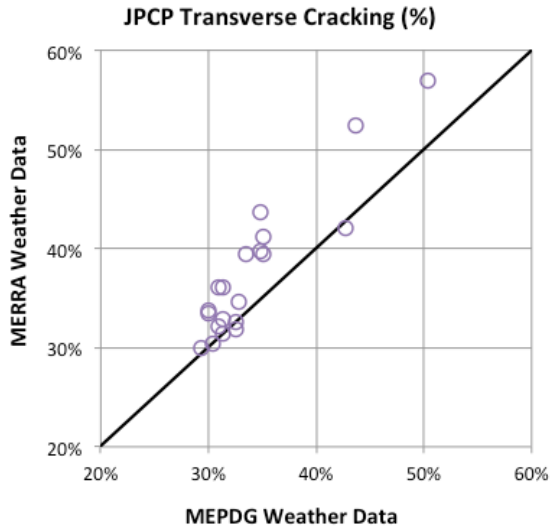

Figure 95. Graph. Comparison of MEPDG JPCP transverse cracking predictions using MERRA versus MEPDG weather data.

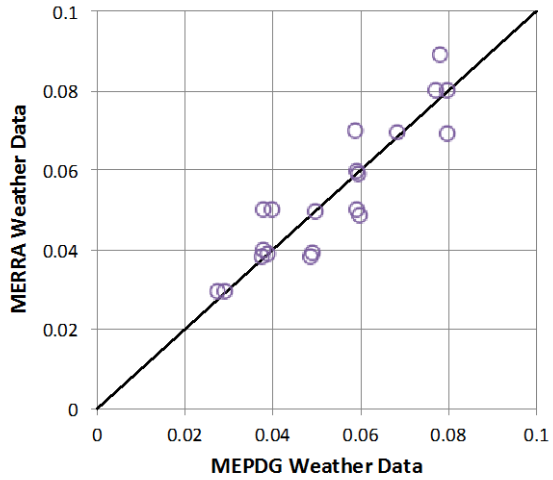

Figure 96. Graph. Comparison of MEPDG JPCP joint faulting predictions (inches) using MERRA versus MEPDG weather data.

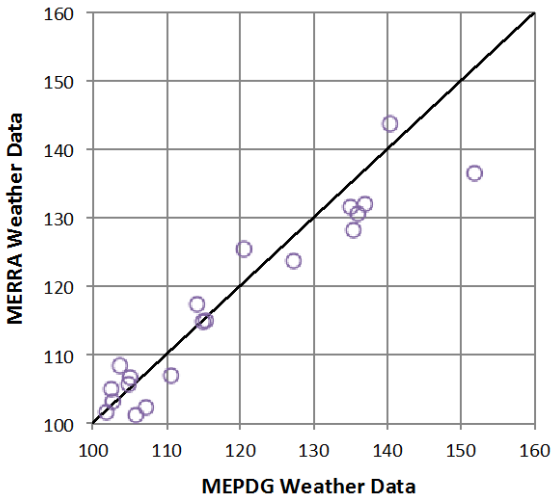

Figure 97. Graph. Comparison of MEPDG rigid pavement IRI predictions (inches/mi) using MERRA versus MEPDG weather data.

Overall, the comparisons of MEPDG predicted performance for both flexible and rigid pavements using MERRA versus MEPDG weather data are close and acceptable for engineering design. Based on the earlier statistical comparisons among the various climate data sources, the agreement in predicted performance using MERRA versus USCRN ground truth and/or MEPDG versus USCRN would likely show similar scatter in agreement as seen in figure 90 through figure 97. However, it is impossible to demonstrate this because the USCRN data lack the wind speed and cloud cover inputs required by the MEPDG software.

RECOMMENDATIONS

The results of the more extensive statistical and pavement performance comparisons reported here support the original recommendation that LTPP should adopt MERRA as a data source for its next update to the climate data module and develop a tool to extract and use this data for engineering applications.

CHAPTER 7. RECOMMENDATIONS

This study effort started out on the premise that improvements to the existing LTPP approach using ground-based weather observations to describe general climate statistics at its test sites could be used to satisfy current MEPDG climate input requirements and emerging infrastructure research needs. However, in the course of this research, the study team discovered a new source of climate data, MERRA, which provides a continuous hourly estimate of all of the climate-related data based on state-of-the-art global modeling.

The current MEPDG pavement performance models were used as an evaluation tool to compare and contrast the influence of weather histories obtained from onsite AWS, OWS, VWS, and MERRA data sources. In this study, limitations in the current climate data and modeling incorporated in the MEPDG and accompanying AASHTOWare Pavement ME Design® software were also discovered. These findings either suggest that the current MEPDG models are not appropriate for this type of climate data evaluation or that these models can be improved, especially if MERRA is the source of climate data. Regardless, the MEPDG models were chosen as the evaluation tool because they represent the most advanced models in pavement performance forecasting today.

SUMMARY OF RECOMMENDATIONS

Based on the results of this phase of the research effort, the study team recommends the following:

1. The LTPP program should use the MERRA dataset as the basis for continuous hourly climate data histories for its test locations.

2. Using the MERRA data set, LTPP should calculate the same derived computed climate statistics as shown in table 1.

3. The LTPP program should not add the TMI as a new computed parameter to the climate module. There is no compelling reason to include it in the LTPP database. It is no longer needed if the MERRA dataset is adopted by LTPP, because MERRA contains the data used to determine TMI.

4. The CLM module in the LTPP database should be modified to contain MERRA data for the cells where LTPP test sections are currently located.

5. The existing LTPP CLM data module should be retained in the LTPP Information Management System as archived data so that the data are still available upon request.

The following portions of this chapter provide more details on the basis of these recommendations.

BENEFITS OF USING MERRA DATA

MERRA is a new source of weather data for use in pavement and other transportation infrastructure modeling applications. As described in chapter 4, MERRA provides continuous

hourly weather data on a relatively fine-grained uniform special grid for 1979 to the present. Most MERRA data elements are fundamental physics-based quantities, many of which are not available from any ground-based or other conventional climate data source. Only a small subset of the MERRA data elements is needed to develop weather inputs for current infrastructure applications such as the MEPDG. The full set of MERRA data elements may enable development of much more powerful infrastructure applications in the future.

MERRA data satisfy all of the major study objectives. They meet the climate data needs for current infrastructure applications such the MEPDG, LTPPBind, HIPERPAV®, and bridge management. The broad range of MERRA data means that it will likely meet the climate data needs for future applications as well. The attention to quality and continuity in MERRA data eliminates the need to deal with temporal changes in position and/or measurement details of OWS histories. The close and uniform spacing of MERRA grid points also eliminate the need for improved weather data interpolation and use of VWS. Lastly, MERRA makes moot the issue of continued location-specific solar radiation measurement, as MERRA provides this information directly at every grid point.

MERRA offers the following benefits compared with conventional ground-based OWS data:

- **Denser, more uniform, and broader spatial coverage**. The ASOS network of first-order ground-based weather stations provides data at approximately 1,000 locations in the contiguous United States. These locations are not distributed uniformly across the country but rather are concentrated in areas with high population density (and an airport). Vast areas of the country have sparse or no ASOS coverage. MERRA data, by contrast, are currently available at more than 3,000 grid points in the contiguous United States and worldwide coverage at similar resolution. MERRA grid points are uniformly distributed at a horizontal spacing of approximately 31.1 mi by 37.3 mi. In other words, no point in the continental United States is more than 24.9 mi from the nearest MERRA grid centroid. This nearest grid point distance will become dramatically smaller when MERRA moves to an approximately 0.62 mi by 0.62 mi horizontal grid spacing; NASA is currently using this higher resolution data in-house, and it is expected to be made available to the public within the next few years.

- **Better temporal frequency and continuity.** MERRA provides weather data at hourly time intervals as required by current state-of-the-art infrastructure modeling applications such as the MEPDG and HIPERPAV®. Daily, monthly, and/or annual statistics are also available directly from MERRA or can be aggregated from the hourly data. There are no gaps in the MERRA histories as often appear in the AWS data and other OWSs. All MERRA data are referenced to Greenwich Mean Time, eliminating issues of local time conversions and discontinuities in the data at changes to/from Daylight Savings Time.

- **Excellent data consistency and quality.** NASA developed MERRA for use in its own modeling applications and satellite retrieval algorithms. To meet these in-house needs, NASA performs rigorous and sophisticated QC checks to ensure that all MERRA data are consistent and correct even as the mix of satellites and other sources of measurement data inevitably change across time and location. LTPP's need for

extensive QC checks such as those in place for the current CLM module will be greatly reduced.

- **Focus on fundamental physical quantities.** MERRA data include data elements that are much more relevant to the fundamental inputs required by thermodynamics-based infrastructure modeling than are available from the first-order ASOS data. For example, MERRA directly provides the shortwave radiation fluxes at the top of atmosphere and ground. In the MEPDG, these quantities are estimated using empirical and semi-empirical relationships that are functions of location, time, and percent sunshine category. Given that net shortwave radiation flux at the surface is the primary driver for pavement temperature distributions, the MERRA data are much more suitable. The ready availability of MERRA data will likely foster improvements to current infrastructure modeling applications such as the MEPDG.

- **Richer and more versatile datasets.** To meet NASA's diverse modeling requirements, MERRA reports hundreds of data elements, although not all of these are at the highest temporal and spatial resolutions. Many of these data elements may be useful to future infrastructure and other modeling applications.

- **Potential for automated updates to LTPP database.** The process of requesting MERRA data, downloading it from the server, extracting and processing the data elements relevant to LTPP needs, and importing these data into the LTPP database has the potential to be highly automated. This could enable more frequent updates to the CLM module at significantly less cost.

- **Improvement over time.** NASA is currently enhancing MERRA to an approximately 1 km spatial resolution. This means that no location will be more than 2,297 ft from the nearest MERRA grid centroid. Significant improvement in conventional ground-based OWS coverage is very unlikely.

- **Reliability analysis capabilities.** MERRA is only one, albeit the most comprehensive, retrospective reanalysis system available. Others have been developed in Europe, Japan, and elsewhere. These various modeling applications could be applied simultaneously to develop ensembles of weather histories. Statistical characterization of these ensembles could provide a rational basis for quantifying the uncertainty of predicted infrastructure performance due to the weather inputs.

MERRA does, of course, have some limitations, including the following:

- **Grid points are not at project location.** The current version of MERRA will have a grid point centroid no further than about 40 km from any project location. This is generally sufficient for the roughly 70 percent of the United States with relatively flat terrain. This distance may not be sufficient in mountainous regions with isolated microclimates but in general, there will be no OWS that can realistically represent these microclimate weather histories either. The current version of MERRA is thus no worse than the OWSs in this regard, and MERRA will be significantly better after the 1 km horizontal resolution upgrade is released to the public. AWSs can obviously

capture future (but not historical) climate conditions at a specific site, but it is unrealistic to expect deployment of these instruments at project sites other than for research purposes.

- **Spatial averaging over grid cell volume.** Some MERRA data represent averages over the grid cell volume as opposed to point measures provided by OWSs. However, given the MERRA grid points are often located closer to project sites than any OWS, the question is "Which is worse—spatially averaged values around the vicinity of the site or point values at the wrong point?" This arguable limitation of the MERRA data will become less important as the MERRA grid point resolution increases and associated grid cell volume decreases in the future.

- **MERRA data begin in 1979**. For LTPP test sections built before 1979, MERRA will not be able to provide a complete climate history over the entire service life of the project. However, OWS data prior to 1980 are also very sparse, especially at hourly time intervals. MERRA is thus no worse than OWS data in this regard. In addition, it is unclear how important these earlier climate data are to current infrastructure modeling applications.

- **MERRA hourly data storage will require changes to LTPP database.** Hourly weather data are required for current state-of-the-art infrastructure modeling applications such as the MEPDG and HIPERPAV®. The LTPP database will therefore need to be restructured to accommodate these data regardless of whether they come from MERRA or OWSs.

In summary, MERRA offers many benefits and very few if any significant limitations for use as the source of climate data for transportation infrastructure modeling applications. It is thus clear that MERRA should be the source for climate data in LTPP.

In addition to providing the weather inputs required for applications such as the MEPDG, the uniformly gridded MERRA data will also make the development of more precise climate zone maps easier. For example, figure 98 shows a LTPP climate zone classification map that was published during the test section recruitment phase of the program. In some places, this map was altered to adhere to State boundaries to make it easier for participating highway agencies to complete the test section nomination form. Climate zones do not follow State boundaries. Unfortunately, this stylized climate zone map has been inappropriately used for other applications; for example this figure appears in the early MEPDG literature. The uniformly gridded MERRA data will make it much easier to develop an updated climate zone map in the style of figure 99 that much more precisely demarcates the zone boundaries.

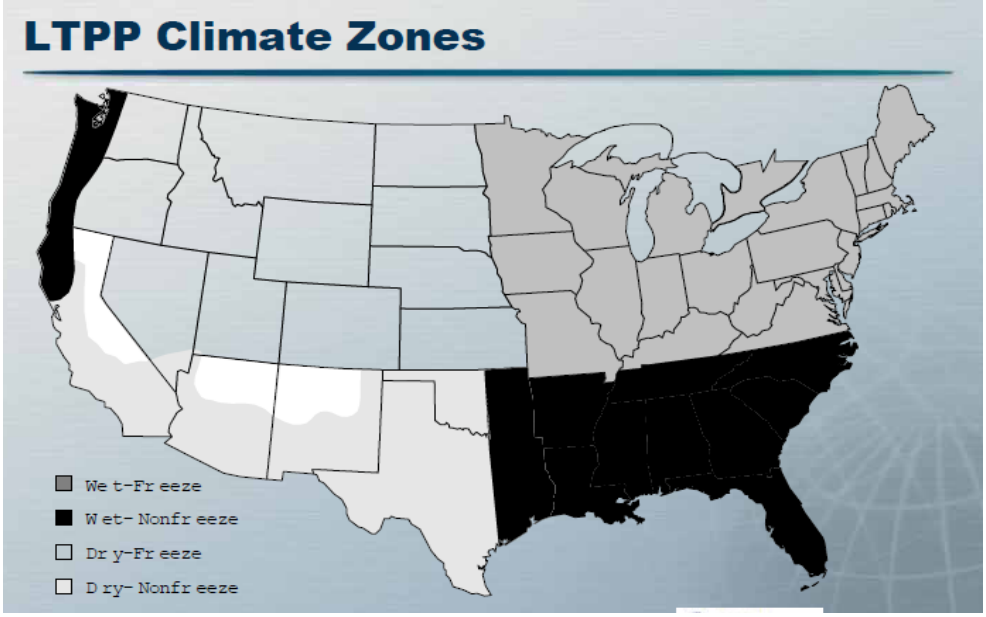

Figure 98. Map. LTPP climate zone map.

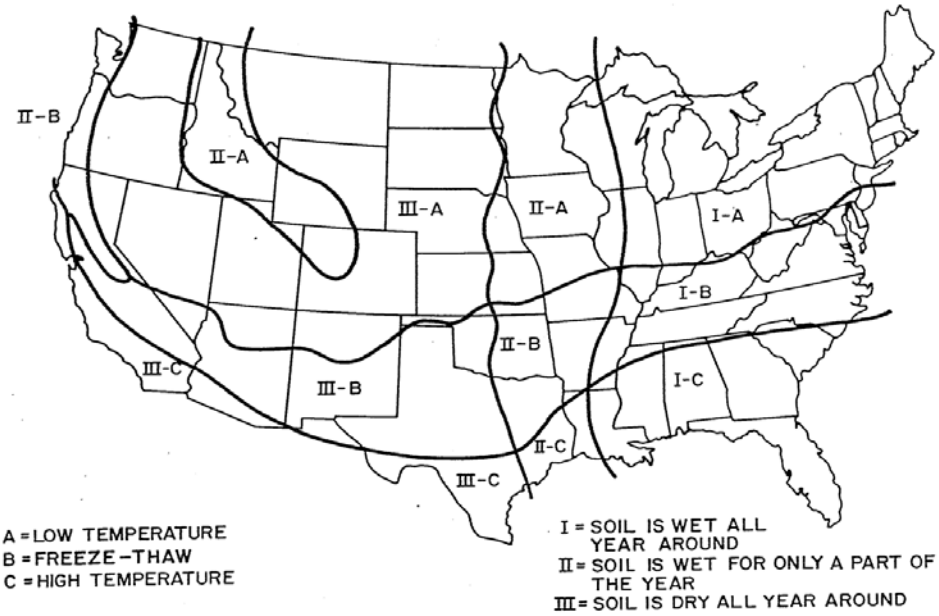

Source: M.I. Darter

Figure 99. Map. Example of more realistic climate zone map.[70]

Another potential LTPP product made possible by MERRA is a “weather anywhere” interactive application. Using a graphical map, a user can click a location and the program returns summary climate statistics. The output could be further refined to include inputs tailored to the AASHTOWare Pavement ME Design® software, HIPERPAV®, and other infrastructure modeling software. This tool is currently under production by the project team.

CLIMATE INDICES

Based on the project team's review of the existing LTPP CLM module, there is no compelling need to eliminate any of the climate indices currently in the database. These indices all have valid use over a range of applications, and their implementation in the LTPP database involves minimal storage and processing.

One specific objective of this project was to examine the calculation and storage of the TMI in the LTPP database. The TMI is a semi-empirical method for classifying the climate of a given location that quantifies the aridity or humidity of a soil-climate system by summing the effects of annual precipitation, potential evapotranspiration, storage deficit, and runoff.[71,64] Inclusion of TMI in the LTPP database was considered early in the program because some existing work on climate zones (e.g., climate zone maps) used it in its formulations. However, TMI has the disadvantage of being a largely empirical index formulated for continental United States conditions and therefore cannot be easily extended to other locations. Zapata et al. suggest a method for extending TMI beyond the continental United States, but the robustness of this method is unclear and its general validity needs further evaluation.[64] The TMI has seen a resurgence of interest in recent years because the MEPDG uses it to determine the equilibrium moisture contents of the unbound pavement materials far above the groundwater table.

The project team has found no compelling reason to incorporate TMI into the LTPP database. The following are the three principal reasons for this conclusion:

1. Although used currently in the MEPDG, TMI is a calculated internal quantity, not a direct model input. TMI values stored in the LTPP database could not be entered as input to the AASHTOWare Pavement ME Design® software and thus would have little direct usefulness to the MEPDG.

2. Because TMI is a semi-empirical index with limitations (e.g., its inability to be calculated outside the continental United States), it is unlikely to be used as a direct model input in any future infrastructure modeling application.

3. In the rare event that TMI values may be desired and assuming that MERRA data are incorporated into the LTPP database, TMI can be calculated on the fly from the appropriate MERRA data elements.

INCORPORATING MERRA DATA INTO THE LTPP DATABASE

If the recommendation to use MERRA data as an additional source of climate data for LTPP test sections is approved, the next consideration is how to add these data to the LTPP database. The MERRA dataset requires adaptation to specific user needs. The following activities and data storage constructs are recommended for adaptation of MERRA data to LTPP needs:

- Some MERRA data units need to be converted to conventional weather units common to infrastructure uses. For example, precipitation in MERRA is expressed as a flux rate that needs to be translated into more traditional units of "depth" over a prescribed period of time. For example, rain is traditionally measured by inches per hour or day whereas MERRA units of precipitation are in units of mass/(area * time).

Wind data are presented in eastward and northward vector components to avoid time-based averaging issues related to wind direction.

- The MERRA grid data represent the weather data for all test sections included in the grid boundaries. Interpolation of weather data is no longer needed. MERRA in essence performs a physics-based interpolation at each grid cell location.

- A new table needs to be developed to associate LTPP test site locations to the appropriate MERRA grid cell.

- Based on previous LTPP experience with weather data, it is recommended that the hourly MERRA data should be parsed into base line datasets containing distinct types of data. While this results in more datasets/tables than originally contained in the MERRA data files, it also provides a rational basis for the higher order climate statistics using existing LTPP database software code.

- A new LTPP database nomenclature needs to be developed to distinguish between MERRA data and the older OWS/VWS ground-based observations. The nomenclature used in this report is CLM_MERRA_*datataype_time*, where *datatype* follows the current climate categories of PRECIP, TEMP, WIND, and HUMIDITY, plus the new SOLAR category for solar radiation related data. Time is HOUR, DAY, MONTH, and ANNUAL.

- New data can be added to tables. Examples of potential new data additions include the following:

  - Evaporation to the PRECIP tables.

  - Snow to the PRECIP tables.

  - Average soil moisture at various depths to the PRECIP tables.

  - Albedo, surface emissivity, shortwave radiation, longwave radiation, and cloud cover to the new solar radiation tables.

- MERRA data are delivered in a flat file format. One of the first steps will be to translate the file format into a relational database format. The raw MERRA data will be stored in tables in native units for QC purposes and to make automating updates, extraction, and population of the new hourly climate data tables easier. Three MERRA analysis products are recommended for LTPP, and some of the data of interest in the files include the following:

  - **tavg1_2d_slv-Nx**—This includes hourly specific humidity and air temperature data.

  - **tavg1_2d_flx_Nx**—This includes surface evaporation, snowfall, precipitation, total precipitation, and total reevaporation of precipitation.

- **tavg1_2d_rad_Nx**—This includes data associated with solar radiation, including albedo, shortwave radiation, longwave radiation, and cloud fraction.

- The raw MERRA database tables are not envisaged as being included in the LTPP SDR because they are intended to mirror the raw data structure, including field names, obtained from the data source. This will decrease data user support requirements by LTPP because the raw data formats are not in customary units employed for civil engineering infrastructure modeling purposes and use nonintuitive variable names.

Figure 100 shows the conceptual computational and structure for climate data for LTPP based on MERRA data. The process starts with obtaining the MERRA data analysis products, which are delivered in a data file format. In the step that transforms the data file formats to database tables, the MERRA raw hourly data are parsed down to only the grid cells where LTPP test sections are located to save data storage space on the LTPP server because the total size of the three primary files are more than 17 terabytes. The MERRA raw hourly data are then both transformed into customary civil engineering units and split into five climate data categories to populate the CLM_MERRA_*datataype*_HOUR tables. These tables are recommended for inclusion in the LTPP SDR as are the remaining DAY, MONTH, and ANNUAL tables. After computation of the day tables from the hourly tables, the remaining month and annual tables will contain the climate indices included in the current LTPP CLM tables. Not shown in this figure is the table that will link test sections to MERRA grid cells, because the key fields in the CLM_MERRA_*datataype_time* tables will be based on MERRA grid cells to save data storage space.

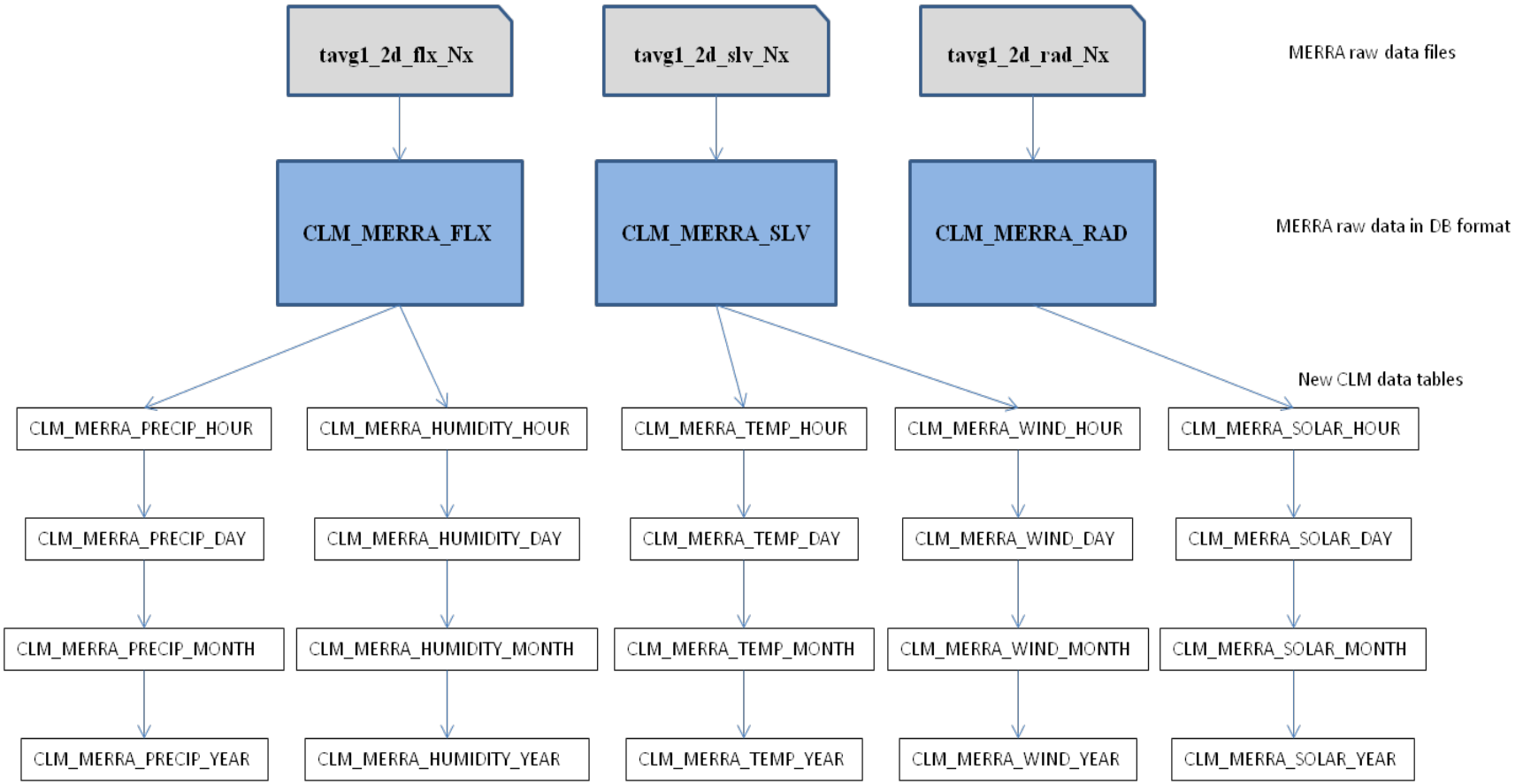

Figure 100. Flowchart. Conceptual computational and data storage structure for MERRA-based LTPP climate data.

REFERENCES

1. Schwartz, C.W., Elkins, G.E., Li, R., Visintine, B.A., Forman, B., Rada, G., and Groeger, J.L. *Evaluation of LTPP Climatic Data for Use In Mechanistic-Empirical Pavement Design Guide (MEPDG) Calibration and other Pavement Analyses*. FHWA-HRT-13-### (Draft), Federal Highway Administration, McLean, VA, 2012.

2. Li, R., Schwartz, C.W., and Forman, B.. "Sensitivity of Predicted Pavement Performance to Climate Characteristics," *ASCE Airfield and Highway Pavements Conference*, Los Angeles, CA, June 2013, pp. 760–771.

3. American Association of State Highway and Transportation Officials. *Mechanistic-Empirical Pavement Design Guide, Interim Edition: A Manual of Practice*. American Association of State and Highway Transportation Officials, Washington, DC, 2008.

4. National Oceanic and Atmospheric Administration. "NOAA's National Weather Service Glossary," < http://w1.weather.gov/glossary/index.php?word=weather:>, October 1, 2011.

5. Solomon, S., Qin, D., Manning, M., Chen, Z., Marquis, M., Avery, K.B., Tignor, M., and Miller, H.L. (eds.). *Contribution of Working Group I to the Fourth Assessment Report of the Intergovernmental Panel on Climate Change*. Cambridge University Press, Cambridge, United Kingdom, and New York, NY, 2007, pp. 996.

6. National Cooperative Highway Research Program (NCHRP). *Mechanistic-Empirical Design of New and Rehabilitated Pavement Structures. Final Report, NCHRP Project 1-37A*, National Cooperative Highway Research Program, National Research Council, Washington, DC, 2004.

7. Strategic Highway Research Program. *Development of LTPP Climatic Database*, SHRP-P-621, *National Academy of Sciences*, Washington, DC, 1993.

8. American Association of State Highway and Transportation Officials. *AASHTO Guide for Design of Pavement Structures*. American Association of State Highway and Transportation Officials, Washington, DC, 1993.

9. Zaghloul, S., Ayed, A., Abd El Halim, A., Vitillo, N., and Sauber, R. "Investigations of Environmental and Traffic Impacts on Mechanistic-Empirical Pavement Design Guide Predictions, Geology and Properties of Earth Materials," *Transportation Research Record, Journal of the Transportation Research Board 1967*, 2006, 148–159.

10. Johanneck, L. and Khazanovich, L. "Comprehensive Evaluation of Effect of Climate in Mechanistic-Empirical Pavement Design Guide Predictions," *Transportation Research Record: Journal of the Transportation Research Board, 2170*, 2010, pp 45–55.

11. Lee, M.C. *Mechanistic-Empirical Pavement Design Guide: Evaluation of Flexible Pavement Inputs*. M.S Thesis, University of Arkansas, Little Rock, AK, 2004.

12. Masad, S.A.. *Sensitivity Analysis of Flexible Pavement Response and AASHTO 2002 Design Guide for Properties of Unbound Layers*. Master's Thesis, Texas A&M University, College Station, TX, 2004.

13. Masad, S. and Little D.N. "Sensitivity Analysis of Flexible Pavement Response and AASHTO 2002 Design Guide for Properties of Unbound Layers," Project ICAR 504-1, International Center for Aggregates Research, Austin, TX, 2004.

14. El-Basyouny, M.M. and Witczak, M.W. "Calibration of Alligator Fatigue Cracking Model for 2002 Design Guide," *Transportation Research Record: Journal of the Transportation Research Board, 1919*, 2005, pp. 77–86.

15. El-Basyouny, M.M., Witczak, M.W., and El-Badawy, S. "Verification for the Calibrated Permanent Deformation Models for the 2002 Design Guide." *Journal of the Association of Asphalt Paving Technologists*, *74*, 2005, pp. 601–652.

16. El-Basyouny, M.M. and Witczak, M.W. "Verification of the Calibrated Fatigue Cracking Models for the 2002 Design Guide," *Journal of the Association of Asphalt Paving Technologists*, *74*, 2005, pp. 653–695.

17. Schwartz, C.W. "Evaluation of the Witczak Dynamic Modulus Prediction Model," *Annual Meeting of Transportation Research Board (CD-ROM)*, Washington, DC, 2005.

18. Brown, S.F., Thompson, M., and Barenberg, E. "NCHRP Research Results Digest 307: Independent Review of the Mechanistic-Empirical Pavement Design Guide and Software," *Transportation Research Board, National Research Council*, Washington, DC, 2006.

19. Carvalho, R. and Schwartz, C.W. "Comparisons of Flexible Pavement Designs: AASHTO Empirical Versus NCHRP Project 1-37A Mechanistic-Empirical," *Transportation Research Record: Journal of the Transportation Research Board, 1957*, 2006, pp. 167–174.

20. Chehab, G.R. and Daniel, J.S. "Evaluating Recycled Asphalt Pavement Mixtures With Mechanistic-Empirical Pavement Design Guide Level 3 Analysis," *Transportation Research Record: Journal of the Transportation Research Board, 1962*, 2006, pp. 90–100.

21. Graves, R.C. and Mahboub, K.C. "Flexible Pavement Design: Sensitivity of the NCHRP 1-37A Pavement Design Guide, A Global Approach," *Proceedings, ASCE Airfield and Highway Pavement Specialty Conference*, Atlanta, GA, 2006, pp. 224–235.

22. Graves, R.C. and Mahboub, K.C. "Pilot Study in Sampling-Based Sensitivity Analysis of NCHRP Design Guide for Flexible Pavements," *Transportation Research Record: Journal of the Transportation Research Board, 1947*, 2006, pp. 123–135.

23. Khazanovich, L., Celauro, C. and Chadbourn, B. "Evaluation of Subgrade Resilient Modulus Predictive Model for Use in Mechanistic-Empirical Pavement Design Guide,"

Transportation Research Record: Journal of the Transportation Research Board, 1947, 2006, pp. 155–166.

24. Kim, S., Ceylan, H., Gopalakrishnan, K., and Heitzman, M. "Sensitivity Study of Iowa Flexible Pavements Using Mechanistic-Empirical Pavement Design Guide," *Annual Meeting of Transportation Research Board (CD-ROM)*, National Research Council, Washington, DC, 2006. (http://pubsindex.trb.org/view.aspx?id=777279)

25. Mohammad, L.N., Wu, Z., Obulareddy, S., Cooper, S. and Abadie, C. "Permanent Deformation Analysis of Hot-Mix Mixtures Using Simple Performance Tests and 2002 Mechanistic-Empirical Pavement Design Software," *Transportation Research Record, Journal of the Transportation Research Board, 1970*, 2006, pp. 133–142.

26. Yin, H., Chehab, G.R. and Stoffels, S.M. "A Case Study: Assessing the Sensitivity of the Coefficient of Thermal Contraction of AC Mixtures on Thermal Crack Prediction," *Asphalt Concrete: Simulation, Modeling, and Experimental Characterization—Proceedings of the Symposium on Mechanics of Flexible Pavements, part of the 2005 Joint ASME/ASCE/SES Conf. on Mech. and Mater*, Geotechnical Special Publication, *146*, 2006, pp. 115–123.

27. Hoerner, T.E., Zimmerman, K.A., Smith, K.D. and Cooley, L.A. "Mechanistic-Empirical Pavement Design Guide Implementation Plan" Report No. SD2005-01, *South Dakota Department of Transportation*, Pierre, SD, 2007.

28. Kim, S., Ceylan, H. and Kasthurirangan, G. "Effect of M-E Design Guide Inputs on Flexible Pavement Performance Predictions," *Road Materials and Pavement Design*, *8*(3), 2007, pp. 375–397.

29. Li, Q., Wang, K.C.P., and Hall, K.D. "Verification of Virtual Climatic Data in MEPDG Using the LTPP Database," *International Journal of Pavement Research and Technology, 3*(1), 2010, pp. 10–11.

30. El-Basyouny, M.M. and Jeong, M.G. "Effective Temperature for Analysis of Permanent Deformation and Fatigue Distress on Asphalt Mixtures," *Transportation Research Record, Journal of the Transportation Research Board*, *2127*, 2009, pp 155–163.

31. Hermansson, A. "Simulation Model for Calculating Pavement Temperatures Including Maximum Temperature," *Transportation Research Record, Journal of the Transportation Research Board*, *1699*, 2000, pp. 134–141.

32. Hermansson, A. "Mathematical Model for Calculation of Pavement Temperatures: Comparison of Calculated and Measured Temperatures," *Transportation Research Record, Journal of the Transportation Research Board*, *1764*, 2001, pp. 180–188.

33. Hermansson, A. "Mathematical Model for Paved Surface Summer and Winter Temperature: Comparison of Calculated and Measured Temperatures," *Cold Regions Science and Technology, 40*(1-2), 2004, pp. 1–17.

34. Zubair, A., Marukic, I., Zaghloul, S., and Vitillo, N. “Validation of Enhanced Integrated Climatic Model Predictions With New Jersey Seasonal Monitoring Data,” *Transportation Research Record, Journal of the Transportation Research Board, 1913*, 2005, pp. 148-161.

35. Ho, C. and Romero, P. “Low Design Temperatures of Asphalt Pavements in Dry-Freeze Regions: Predicting by Means of Solar Radiation, Transient Heat Transfer, and Finite Element Method,” *Transportation Research Record, Journal of the Transportation Research Board, 2127*, 2009, pp. 60–71.

36. Zuo, G., Drumm, E.C., and Meier, R.W. “Environmental Effects on the Predicted Service Life of Flexible Pavements,” *Journal of Transportation Engineering, 133*(1), 2007, pp. 47–56.

37. Schindler, A.K., Ruiz, J.M., Rasmussen, R.O., Chang, G.K., and Wathne, L.G. “Concrete Pavement Temperature Prediction and Case Studies With the FHWA HIPERPAV Models,” *Cement and Concrete Composites, 26*(5), 2004, pp. 463–471.

38. Canadian National Climate Data and Information Archive <http://climate.weatheroffice.gc.ca/climateData/canada_e.html> (September 8, 2012).

39. Pisano, P. “ITS Research Success Stories,” *Clarus*, 2011. <http://www.weatherunderground.com/> (August 12, 2011).

40. National Climatic Data Center. METAR Homepage. <http://weather.noaa.gov/weather/coded.html> (October 2011).

41. Federal Aviation Administration. Aviation Weather Services. Advisory Circular, AC 00-45G, Change 1. 2010.

42. National Climatic Data Center. USCRN Homepage. http://www.ncdc.noaa.gov/crn/ (August 22, 2012).

43. National Weather Service. “NWS ASOS Program,” <http://www.nws.noaa.gov/asos/index.html> (September 1, 2011).

44. Rienecker, M.M., and coauthors. “MERRA—NASA’s Modern-Era Retrospective Analysis for Research and Applications,” *Journal of Climate, 24*, 2011, pp. 3,624–3,648.

45. National Aeronautics and Space Administration (NASA) Goddard Space Flight Center. “MERRA: Modern-Era Retrospective Analysis for Research and Applications.” <https://gmao.gsfc.nasa.gov/merra/>. (July 10, 2012)

46. Kalnay, E., and coauthors. “The NCEP/NCAR 40-Year Reanalysis Project,” *Bulletin of the American Meteorological Society, 77*, 1996, pp. 437–471.

47. Uppala, S.M., and coauthors. “The ERA-40 Re-Analysis,” *Quarterly Journal of the Royal Meteorological Society, 131*, 2005, pp. 2,961–3,012.

48. Onogi, K., and coauthors. “JRA-25: Japanese 25-Year Reanalysis Project—Progress and Status,” *Quarterly Journal of the Royal Meteorological Society, 131*, 2005, pp. 3,259–3,268.

49. Reichle, R.H., Koster, R.D., De Lannoy, G.J.M., Forman, B.A., Liu, Q., Mahanama, S., and Toure, A. “Assessment and Enhancement of MERRA Land Surface Hydrology Estimates,” *Journal of Climate, 24*, 2011, pp. 6,322–6,338.

50. Tighe, L.S., Smith, J., Mills, B., and Andrey, J. “Using the MEPDG to Assess Climate Change Impact on Southern Canadian Roads,”, *7th International Conference on Managing Pavement Assets (ICMPA)*, Calgary, Canada, 2008, pp. 96–108.

51. Schwartz, C.W. and Li, R. “Sensitivity of Predicted Flexible Pavement Performance to Unbound Material Hydraulic Properties,” *GeoFlorida 2010: Advances in Analysis, Modeling, and Design, Geotechnical Special Publication 199*, ASCE, 2010, p. 2,672 (doi 10.1061/41095(365)271).

52. Schwartz, C.W., Li, R., Kim, S., Ceylan, H., and Gopalakrishnan, K. “Sensitivity Evaluation of MEPDG Performance Prediction,” Final Report of National Co-operative Highway Research Program 1-47 Project (available online). *Transportation Research Board, National Research Council*, Washington, DC, 2012.

53. Ceylan, H., Kim, S., Schwartz, C.W., Li, R., and Gopalkrishnan, K. “Effect of PCC Material Properties on MEPDG Rigid Pavement Performance,” *10th International Conference on Concrete Pavements*, Quebec, Canada, July 2012, pp. 236–251.

54. Li, R., Schwartz, C.W., Kim, S., and Ceylan, H. “Local Sensitivity of Mechanistic-Empirical Flexible Pavement Performance Predictions to Unbound Material Property Inputs,” *2012 Geo-Congress*, Oakland, CA, March 2012, pp. 1,495–1,504.

55. Cacuci, D.G. *Sensitivity and Uncertainty Analysis Theory: Volume I*, Chapman and Hall/CRC, Boca Raton, FL, 2003.

56. Saltelli, A., Ratto, M., Andres, T., Campolongo, F., Cariboni, J., Gatelli, D., Saisana, M., and Tarantola, S. *Global Sensitivity Analysis: The Primer*, John Wiley and Sons Ltd., England, 2008.

57. Alam, M., Fekpeet, E., and Majed, M. *FHWA FAF2 Freight Traffic Analysis Report*, Federal Highway Administration, Washington, DC, 2007.

58. Baker, D.G., and Haines D.A. *Solar Radiation and Sunshine Duration Relationship in the North-Central Region and Alaska*, Technical Bulletin 262, Experiment Station, University of Minnesota, Minneapolis, MN 1969.

59. Cosgrove, B.A., Lohmann, D., Mitchell, K.E., Houser, P.R., Wood, E.F., Schaake, J.C., Robock, A., Marshall, C., Sheffield, J., Duan, Q., Luo, L., Higgins, R.W., Pinker, R.T., and Tarpley, J.D.” Real-Time and Retrospective Forcing in the North American Land

Data Assimilation System (NLDAS) Project," *Journal of Geophysical Research*, *108*(D22),2003, doi:10.1029/2002JD003118.

60. National Oceanic and Atmospheric Administration, U.S. Department of Commerce, Federal Aviation Administration, U.S. Navy, U.S. Department of the Air Force, *Automated Surface Observing System: ASOS User's Guide*, Washington, D.C., 1998.

61. Dempsey, B.J., Herlach, W.A., and Patel, A.J. *The Climatic-Material-Structural Pavement Analysis Program*, FHWA/RD-84/115, 3, Final Report, Federal Highway Administration, Washington, DC, 1985.

62. Lytton, R.L., Pufahl, D.E., Michalak, C.H., Liang, H.S., and Dempsey, B.J. *An Integrated Model of the Climatic Effects on Pavements*. FHWA-RD-90-033, Federal Highway Administration, McLean, VA, 1993.

63. Larson, G., and B. J. Dempsey. *Integrated Climatic Model, Version 2.0*. Report No. DTFA MN/DOT 72114, Newmark Civil Engineering Laboratory, University of Illinois at Urbana-Champaign, IL, 1997.

64. Zapata, C.E., Perera, Y.Y. and Houston, W.H. "Matric Suction Prediction Model in New AASHTO Mechanistic–Empirical Pavement Design Guide," *Transportation Research Record, Journal of the Transportation Research Board*, *2101*, 2009, pp. 53–62.

65. Vehrencamp, J.E. "Experimental Investigation of Heat Transfer at Air-Earth Interface," American Geophysical Union, Washington DC *Transportation*, 34(1), 1953.

66. Geiger, R. *The Climate Near Ground*, Harvard University Press, Cambridge, MA, 1959.

67. Brock, F.V., Crawford, K.C., Elliott, R.L., Cuperus, G.W., Stadler, S.J., Johnson H.L., and Eilts, M.D. "The Oklahoma Mesonet: A Technical Overview," *J. Atmospheric and Oceanic Technology*, *12*, 1995, pp. 5–19.

68. Groisman, P.Y., and Legates, D.R. "The Accuracy of United States Precipitation Data," *Bulletin of the American Meteorology Society*, *75*, 1994, pp. 215–227.

69. Google®, Inc. *Sites used for evaluation of MEPDG performance predictions using MEPDG and MERRA climate data*. Accessed June 30, 2014. https://www.google.com/maps/d/edit?mid=zcHlzMa1-Xeo.kL-97GvytZCc.

70. Shahin, M.Y., Darter, M.I., Kohn, S.D, *Development of a Pavement Maintenance Management System*, Volume I–V, U.S. Air Force Engineering Services Center, Tyndell Air Force Base. 1977.

71. Thornthwaite, C.W. "An Approach Toward a Rational Classification of Climate," *Geophysical Review*, *38*(1), 1948, pp. 55–94.

HRDI-30/05-15(500)E